U.PORTO

FEUP FACULDADE DE ENGENHARIA
UNIVERSIDADE DO PORTO

COMPOSITE PLATE GIRDER BRIDGES

A State-of-the-Art Report of UK Practice

JOSÉ PEDRO VILAS BOAS DE MONTALVÃO FERNANDES

Dissertation submitted for the partial fullfillement of the requirements to the degree of

MASTER'S IN CIVIL ENGINEERING — SPECIALISATION IN STRUCTURES

Professor Dr. José Miguel de Freitas Castro

Dr. Ricardo Nuno Tavares Teixeira

JANUARY 2016

MESTRADO INTEGRADO EM ENGENHARIA CIVIL 2015/2016

DEPARTAMENTO DE ENGENHARIA CIVIL

Tel. +351-22-508 1901

Fax +351-22-508 1446

✉ miec@fe.up.pt

Editado por

FACULDADE DE ENGENHARIA DA UNIVERSIDADE DO PORTO

Rua Dr. Roberto Frias

4200-465 PORTO

Portugal

Tel. +351-22-508 1400

Fax +351-22-508 1440

✉ feup@fe.up.pt

🌍 http://www.fe.up.pt

Reproduções parciais deste documento serão autorizadas na condição que seja mencionado o Autor e feita referência a *Mestrado Integrado em Engenharia Civil - 2015/2016 - Departamento de Engenharia Civil, Faculdade de Engenharia da Universidade do Porto, Porto, Portugal, 2016*.

As opiniões e informações incluídas neste documento representam unicamente o ponto de vista do respetivo Autor, não podendo o Editor aceitar qualquer responsabilidade legal ou outra em relação a erros ou omissões que possam existir.

Este documento foi produzido a partir de versão eletrónica fornecida pelo respetivo Autor.

To João and Tiago,
For the infinite joy they bring.

To Sofia Marques da Silva,
For seeding the will.

Everything should be made as simple as possible, but no simpler.
Albert Einstein

ACKNOWLEDGMENTS

The author would like to thank his employer WSP | Parsons Brinckerhoff in the persons of David Gulick, Andrew Porter, and especially Kelly Croke for their sponsorship in the undertaking of this work.

To Professor José Miguel Castro for his willingness to tutor this dissertation written at a distance regardless of the constraints, and for his review and constructive criticism of the work.

A special thanks to Dr. Ricardo Teixeira, tutor, colleague and friend. For his unflinching support, review of the text, and especially for the long hours of discussion about any subject in structural engineering.

To Tony Harris, Head of Discipline – Bridges at WSP | Parsons Brinckerhoff, for his valuable comments and insights.

To my colleagues and friends Tom Corcoran and Stephen Heaney for their comments and long hours of fruitful discussion.

Finally, to acknowledge Elfyn Williams at Welsh Government for providing the data on existing road bridges in Wales and Richard Stonehouse at Mabey Bridge for the data on fabrication costs used in Chapter 2.

ABSTRACT

The United Kingdom has a rich history in the design and construction of steel bridges. This is owed in great part to having been the birthplace of the Industrial Revolution, when advances in scientific knowledge and manufacture process enabled the economic production of large quantities of steel.

The invention of the steam-engine train and the construction of railways that followed provided a fertile ground for engineers of the time to continually experiment with the new material. In the following century the construction of bridges would reach spans unimaginable until then. With the rise of the automobile in the 20th century and the expansion of motorways in post-war Europe the ground was provided for the construction of many new bridges. It was in this context that steel-concrete composite bridges first made their appearance in the 1960's. Since then composite bridges underwent continuous development to their present types. Since then composite bridges evolved continuously to the deck types that can be seen today.

This dissertation intends to present a review of the state-of-the-art of UK practice in the analysis and design of steel-concrete composite bridges. Following an historical background to the evolution of steel bridges an overview of the presence of composite bridges within existing road bridges in service is set out. Typical deck cross-sections in use in the UK construction industry and their respective preferred range of application are presented, as well as information on plate girder fabrication costs.

The methods used in practice today for the global analysis of composite bridge decks are addressed in following. The design actions and the rules for combinations of actions in current design codes (the Eurocodes) that define ultimate and serviceability limit states are presented. The quantification of time dependant properties of concrete and a general view of the analysis models at the disposal of practising engineers are provided.

A review of the design of composite cross-sections follows, starting with the cross-section classification process and the explanation of its consequences in the cross-section resistances. The verification of cross-section resistances to bending flexure, vertical shear force, combined bending and vertical shear force, and longitudinal shear force for ultimate limit states is presented in detail. The importance of serviceability limit state checks is highlighted. Verifications of stress limitations in structural steelwork, reinforcing steel and concrete are presented as well as the control of concrete cracking by limiting crack widths.

The presentation of a case study of the preliminary design of a steel-concrete composite viaduct in Wales demonstrates how the subjects covered all come together in the design of a bridge structure. It is shown how the brief requirements and the site constraints to be addressed dictated the choice of the type of superstructure, in this case a solution typical of the UK which is the ladder deck. The design actions to be considered and the type of model chosen for the global analysis of the deck are then presented. These are followed by the validation of the design by means of cross-section verifications for ultimate limit states. A summary of the merits of the proposed solution and its economy of design concludes the dissertation.

KEYWORDS: bridge, steel, composite, analysis, design.

RESUMO

O Reino Unido tem uma história rica no projecto e construção de pontes em aço. Tal deve-se em grande parte a ter sido o berço da Revolução Industrial, quando progressos no conhecimento científico e nos processos de fabrico possibilitaram a produção económica de aço em grandes quantidades.

A invenção do comboio a vapor e a construção de ferrovias que se seguiu proporcionaram terreno fértil para os engenheiros da época experimentarem o novo material, com a construção de pontes no século seguinte a atingir vãos até então inimagináveis. Com o surgir do automóvel no século XX e a expansão da rede de autoestradas no pós-guerra proporcionou-se a construção de grande número de novas pontes. Foi neste contexto que as pontes mistas aço-betão fizeram a sua primeira aparição nos anos sessenta. Desde então as pontes mistas evoluíram continuamente até às tipologias de tabuleiros que se podem ver nos dias de hoje.

Esta dissertação pretende apresentar uma revisão do estado-da-arte da prática no Reino Unido da análise e projecto de pontes mistas aço-betão. Após um enquadramento histórico da evolução das pontes em aço uma visão geral da presença das pontes mistas entre as pontes rodoviárias em service é estabelecida. As secções transversais típicas em uso na indústria da construção do Reino Unido e o seu respectivo campo de aplicação preferencial são apresentadas, bem como informação sobre custos de fabricação de vigas de alma cheia.

Os métodos usados hoje na análise global de tabuleiros de pontes mistas serão abordados de seguida. As acções de cálculo e as regras para combinações de acções dos códigos de projecto actuais (os Eurocódigos) que definem os estados limite último e de serviço são apresentadas. A quantificação das propriedades diferidas do betão e uma visão geral dos modelos de análise à disposição do engenheiro são fornecidas.

Segue-se uma revisão do projecto de secções mistas, com início no processo de classificação de secções e a explicação das suas consequências para a resistência da secção. A verificação das resistências à flexão, ao esforço transverso, à combinação entre flexão e esforço transverso, e ao esforço rasante é apresentada detalhadamente. A importância da verificação de estados limite de service é sublinhada. As verificações de limitação de tensões no aço estrutural, nas armaduras e no betão são apresentadas bem como o controlo de fissuração do betão pela limitação da abertura de fendas.

A apresentação de um caso de estudo do estudo prévio de um viaduto misto aço-betão em Gales demonstra como os temas cobertos se combinam no projecto de uma ponte. É mostrado como os requisitos do caderno de encargos e os condicionantes locais a abordar ditaram a escolha do tipo de superestrutura, neste caso uma solução típica do Reino Unido que é o tabuleiro bi-viga com carlingas. As acções de cálculo a considerar e o modelo adoptado para a análise global do tabuleiro são apresentados. Segue-se a validação da solução através das verificações da secção para o estado limite último. Um resumo das mais-valias da solução proposta e da economia do seu projecto conclui a dissertação.

PALAVRAS-CHAVE: ponte, aço, mista, análise, projecto.

TABLE OF CONTENTS

ACKNOWLEDGEMENTS i

ABSTRACT iii

RESUMO v

1 INTRODUCTION 1

1.1. GENERAL CONSIDERATIONS 1

1.2. HISTORICAL BACKGROUND 2

1.3. GENERAL OBJECTIVES 2

1.4. DISSERTATION CONTENTS 3

2 STATE-OF-THE-ART IN THE UK 5

2.1. HISTORICAL OVERVIEW OF STEEL BRIDGES IN BRITAIN 5

2.1.1. PIONEERS OF THE GEORGIAN ERA 5

2.1.2. VICTORIAN RAILWAY ENGINEERING 10

2.1.3. EDWARDIAN ENGINEERING AND THE ARRIVAL OF STEEL 15

2.1.4. BRIDGE ENGINEERING IN THE INTERWAR PERIOD 18

2.1.5. EVOLUTION OF BRIDGES FROM THE POST-WAR ERA TO PRESENT DAY 20

2.2. COMPOSITE BRIDGES WITHIN ROAD NETWORKS IN WALES 29

2.2.1. EXISTING BRIDGE DISTRIBUTION BY CONSTRUCTION TYPE 29

2.2.2. EXISTING BRIDGE DISTRIBUTION BY SPAN RANGE 30

2.2.3. EXISTING BRIDGE DISTRIBUTION BY CONSTRUCTION DATE 30

2.2.4. CONSTRUCTION TYPE IN RELATION TO SPAN RANGE 31

2.3. TYPICAL COMPOSITE BRIDGE DECKS FROM UK PRACTICE 32

2.3.1. MULTI GIRDER BRIDGE DECK CROSS SECTIONS 33

2.3.2. TWIN GIRDER BRIDGE DECK CROSS SECTIONS 34

2.3.3. MULTIPLE COMPACT BOX BRIDGE DECK CROSS SECTIONS 35

2.3.4. OPEN TOP TRAPEZOIDAL BOX BRIDGE DECK CROSS SECTIONS 36

2.4. ECONOMY AND FABRICATION COSTS 38

3 GLOBAL ANALYSIS OF COMPOSITE DECKS 41

3.1. OVERVIEW OF DESIGN ACTIONS 41

3.1.1. DEAD LOADS – SELF-WEIGHT OF STRUCTURE 42
3.1.2. SUPERIMPOSED DEAD LOADS - SELF-WEIGHT OF NON-STRUCTURAL ELEMENTS 43
3.1.3. THERMAL ACTIONS – TEMPERATURE DIFFERENCE COMPONENTS 44
3.1.4. ROAD TRAFFIC ACTIONS ON BRIDGES 45
3.1.4.1. Models of Road Traffic Actions 45
3.1.4.2. Division of the Carriageway and Load Application 46
3.1.4.3. Load Model 1 48
3.1.4.4. Load Model 2 50
3.1.4.5. Load Model 3 50
3.1.4.6. Load Model 4 53
3.1.4.7. Loading on Footways and Cycletracks 53
3.1.4.8. Groups of Traffic Loads 53
3.2. COMBINATIONS OF ACTIONS FOR ROAD BRIDGES 54
3.2.1. LIMIT STATE DESIGN TO THE PARTIAL FACTOR METHOD 54
3.2.2. ULTIMATE LIMIT STATE COMBINATIONS 55
3.2.3. SERVICEABILITY LIMIT STATE COMBINATIONS 56
3.2.4. PARTIAL SAFETY FACTORS FOR ACTIONS 58
3.3. TIME DEPENDENT PROPERTIES OF CONCRETE 60
3.3.1. SHRINKAGE OF CONCRETE 60
3.3.2. CONCRETE CREEP 63
3.4. STRUCTURAL ANALYSIS OF COMPOSITE DECKS 65
3.4.1. STRUCTURAL MODELLING FOR ANALYSIS 65
3.4.2. STRUCTURAL STABILITY 67
3.4.3. EFFECTIVE WIDTH OF FLANGES FOR SHEAR LAG 68
3.4.4. MODULAR RATIOS FOR CONCRETE 71
3.4.5. EFFECTS OF CRACKING OF CONCRETE 72
3.4.6. PRIMARY AND SECONDARY EFFECTS OF CONCRETE SHRINKAGE 73

4 DESIGN OF COMPOSITE CROSS-SECTIONS 81

4.1. CLASSIFICATION OF CROSS-SECTIONS 81
4.1.1. DETERMINATION OF THE CROSS-SECTION CLASS 82
4.1.2. EFFECTIVE SECTION OF CLASS 4 CROSS-SECTIONS 83
4.2. CROSS-SECTION VERIFICATION FOR ULTIMATE LIMIT STATES 86
4.2.1. CROSS-SECTION BENDING RESISTANCE 86

4.2.1.1. Plastic Resistance Moment 86
4.2.1.2. Non-Linear Resistance Moment 88
4.2.1.3. Elastic Resistance Moment 90
4.2.2. Cross Section Resistance to Vertical Shear 92
4.2.2.1. Plastic Resistance to Vertical Shear 93
4.2.2.2. Shear Buckling Resistance to Vertical Shear 94
4.2.2.3. Bending and Vertical Shear Interaction 98
4.2.3. Cross Section Resistance to Longitudinal Shear 101
4.2.3.1. Longitudinal Shear Force for Beams in Bridges 102
4.2.3.2. Design Resistance of Headed Stud Connectors 105
4.2.3.3. Detailing of the Shear Connection 106
4.3. Cross-Section Verification for Serviceability Limit States 108
4.3.1. Stress Limitations for Bridges 108
4.3.1.1. Concrete Compressive Stress Limits 109
4.3.1.2. Reinforcing Steel Tensile Stress Limits 109
4.3.1.3. Steelwork Stress Limits 110
4.3.1.4. Limitation of Longitudinal Shear Force of Connectors 111
4.3.2. Web Breathing 111
4.3.3. Cracking of Concrete 112
4.3.3.1. Minimum Reinforcement for Restraint of Imposed Deformations 113
4.3.3.2. Control of Cracking Due to Direct Loading 114

5 CASE STUDY – THE RIVER SEIONT VIADUCT 117

5.1. Introduction and Background 117
5.1.1. The A487 Caernarfon to Bontnewydd Bypass 117
5.1.2. Options Development for The River Seiont Viaduct 119
5.2. Proposed Structure 121
5.2.1. Description of structure and design working life 122
5.2.2. Deck Cross-Section of the Viaduct 123
5.2.3. Materials 125
5.3. Design Actions and Combinations 125
5.3.1. Permanent Actions 125
5.3.2. Shrinkage 126
5.3.3. Thermal Actions 127

5.3.4. Road Traffic Actions 127
5.3.5. Combinations of Actions 129
5.4. Global Analysis of the Viaduct 130
5.4.1. Effective Width of Flanges for Shear Lag 130
5.4.2. Modular Ratios for Concrete 130
5.4.3. Effects of Cracking of Concrete 132
5.4.4. Structural Analysis Model 132
5.4.5. Linear Elastic Analysis 134
5.5. Cross-Section Verification at ULS 137
5.5.1. Bending Resistance of the Span Cross-Section 137
5.5.2. Bending Resistance of the Pier Cross-Section 139
5.5.3. Shear Resistance of Pier Cross-Section 143
5.5.4. Bending and Vertical Shear Interaction of Pier Cross-Section 145
5.6. Material Quantities and Steel Consumption 147

6 CONCLUSIONS 149

6.1. Closing Remarks 149
6.2. Future Works 151

TABLE OF FIGURES

Fig. 2.1 – The Iron Rolling Mill, Adolph Von Menzel 1875 (from *Google Art Project*) 6

Fig. 2.2 – The Cast Iron Bridge near Coalbrookdale, painting by William Williams, 1780 (from *bbc.co.uk*) 7

Fig. 2.3 – The Iron Bridge over the River Severn at Buildwas (from *Shrewsbury Museum Service*) 8

Fig. 2.4 – The Pontcysyllte Aqueduct (from *whc.unesco.org*) 9

Fig. 2.5 – The Menai Straight Bridge (from *wikipedia.org*) 10

Fig. 2.6 – The Clifton Suspension Bridge (from *wikipedia.org*) 11

Fig. 2.7 – The Windsor Railway Bridge (from *wikipedia.org*) 12

Fig. 2.8 – The Royal Albert Bridge (from *bbc.co.uk*) 13

Fig. 2.9 – The Britannia Bridge (from *denbighshirearchives.wordpress.com*) 14

Fig. 2.10 – The Forth Bridge (from *wikipedia.org*) 16

Fig. 2.11 – The Tower Bridge (from *bbc.co.uk*) 16

Fig. 2.12 – Connel Bridge (from *rcahms.gov.uk*) 17

Fig. 2.13 – Queen Alexandra Bridge under construction (from *urbanglasgow.co.uk*) 18

Fig. 2.14 – Tyne Bridge (from *wikipedia.org*) 19

Fig. 2.15 – Billingham Bridge (from *geograph.co.uk*) 19

Fig. 2.16 – Pelham Bridge (from *geograph.co.uk*) 20

Fig. 2.17 – First Severn Crossing (from *severnbridge.co.uk*) 21

Fig. 2.18 – Tay Estuary Road Bridge (from *songofthepaddle.co.uk*) 21

Fig. 2.19 – Tinsley Viaduct (from *sabre-roads.co.uk*) 22

Fig. 2.20 – Raith Bridge (*James Brown,* 2010) 23

Fig. 2.21 – Cantilever construction of the Cleddau Bridge (*Robert Matera-Byford*, 2009) 23

Fig. 2.22 – Saltings Viaduct (from *SWTRA*) 24

Fig. 2.23 – Friarton Bridge (from *geograph.org.uk*) 25

Fig. 2.24 – Humber Bridge under construction (from *geograph.org.uk*) 26

Fig. 2.25 – Queen Elizabeth II Bridge (from *sevenoakschronicle.co.uk*) 26

Fig. 2.26 – Hulme Bridge (from *wikipedia.org*) 27

Fig. 2.27 – River Usk Bridge (from *newsteelconstruction.com*) 28

Fig. 2.28 – River Usk Bridge under construction (from *mabeybridge.com*) 28

Fig. 2.29 – Existing bridge distribution by construction type 29

Fig. 2.30 – Existing bridge distribution by span range 30

Fig. 2.31 – Existing bridge distribution by construction date 31

Fig. 2.32 – Bridge construction type in relation to span range 32

Fig. 2.33 – Multi girder deck cross section (from *Steel Detailers Manual*, Blackwell Science, 2002)... 33

Fig. 2.34 – Twin girder deck with transverse girders cross section (from *Steel Detailers Manual*, Blackwell Science, 2002) 34

Fig. 2.35 – Multiple closed box deck cross section (from *Steel Detailers Manual*, Blackwell Science, 2002) 36

Fig. 2.36 – Open top trapezoidal box deck cross section (from *Steel Detailers Manual*, Blackwell Science, 2002)..... 37

Fig. 2.37 – Open top box section with and without longitudinal stiffening (from *Guidance Notes on Best Practice in Steel Bridge Construction*, SCI, 2010) 37

Fig. 3.1 – Typical cross section of a single carriageway road bridge..... 43

Fig. 3.2 – Normal procedure for the definition of the temperature difference component. 44

Fig. 3.3 – Simplified procedure for the definition of the temperature difference component. 44

Fig. 3.4 – Examples of carriageway widths *w* to consider (from *Designers Guide to Eurocode 1*, Thomas Telford, 2010) 46

Fig. 3.5 – Possible notional lane definition for worst effects from LM1 on girder G1. 47

Fig. 3.6 – Possible notional lane definition for worst effects from LM1 on girder G2. 48

Fig. 3.7 – Longitudinal and plan application of Load Model LM1 as per UKNA of EN1990..... 49

Fig. 3.8 – Load Model LM2 consider (from *Designers Guide to Eurocode 1*, Thomas Telford, 2010) . 50

Fig. 3.9 – Configuration of SV80 vehicle (from *UK National Annex to EN 1991-2:2003*, BSI, 2008) ... 51

Fig. 3.10 – Configuration of SOV-250 vehicle (from *UK National Annex to EN 1991-2:2003*, BSI, 2008) 51

Fig. 3.11 – Application of SV or SOV vehicle with Load Model 1 (from *UK National Annex to EN 1991-2:2003*, BSI, 2008) 52

Fig. 3.12 – Time dependant evolution of concrete shrinkage strain (h_0=250mm, t_s=1d, RH=80%) 62

Fig. 3.13 – Development of creep coefficient over time (h_0=250mm, f_{ck}=35MPa, RH=80%) 64

Fig. 3.14 – Example of finite element grillage model 66

Fig. 3.15 – Example of finite element hybrid model 66

Fig. 3.16 – Example of finite element shell model..... 67

Fig. 3.17 – Bending stress distribution in wide flanges due to shear lag effect. 69

Fig. 3.18 – Equivalent span Le for continuous girders (from *EN1994-2, BSI, 2010*). 70

Fig. 3.19 – Non-uniform longitudinal stress at mid-plane of the concrete flange of a hybrid model. 70

Fig. 3.20 – Cracked regions over an internal support as per the simplified method. 73

Fig. 3.21 – Eccentricity between slab mid-plane and centroid of composite section..... 74

Fig. 3.22 – Structural analysis diagram of a simply supported composite beam. 75

Fig. 3.23 – Bending moment due to shrinkage effects in a simply supported composite beam. 75
Fig. 3.24 – Uncracked section stresses due to primary shrinkage effects. 75
Fig. 3.25 – Structural analysis diagram of a continuous uncracked composite beam. 76
Fig. 3.26 – Bending moments due to shrinkage effects in a continuous uncracked composite beam. 76
Fig. 3.27 – Uncracked section stresses due to primary and secondary shrinkage effects. 76
Fig. 3.28 – Structural analysis diagram of a continuous composite beam with cracked regions. 77
Fig. 3.29 – Bending moments due to shrinkage effects in a composite beam with cracked regions. .. 77
Fig. 3.30 – Cracked section stresses due to secondary shrinkage effects. 78
Fig. 4.1 – Effective web of Class 4 cross-section. 85
Fig. 4.2 – Stress distribution for plastic sagging resistance moment. 87
Fig. 4.3 – Stress distribution for plastic hogging resistance moment. 87
Fig. 4.4 – Stress distribution on effective section for plastic hogging resistance moment. 88
Fig. 4.5 – Stress-strain diagrams for non-linear resistance model. 89
Fig. 4.6 – Stress distribution for elasto-plastic sagging resistance moment. 90
Fig. 4.7 – Cumulative stresses for calculation of the elastic resistance moment. 91
Fig. 4.8 – Pure shear stress state in a web plate (from *Design of Plated Structures*, ECCS, 2010) 94
Fig. 4.9 – Post-critical stresses in a web plate (from *Design of Plated Structures*, ECCS, 2010) 94
Fig. 4.10 – Mechanical model of the rotated stress field (from *Commentary and Worked Examples to EN1993-1-5*, ECCS, 2007) 95
Fig. 4.11 – Reduction curves for shear buckling and critical shear stress 98
Fig. 4.12 – Plastic stress distribution modified by the effect of vertical shear (from *EN 1994-2:2005*, BSI, 2008) 99
Fig. 4.13 – Region to consider the interaction of bending moment and shear force (from *Design of Plated Structures*, ECCS, 2010) 101
Fig. 4.14 – Definition of an inelastic length for the determination of longitudinal shear force (from *EN 1994-2:2005*, BSI, 2008) 103
Fig. 4.15 – Variation of normal force in the concrete slab with bending moment (from *Designers Guide to EN1994-2*, Thomas Telford, 2006) 103
Fig. 4.16 – Determination of the longitudinal shear force from primary shrinkage at the end of a beam (from *Designers Guide to EN1994-2*, Thomas Telford, 2006) 104
Fig. 4.17 – Typical potential surfaces of shear failure (from *EN 1994-2:2005*, BSI, 2008) 107
Fig. 5.1 – A487 Caernarfon to Bontnewydd Bypass Preferred Routes 118
Fig. 5.2 – Horizontal alignment of the A487 over River Seiont 119
Fig. 5.3 – Plan of River Seiont Viaduct. 122
Fig. 5.4 – Elevation of River Seiont Viaduct. 122

Fig. 5.5 – A487 Carriageway over River Seiont Viaduct 123
Fig. 5.6 – Typical cross section of River Seiont Viaduct 124
Fig. 5.7 – Elements of the deck cross-section of River Seiont Viaduct..... 126
Fig. 5.8 – Notional lanes for most adverse effects on left girder 128
Fig. 5.9 – Notional lanes for most adverse effects on right girder..... 129
Fig. 5.10 – Notional cross-sections of spans 2 and 3. 132
Fig. 5.11 – Three-dimensional line beam model of River Seiont Viaduct. 133
Fig. 5.12 – Bending moment diagram due to effects of permanent actions. 134
Fig. 5.13 – Bending moment diagrams due to effects of shrinkage. 134
Fig. 5.14 – Bending moment envelopes due to effects of road traffic actions. 135
Fig. 5.15 – Bending moment diagram due to effects of temperature difference. 135
Fig. 5.16 – ULS bending moment envelope. 136
Fig. 5.17 – ULS shear force envelope. 136
Fig. 5.18 – Plastic stress distribution on effective Class 2 cross-section. 141
Fig. 5.19 – Web panels on longitudinal girders of River Seiont Viaduct. 143

TABLE OF TABLES

Table 2.1 - Typical distribution of work hours to girder weight for UK steel fabrication. 38
Table 3.1 - Number and width notional lanes..... 47
Table 3.2 - Load Model 1 characteristic values and UK National Annex adjustment factors. 48
Table 3.3 - Characteristic values of the multi-component action of group traffic loads. 54
Table 3.4 - Partial factors for design values of actions (STR/GEO) Set B (from EN1990) 58
Table 3.5 - Recommended values of ψ factors for road bridges (from EN1990)..... 59
Table 3.6 - Basic combinations at ULS (STR/GEO) for analysis of road bridges decks. 60
Table 4.1 - Maximum width-to-thickness ratios for compression parts as per Table 5.2 of EN1993-1-1. 82
Table 4.2 - Shear buckling factor as per Table 5.1 of EN1993-1-5..... 96
Table 4.3 - Recommended values of w_{max} as per Table 7.101N of EN1992-2. 112
Table 5.1 – Structural steelwork grades used in the River Seiont Viaduct. 124
Table 5.2 – Structural steelwork grades used in the River Seiont Viaduct. 125
Table 5.3 – Concrete grades used in the River Seiont Viaduct. 125
Table 5.4 – Permanent actions on River Seiont Viaduct. 126
Table 5.5 – Combinations of actions considered for preliminary design..... 129
Table 5.6 – Effective widths of the concrete flange..... 130
Table 5.7 – Axial forces on the steel section elements. 137
Table 5.8 – Axial forces and lever arms of the composite cross-section elements. 138
Table 5.9 – Axial forces on cross-section elements for plastic stress distribution. 139
Table 5.10 – Axial forces on the cross-section web for plastic stress distribution. 140
Table 5.11 – Axial forces and lever arms of the effective cross-section elements. 142
Table 5.12 – Axial forces and lever arms considering reduced steel strength of web. 147
Table 5.13 – Structural steelwork quantities based on preliminary design. 148

1 INTRODUCTION

1.1. GENERAL CONSIDERATIONS

Since the dawn of Humanity we have tried to better our lives by producing tools and utensils to ease our chores and by building shelters where Nature provided few or any. The birth of ancient civilisations spawned complex societies where the separation of Humans from the natural environment would become the norm. The urbanisation process and its increased concentration of human populations would precipitate the desire of the ruling political and religious elites for monumental architectural works to affirm authority, but most importantly, would spark the need for engineering works such as aqueducts, bridges, canals and roads that enabled the new social fabric to exist.

The evolution of bridge construction has followed a parallel path with the development and transitions experienced by Human societies throughout history. The expansion of early empires brought about a dissemination of engineering works around the globe. However, the slow evolution of science and technology in the centuries to follow meant that construction technology had not changed greatly by the Middle Ages. With the advent of the Renaissance history would be proppelled into the Modern Age, with the seafaring discovery voyages bringing about a global world. The new-found prosperity enabled master builders to strive for bolder designs, but it would not be until the scientific revolution of the Enlightnment that bridge engineering would break away from its past.

With the Industrial Revolution an unseen rate of technological progress pushed the boundaries of possibility to new heights. There were new scientific methods to analyse and design bridges, new materials to be used in their construction, and new machinery with which to build them. The construction of roads and railways in the 1800's was a fertile ground for the development of modern bridge engineering, with the rise of steel as the material of choice for major bridges. The progress made during the 19th century is best put in context by the evolution of main span length. When the Pont de Vieille-Brioude collapsed in1822 its 54m masonry arch span was thought to have been the World's largest for the last 300 years. The steel arch of Eiffel's Garabit Viaduct on the Clermont-Ferrand to Béziers railway had a record span of 165m when completed in 1886.

Since it was first introduced in the late 1800's steel remained the material of choice for the construction of long span bridges throughout the 20th century. The development of reinforced concrete at the turn of the century and that of prestressed concrete in postwar presented two new materials that proved to be very competitive for short and medium spans. The higher cost of steel only decks meant that these would be better suited for long spans where the added weight of concrete was detrimental.

From the 1960's onwards the development of steel-concrete composite decks again turned the tables on prestressed concrete by providing an economical alternative to for medium span ranges. By providing steel girders and a reinforced concrete deck slab with an interface connection that enables

the composite behaviour of the cross-section an efficient structural type was created. Where speed of construction with minimal traffic disruption is required composite bridges are today challenged only by precast concrete solutions.

The advances in the last 30 years in automated fabrication processes and in construction equipment have rendered composite bridges as high-quality solutions from a technological and economical perspective. Innovative designs making use of high strength steels in the flanges of hybrid girders and cross-sections with double composite action are expanding the optimal range of application of composite bridges. Today's trends of off-site construction for quality control, the constraints from existing road and rail traffic, the short programmes for delivery of major engineering works schemes, all seem to point to a greater relevance of composite bridges in the near future.

1.2. HISTORICAL BACKGROUND

With a strong tradition in the construction of steel bridges the United Kingdom was naturally among the pioneering nations were composite bridge construction was introduced. The expansion of the motorway network during the 1950's and 1960's provided the opportunity for composite bridges to be brought to the fore.

After an initial process of experimentation with the new bridge type designers grew more and more confident in its possibilities and devised designs that were ever more innovative and bold. The fast rate of innovation that steel bridge construction was experiencing in the early 1970's would suffer a serious setback due to a set of spectacular accidents with box girder bridges. The loss of public confidence together with new regulations that imposed tighter requirements on fabrication would render steel construction less competitive than before.

The process of standardisation of construction regulations launched by the European Commission led to abundant investigation on the behaviour of steel and composite structures. Contributions from practising engineers and academics from across the continent were included in new design standards: the Eurocodes. With previous shortcomings in theoretical models resolved and with the advances in computer structural analysis software of the past three decades practicing engineers have had the know-how and the means to innovate.

1.3. GENERAL OBJECTIVES

The purpose of this work is to provide an overview of the current practice and trends in the design of composite bridges in the United Kingdom. In order to achieve this, an insight into the historical context in which steel bridges appeared in Britain and their evolution until the present day provides the background that lead to the composite bridges designed and built in recent decades.

An outline of the actions and design situations prescribed by current standards as the functional requirements for which bridges are designed in the UK, together with a review of the models applicable to the analysis of bridge superstructures and commentary on the design and verification of cross-sections are intended to provide a broad view of the state-of-the-art of composite bridge design.

1.4. DISSERTATION CONTENTS

Following a brief introduction with the background and objectives of this dissertation a review of the state-of-the-art of composite bridges in the United Kingdom is presented. The next chapter will provide an overview of the standards defining the actions on bridges and an outline of methodologies for the global analysis of composite decks from the perspective of the practising engineer. An overview of the design verifications of member resistances as well as of serviceability criteria will then be addressed. A case study presentation of the preliminary design of a highway viaduct in Wales will provide justification for the choice of a composite solution as the best suited to the brief's requirements. The closing remarks present the lessons learned and main conclusions as well as possible future developments.

The contents of this dissertation are presented over five chapters.

In Chapter 2 the historical evolution of steel bridges in Britain since the Industrial Revolution to present day is described, followed by a quantitative analysis of existing road bridges in Wales to put in context composite bridges in terms of market share and span range. The types of composite decks most commonly used in the construction of bridges in the UK are then presented and their range of application discussed. The chapter closes with a commentary on the fabrication costs of plated girders and considerations for economic design.

Chapter 3 covers the global analysis of composite bridge decks. It starts by presenting an overview of the actions prescribed by the Eurocodes for the design of bridges, and proceeds to illustrate the rules for combinations of actions that define design situations for serviceability and ultimate limit states. The modifications enforced by the UK National Annexes are commented upon. An outline of the modelling approaches at the disposal of designers for the analysis of composite decks is presented, along with their strong points and limitations. To finalise, the effects of concrete cracking and shrinkage on composite structures are explained.

In Chapter 4 the design of composite cross-sections is covered in detail. The chapter begins by presenting the cross-section classification process and explaining its repercussions on the cross-section resistance. The concept of effective cross-sections is introduced. In following, the verifications of cross-section resistances for ultimate limit states are developed upon, and the resistances to bending flexure, vertical shear and longitudinal shear presented. The chapter then concludes with the presentation of the serviceability criteria that ensure adequate functioning under normal use, in the form of stress limitations and concrete crack width checks.

Chapter 5 presents a case study of the design of a highway viaduct in Wales. The definition of the highway route and the options of suitable bridge structures considered for the scheme are presented. The proposed structure for the River Seiont Viaduct is described with its span arrangement, deck cross-section and materials. The actions considered in the design of the superstructure are listed and quantified and the relevant combinations of actions defined. The global analysis approach is explained, the analysis model adopted for the structure described and the analysis results presented. Finally, cross-section verifications for ultimate limit states validating the design are presented in detail.

The dissertation concludes by summarising the lessons learned in relation to each of the subjects covered in the previous chapters and by proposing fields for future development of the work.

2 STATE-OF-THE-ART IN THE UK

2.1. HISTORICAL OVERVIEW OF STEEL BRIDGES IN BRITAIN

2.1.1. PIONEERS OF THE GEORGIAN ERA

With its birthplace in Britain, the advent of the Industrial Revolution circa 1760 was to change profoundly the way western society was organized until then. An unprecedented growth in the productive power of the economy would enable for the first time in history the improvement of living standards of the masses of ordinary people (Lucas, 2002).

It is consensual today that the First Industrial Revolution was an event that took place somewhere between 1760 and 1840. An accelerated transition from an agricultural based economy to the new manufacture based industrial economy brought about the shift from hand production methods to the use of machinery, the replacing of wood as the primary energy source by coal, as well as new chemical and iron production processes. For many historians the invention of the steam engine in 1781 by James Watt was the pivotal point of this new age.

While this statement is obviously open to dispute, the invention of the steam engine can be seen as the reaching of a critical threshold. It was at this point that the new machine (itself a product of the on-going larger process) combines and harnesses the full potential of the innovations brought about in diverse fields.

Had it not been for the insights into Thermodynamics stemming back to the Age of Enlightenment with the formulation of Boyle´s Law in 1662 or for the use of coal, which was far more efficient than wood as fuel and made new iron production processes economically viable, this new invention would not have been possible. Producing continuous rotary motion the steam engine would be placed wherever there was a water and coal supply, powering a wide range of machinery.

The use of iron in structural applications was not a novelty in itself, since master builders of the Middle Ages had already employed iron rods as ties in the construction of gothic cathedrals. The architects of the Renaissance further exploited its use, with a well-known example being the chains that sustain the thrust from the dome of St. Peter's Cathedral. Nevertheless, the use of iron as the material of choice for the main load bearing elements of a structure was still neither technically nor economically viable at that time.

Within this historical context it is telling that the first application of iron as the sole material of a bridge structure would take place in the heart of a coal mining and iron producing industrial centre - the village of Coalbrookdale in the Severn Gorge. It was in this very place that in 1709 Abraham Darby had begun to fuel a blast furnace with coke in place of charcoal, paving the way for the cheaper production of pig iron, which in turn finery forges would transform into bar iron (Landes, 1969). The

coking coal of the region contained fewer impurities than usual and produced an iron of superior quality (Fig. 2.1).



Fig. 2.1 – The Iron Rolling Mill, Adolph Von Menzel 1875 (from *Google Art Project*)

The Severn Gorge in Shropshire was a site where good deposits of coal, iron ore, limestone and clay could be easily mined, with the Severn River providing natural means of transport out to sea. While the river was a key trading route it was also a barrier to travel about the gorge. The boat traffic on the river and the steep banks meant that a bridge at the site should be of single span and provide adequate headroom for ships to pass (Cossons and Trinder, 2002).

In 1773 architect Thomas Farnolls Pritchard suggested building a bridge out of cast iron. Following a petition to Parliament for leave to construct an iron bridge in 1773 and the raising of a subscription of three to four thousand pounds in 1775, the Act to build a bridge received Royal Assent in March 1776. Construction of the bridge broke ground in November 1777 starting with the masonry abutments, with the cast iron arch ribs being lifted into place in 1779. The completed bridge opened to traffic in January 1st of 1781 with its five arch ribs spanning 30.6m across the river (Fig. 2.2) (Smith, 1979).

With the death of Thomas Farnolls Pritchard just one month after construction began, it is not clear to which extent the completed structure reflects his original design, with a foreman at the foundry being credited for drawing detailed designs of the members that were typical of carpentry joining details.



Fig. 2.2 – The Cast Iron Bridge near Coalbrookdale, painting by William Williams, 1780 (from *bbc.co.uk*)

The prominent engineers of the time quickly understood that the new material brought about extended possibilities to their works and intended to put them to use by further exploring its capabilities and understanding its behaviour. In 1795, Thomas Telford, at the time Shropshire's County Surveyor, designed a new cast iron bridge over the Severn at Buildwas to replace a medieval stone bridge. Telford's design was also of a single span arch bridge, with a 39.6m clear span at the arch springing's.

The design consisted of five main flat arches supporting the carriageway strengthened on both sides of the deck by outer arched ribs that sprang below the arch rising above the deck at the arch crown (Fig. 2.3). In Telford´s own words, this arrangement introduced "more of the principle of timber trussing than of masonry". Despite the larger span the new bridge used only 181 tonnes of iron as opposed to the 385 tonnes of its predecessor in Coalbrookedale, a clear demonstration of efficiency and evolution of design (Smiles, 1862; Skempton et al, 2002).

As is typical with the introduction of a new material, engineers will first employ it in similar fashion to previous experience. The linear elements made from iron bars resembled more closely timber structures such as the Old Walton Bridge, a 39m span timber lattice arch built in 1750 to a design by William Etheridge, than the solid elliptical masonry vaults of the day. Telford quickly envisaged new

structural and construction forms made possible by the new material, and within a decade would design radical new structures made of cast iron.

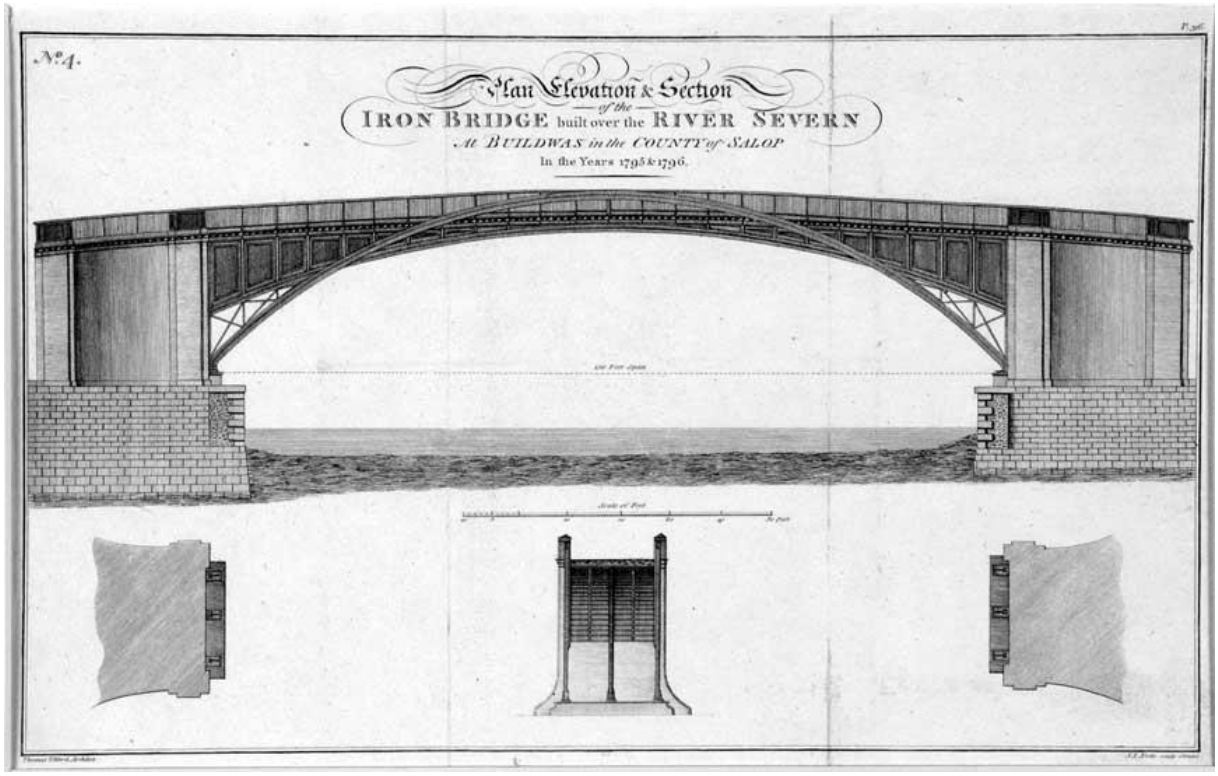


Fig. 2.3 – The Iron Bridge over the River Severn at Buildwas (from *Shrewsbury Museum Service*)

The Pontcysyllte Aqueduct in north east Wales was completed in 1805 as part of the Ellesmere Canal, having taken about ten years between design and construction. It is a 307m long aqueduct crossing the River Dee valley some 38m above the river bed. The superstructure consists of nineteen 16m spans with the deck comprising cast iron troughs over cast iron arch ribs, and is supported by eighteen hollow masonry piers (Fig. 2.4).

The cast iron troughs effectively materialized a cross section that fulfilled both structural and functional requirements, by being both a load bearing element as well as the canal itself. The troughs were made of flanged plates bolted together, with the peculiarity of being shaped as typical stone arch voussoirs, a decorative feature following the lines of the stiffening plates of the cast iron arches beneath (rcahmw, 2010).

A prolific designer, Telford would continue to explore the use of cast iron in his later works by using it in various bridge types, from the shallow arch with lattice spandrels of the Craigellachie Bridge (1814) and the Holt Fleet Bridge (1828), to the chain cables of the Conwy Suspension Bridge (1826) and the Menai Straight Suspension Bridge (1826) (Fig. 2.5).



Fig. 2.4 – The Pontcysyllte Aqueduct (from *whc.unesco.org*)

It should be noted that Telford was a self-taught engineer, with no formal training on natural sciences such as Mathematics and Physics. He may have overcome this gap with an intuitive understanding of structural behaviour, possibly influenced by his early days as a stonemason apprentice, and also by the study of reduced models as well as conducting strength tests on materials.

British engineers of the day were not deeply interested in theoretical studies and Telford himself had a particular distaste for mathematics, having never become acquainted with the elements of geometry. At the time there was a general view from engineers that problems of determining adequate strength were better addressed by means of tests. Telford's approach regarding the cables for his suspension bridges was to test his cables by submitting them to strains similar to those in the bridge itself (Timoshenko, 1953).

By the second half of the 18th century the newly developed puddling process had replaced the charcoal-fuelled finery forge process for producing wrought iron. The subsequent rolling process for consolidating wrought iron was fifteen times faster than hammering. By combining these two processes structural grade iron could now be produced at low cost (Landes, 1969). Unlike its predecessor cast iron, wrought iron is ductile and will undergo considerable elongation before tensile failure. It was this innovation that made possible the use of wrought iron cable chains and enabled Telford to design his long span suspension bridges.



Fig. 2.5 – The Menai Straight Bridge (from *wikipedia.org*)

During the 18th century scientific methods found their practical application to engineering problems as new developments required not only empirical knowledge but the ability to analyse problems rationally. It was in this context that the first engineering schools were founded and the first books on structural engineering published, with France at the forefront of developments. The contributions of Coulomb to the mechanics of elastic bodies and to the theory of retaining walls are particularly noteworthy. In 1794 a new kind of engineering school was to be born in with the founding of the École Polytechnique.

For the first time it was assumed that the various branches of engineering required the same base preparation in subjects as Mathematics, Mechanics, Physics and Chemistry. It was believed that with good training in these fundamental sciences it would not be difficult for the student to acquire special knowledge in any field of engineering. Famous names like Monge, Lagrange, Fourier and Poisson are amongst the teaching body of the school, and the likes of Cauchy, Carnot and Navier will stand out from its first pupils. It is not without irony that following a visit to England Navier would write a treatise on suspension bridges. His review of the most important existing structures and discourse on theoretical methods of analysis would be a reference on the subject for the next fifty years. Navier will also write a seminal book on the strength of materials (Timoshenko, 1953).

During the first half of the 19th century Britain had no schools equivalent to the French, with the technical level of its textbooks being much lower and the country´s engineers lacking the broad scientific education of their counterparts. However, there were still individuals whose genius allowed them to make substantial contributions even in this unfavourable context. Such was the case of Thomas Young, whose characterisation of the elasticity modulus as an intrinsic material constant in 1807 allowed for the accurate prediction of strain in an element regardless of its cross section geometry.

2.1.2. VICTORIAN RAILWAY ENGINEERING

Building on the achievements of their predecessors from the Georgian era the generation of engineers that followed would again expanded the realm of possibilities. At the turn of the 19th century the

growing production of textiles in the North West and coal mining in the North East and Yorkshire needed an alternative for the shipment of good as canal development was restricted by the Pennine mountain range. From the 1830´s onwards several new railway lines for passenger and freight were under construction to link major cities and industrial centres, requiring an array of bridges to be designed and built. In these times of euphoria two men would stand out with their innovative bridge designs: Isambard Brunel and Robert Stephenson.

Isambard Brunel was the son of renowned French engineer Marc Brunel, who had made his way to the United States and then to England in the wake of the French Revolution. Being a product of the French engineering school Marc Brunel wanted his son to have the same high-level education and encouraged him from an early age to study mathematics, engineering principles and drawing. At age fourteen is father sent Isambard to study in France, where after completing his preparation studies at Lycée Henri-IV he would be presented as candidate to none other than the École Polytechnique. Sadly, Isambard would not be allowed to enrol the prestigious school due to the fact that he was a foreign citizen but it is without doubt that these formative years moulded his future.

When in 1829 a competition was held to design a bridge spanning the Avon Gorge in Bristol Brunel was amongst the engineers to submit an entry. When called upon to make a selection from five of the submitted entries the eminent Thomas Telford rejected all and in turn proposed a design of his own. In 1831 a second competition was held for the design of a wrought iron suspension bridge, with Brunel being the winner after much controversy. Brunel´s design set the Egyptian inspired masonry abutments on the steep sides of the gorge with the deck spanning a record 214m about 76m above the river bed (Fig. 2.6). Long delays in construction due to financial difficulties and contractual disagreements meant the bridge would only be completed in 1864, five years after Brunel´s death (Andrews and Pascoe, 2008).



Fig. 2.6 – The Clifton Suspension Bridge (from *wikipedia.org*)

In 1833 Brunel was appointed chief engineer of the Great Western Railway from London to Bristol. The new railway line would showcase his engineering prowess on structures such as Paddington Station, the Ivybridge Viaduct and the Box Tunnel. Completed in 1849, the Windsor Railway Bridge on the Great Western Railway line from Slough to Windsor is a wrought iron bowstring arch structure (Fig. 2.7). With a span of 62m and a rise of just 5.4m it is a fairly shallow arch, a design that apart from the trussed bracings between the vertical hanger rods seems as contemporary today as it may have appeared bold at the time.



Fig. 2.7 – The Windsor Railway Bridge (from *wikipedia.org*)

Brunel´s final design was the Royal Albert Bridge between Plymouth and Saltash (Fig. 2.8), completed in 1859. The structure is 666.8m long comprising 19 spans, with plate girder approach spans up to 28.3m leading up to the main centre spans where two lenticular trusses span 138.7m each with a clearance of 30m to the River Tamar. The lenticular trusses form a self-anchored system, with the thrust from the upper compression chord being taken up by the pair of chains that make up the bottom tension chord. This meant that there was no transfer of large horizontal forces from the arches to the piers, a crucial characteristic since the track alignment was curved to either side of the main crossing (Binding, 1997).

By the mid 1800´s the use of plate girder bridge decks had become common practice, with the girders being built up from web and flange plates riveted together by means of angle sections. Brunel had conducted his own studies and experiments in regards to the optimal shape of girders, with interesting and original cross section designs. On occasions he used triangular shaped cells for the girder flanges and on other instances near circular sections for the compression flange alone with a flat plate tension flange. According to his son and biographer, Isambard Brunel Junior, *"The metal in the top of a girder being in compression, it was important so to dispose it that it should resist the tendency to yield sideways under the strain."* (Brunel, 1870). Scientists such as Euler had looked into the stability of compressed columns more than century earlier, but Brunel glimpsed what engineers today refer to as lateral-torsional buckling of members in flexure.

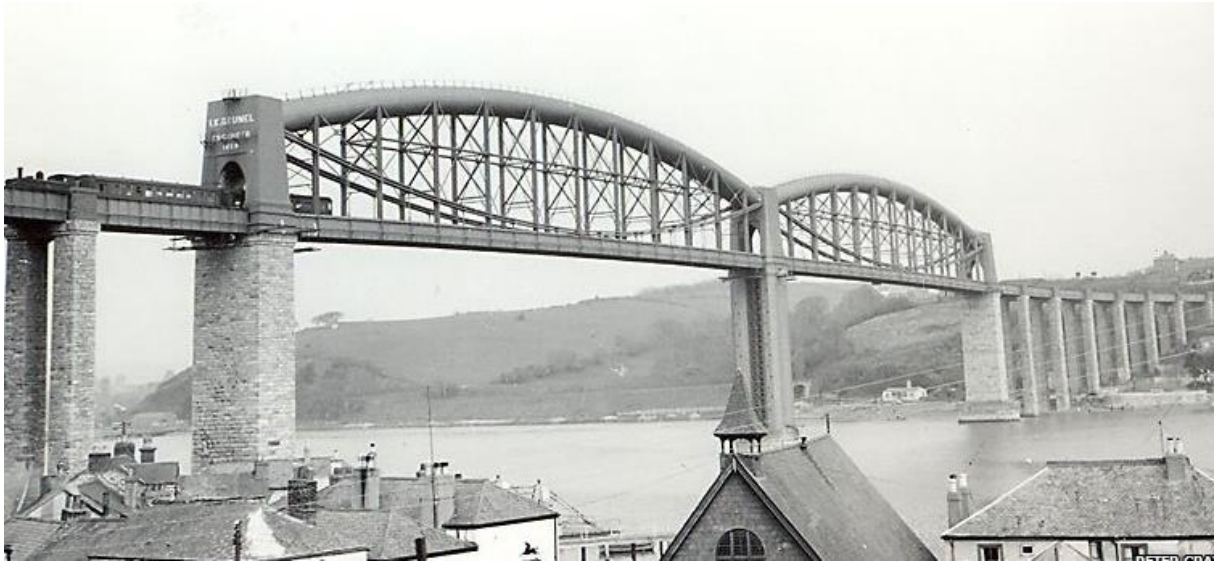


Fig. 2.8 – The Royal Albert Bridge (from *bbc.co.uk*)

Another great innovator was Robert Stephenson, the son of railway pioneer George Stephenson. His father was a renowned civil engineer, a builder of railways and just as famous as a designer of steam locomotives whose 4 feet 8½ inch rail gauge became the standard for most of the world´s railways. From an early age Robert would assist his father in his works, becoming familiar with the construction of major railway works. As early as 1821, aged only eighteen years old, Robert worked alongside his father surveying the Stockton and Darlington Railway. Having been persuaded that his son would benefit from a university education to complement his professional training George Stephenson would have his son attend an academic year at Edinburgh University (Tomlinson, 1915).

In the years to follow Robert would take part in the construction of the Canterbury & Whitstable Railway, the Liverpool & Manchester Railway and the Leicester & Swannington Railway. At age thirty he would be appointed chief engineer of London & Birmingham Railways. By 1850 Robert Stephenson had been involved in the surveying, construction and design of a third of England's railway network (Rolt, 1984). Involved as he was in the construction of new railways Robert would have the opportunity to design numerous bridges, with the works of his maturity being engineering landmarks that are in service to this very day.

The construction of the Chester & Holyhead Railway linking London to the coal port of Holyhead in the island of Anglesey presented the singular problem of a railway bridge having to span over the Anglesey Canal. Given the traffic by large size vessels the Admiralty had set the prerequisites that no scaffolding or centering that would obstruct the passage should be used and that a clearance of 30m was required along the whole span. Stephenson knew full well that Telford´s Menai Suspension Bridge could not be replicated for a railway crossing given its flexibility, and thus devised an original approach to the problem. He would propose a tubular bridge with main spans of 140m made of wrought iron, with a cross section such that trains would run through it (Fig. 2.9) (Clark, 1849).

He would call on William Fairbairn to assist him given his great experience in iron plate structures from shipbuilding works and together they would develop the concept. Fairbairn conducted extensive tests on scale models where it became evident that the compressed flange and web of the tubular cross section would need to be stiffened, which he achieved by means of a cellular structure of the flanges and vertical web stiffeners. The erection process of the bridge was also innovative. A special assembly

procedure was devised in which after the first tube was placed over the piers the adjacent tube was tilted before the riveted connection was made, so that when it was put in a horizontal position a bending moment was induced. In doing so Stephenson and Fairbairn´s intention was to achieve bending moments of similar magnitude at pier and span sections, and represents one of the earliest examples of prestressing by movement of supports. The structure would be in service for 120 years, until a fire led to its collapse in 1970.

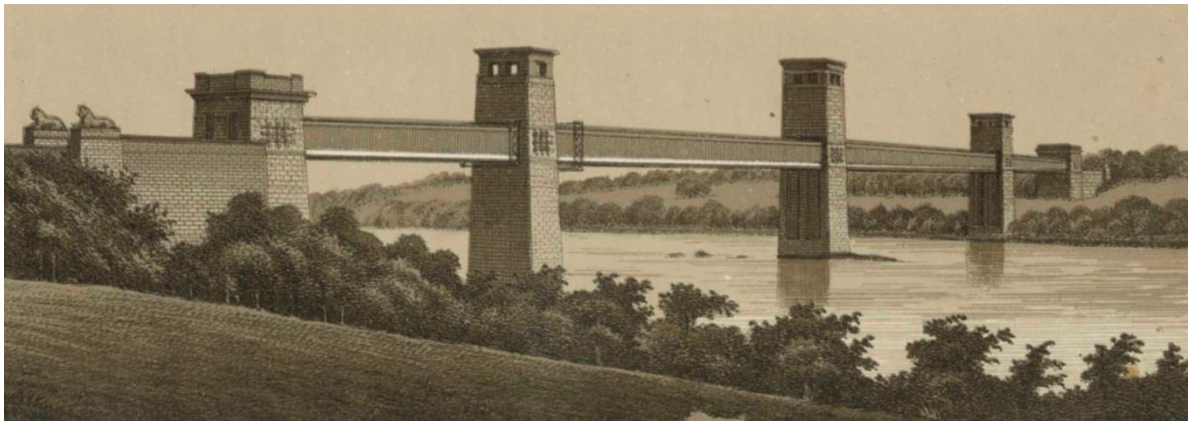


Fig. 2.9 – The Britannia Bridge (from *denbighshirearchives.wordpress.com*)

The construction process showed that not only were the designers aware of the behaviour of the tubular deck as a continuous beam, but also that it could be manipulated to achieve a more favourable state of stress. The purpose was not to replicate the condition as if the bridge had been constructed in one length and placed over the towers, since the strains over the piers would have been greater than in the spans, but rather to equalise the strains and make optimal use of the beam constant section. Again, innovation was enabled by advances in the theory of structures, in this instance the works of Navier on the bending of continuous beams which derived a method similar to the three moment equation for analysis of indeterminate structures. This was the method W. Pole used to help Stephenson select the appropriate tilt angles (Timoshenko, 1953).

The continued expansion of the railways in the second half of the 19th century would bring about several iconic structures. The engineers of the day became familiarised with advances in analysis methods and grew more confident in their understanding of structural behaviour, which in turn led to even more daring designs.

William Baker, who succeeded Robert Stephenson as chief engineer in the London & North Western Railway, designed two significant structures that are still in service: the Battersea Railway Bridge over the Thames and the Runcorn Railway Bridge over the Mersey River. The latter was thought to be the longest bridge in the world upon completion, with wrought iron lattice girders being used for its three 93m main spans (Holt, 1986). The decade would see the construction of two wrought iron arch bridges over the Thames spanning more than 50m, namely the Blackfriars Bridge and the Grosvenor Bridge.

Despite the fact that the construction of force polygons and of the funicular polygon was known since the works of Varignon in the early 18th century, they were only used in the solution of a few particular cases. The works of German engineer Karl Culmann in the field of Graphic Statics in the 1860's were of paramount importance as they presented a systematic approach easily applicable to most structural engineering problems of the day. As an engineer of the Bavarian railroads Culmann was involved in

the design of important railway structures. In 1849 he had the opportunity to visit England and the United States and see first-hand the major bridge works that were being built, and upon his return wrote an extensive study with his observations and criticism of the state-of-the-art of bridge building in these countries. When in 1855 he was called by the already prestigious Zurich Polytechnic to become professor of theory of structures he devoted great effort to the preparation of the lectures and their notes, which would form the core of his 1866 book "Graphic Statics" which influenced the following generations of engineers across Europe (Timoshenko, 1953).

2.1.3. Edwardian Engineering and the Arrival of Steel

At the same time a huge forward leap was taking place in metallurgy, with the 1856 patenting by Henry Bessemer of a new industrial process for the production of steel from molten pig iron. By oxidation with air being blown through the molten iron impurities are removed while also raising the temperature of the iron mass and keeping it molten. The new process enabled the economical production of high quality steel, with early Bessemer converters producing steel for £7 per long ton as opposed to the £50 of the cementation process they replaced. The steel produced was of unpredictable strength, a shortcoming that would be won over by the development of the open hearth furnace (Rosenberg, 1982).

In 1873 the Forth Bridge Company was created with the purpose of building a bridge across the Forth estuary taking rail traffic through the east coast of Scotland. The construction of a bridge at this location was a tremendous engineering challenge given the massive spans required, poor foundation soils and adverse weather conditions typical of the site. The project would provide the opportunity for the design and construction of the first steel bridge in Britain.

The new bridge was to be designed by Thomas Bouch but after the Tay Bridge disaster there was no public confidence on Bouch´s proposed design of a suspension bridge. Following a consultation period in which consulting engineers were invited to present proposals for the bridge a design by John Fowler and Benjamin Baker was chosen (Pannell, 1964).

At the time Fowler was already a renowned engineer, having designed in 1860 the first railway bridge over the Thames, the Grosvenor Bridge. His protégé and associate Benjamin Baker was a talented engineer who had written a book advocating the use of steel in long span bridges. Their proposal consisted of a cantilever bridge with suspended spans with a total length in excess of 2500m, with steel lattice truss approach spans of 51.2m leading up to the 210.3m outer span of the steel cantilever sections followed by the two massive 521.3m main spans (Fig. 2.10). The 521.3m main spans are divided in two 207.3m cantilevers supporting a 106.7m suspended truss span with navigational clearance of 46m.

At the time the Board of Trade regulated the use of steel in construction and restricted its maximum working stress at 5t/sq.in, which was the limit set by the Admiralty for steel plates used in shipbuilding based on a factor of safety of four applied to ultimate strength. Baker was able to obtain steel with a minimum strength of 30t/sq.in and persuaded the Board of Trade to accept a working stress of 7.5t/sq.in (Hayward, 2015). Construction of the bridge took place between 1882 and 1890, with its main spans achieving a world record that would stand for 27 years.

Having such an emblematic design to be the first steel bridge in Britain displayed to engineers and public the possibilities the new material would bring about. With the expansion of railways in Britain during the Edwardian era until the onset of the First World War, steel would be the material of choice for a many number of bridges.



Fig. 2.10 – The Forth Bridge (from *wikipedia.org*)

The last quarter of the 19th century would see great contributions to the Theory of Structures with the most remarkable being the works of Carlo Alberto Castigliano and Otto Mohr. Castigliano was able to provide logical proof that the work done by the external forces applied to an elastic body equals its strain energy, and developed a method to apply this principle to the analysis of statically indeterminate structures. In turn, German engineer Otto Mohr developed a particular application of the principle of virtual work for use in structural analysis while also developing the graphical method for stress analysis that came to be known as Mohr's circle.

In 1894, only two years after the completion of the Forth Bridge, the construction of a new bridge in London over the Thames addressing the need for a crossing that allowed access to tall-masted ships was completed: the Tower Bridge (Fig. 2.11).



Fig. 2.11 – The Tower Bridge (from *bbc.co.uk*)

The design of the bridge came from a partnership of John Wolfe Barry and Henry Marc Brunel, the second son of Isambard Brunel who had been responsible for the design of the Blackfriars Railway Bridge, the London Underground District Line, and Barry Docks. The required clearance for the navigational channel was achieved in an original manner by adopting a central 61m span bascule bridge with two 82m suspended side spans and the suspension cables anchored at the abutments and at the bridge's upper walkways. Both towers are steel structures clad in granite (Smith, 2008).

Another noteworthy design also by John Wolfe Barry is the Connel Bridge (Fig. 2.12), completed in 1903 as part of the Callander and Oban Railway. The structure is a cantilever bridge with inclined piers, resulting in a clear span of 150m with a central suspended span of 71m. When completed, the bridge was the second longest span in Britain.

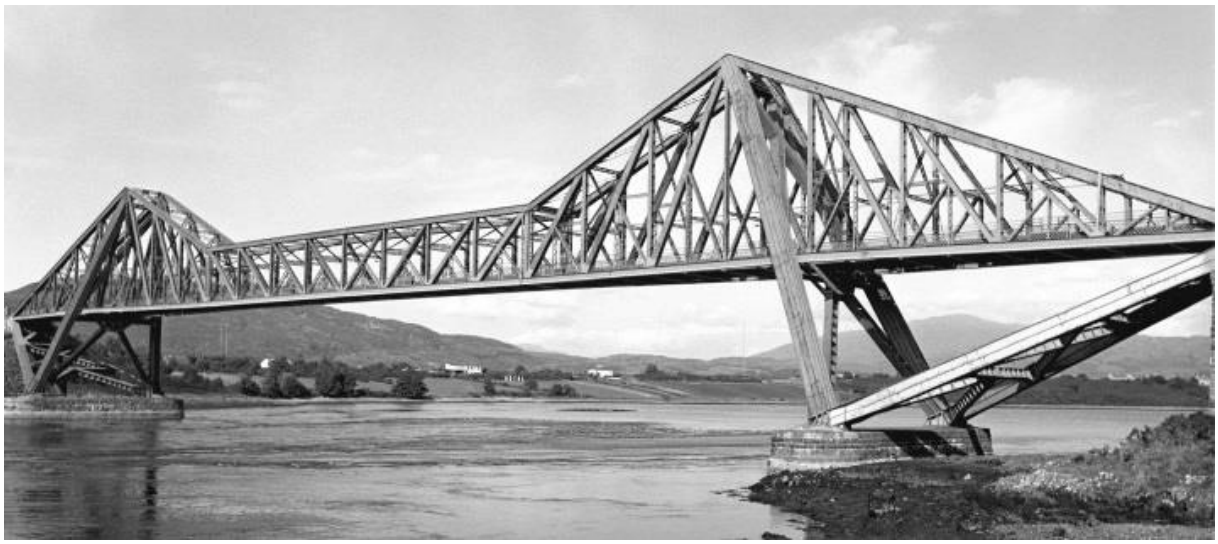


Fig. 2.12 – Connel Bridge (from *rcahms.gov.uk*)

Still in the first decade of the 20th century a notable structure was built over the river Wear in Sunderland, the Queen Alexandra Bridge (Fig. 2.13). When opened in 1909 the double-deck bridge provided access from nearby coalfields to Sunderland's south docks to both rail and road traffic. The steel truss structure comprises three 61m land spans and a main river span of 91.4m, with a navigational clearance of 25.9m. Weighing three times as much as the suspended spans of the Forth Bridge its main river span was heralded at the time as Britain's heaviest span. Since the navigational channel would be in operation throughout the construction of the bridge the construction method of the main river span would be cantilevering the deck truss from both river piers with temporary stays propping the structure.

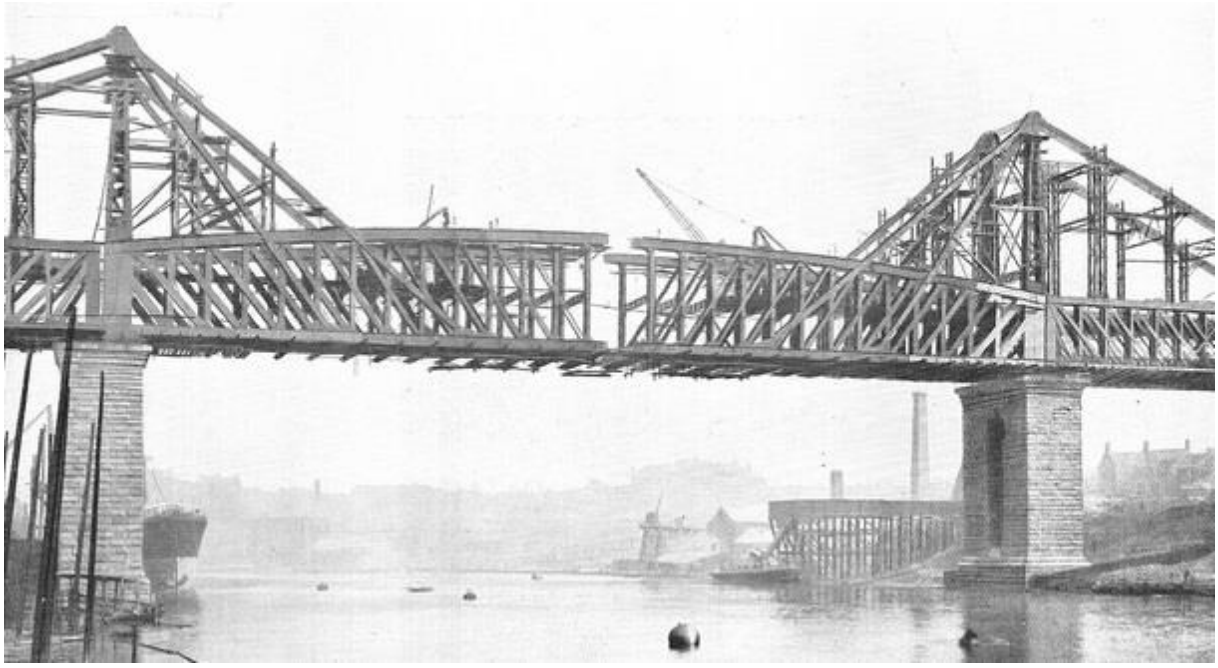


Fig. 2.13 – Queen Alexandra Bridge under construction (from *urbanglasgow.co.uk*)

2.1.4. BRIDGE ENGINEERING IN THE INTERWAR PERIOD

The Edwardian era was a time of peace and prosperity with no severe depressions. While Britain's economy was no longer the world's largest, having fallen behind the United States and Germany, it still held the lead in trade, finance and shipping (Dintenfass and Dourmois, 1999). The outbreak of World War I would end this period of stability and plenty, with Britain suffering great human loss and being forced to use its financial reserves as well as borrow large sums for the war effort.

With the end of the war a serious economic downturn followed and in 1921 a major depression hit with such impact that a decade of stagnation would follow. When the Wall Street stock market crash of 1929 triggered the Great Depression and worldwide economic recession followed the recovering British industry was again hit hard. The consequence would be yet another decade of stagnation. Turmoil again erupted in Europe in 1939 with the onset of World War II with Britain reorienting its industrial production to the war effort and again being forced to borrow large sums to sustain its military expenditure.

In light of the difficult times of the interwar period infrastructure investment was relatively low, with bridge construction being affected as a consequence. Nevertheless, among the bridges built during this period there were interesting designs. The Tyne Bridge (Fig. 2.14) in Newcastle was completed in 1928 and provided a new road crossing downstream to Robert Stephenson's High Level Bridge. The design by Mott, Hay and Anderson (precursor of engineering consultancy Mott Macdonald) consisted of a double pinned arch with a span at the springing's of 161.8m and a rise at the crown of 55m, with a 26m clearance above high water level. In the following year construction in Sunderland of another arch bridge by the same designers would be completed with the opening of the Wearmouth Bridge. Although also an arch, the choice here was for a three-pinned arch with a span of 114m and a water level clearance of 32m.



Fig. 2.14 – Tyne Bridge (from *wikipedia.org*)

Also designed by Mott, Hay and Anderson the 1934 Billingham Bridge (Fig. 2.15) at Stockton-On-Tees was an engineering and technological landmark: the world´s first fully welded bridge. A road bridge over a railway the structure was designed as a five span continuous portal frame (8.5-14.6-19.6-14.6-8.5m). The longitudinal steel girders were welded to the supporting stanchion-legs by the electric arc process, which would only become customary in bridge construction two decades later (Hayward, 2015).



Fig. 2.15 – Billingham Bridge (from *geograph.co.uk*)

In the aftermath of World War II Britain had to rebuild its economy from the loss of huge amounts of wealth, in which it was helped by the Marshall Plan put in place by the United States to fund the rebuilding of European economies at the end of the war. The program aimed to remove trade barriers, modernize industry, adopt modern business procedures and make Europe prosperous again. At the same time, the Bretton Woods Conference established a new set of rules for commercial and financial relations amongst the world major industrial states. During the following two decades, the British economy would experience a period of rapid growth, expanding rapidly and surpassing the size of its economy prior to the war.

2.1.5. Evolution of Bridges from the Post-War Era to Present Day

The 1950's marked the beginning of the motorway age in Britain with the opening of the Preston Bypass, the first 8 mile stretch of the M6, in 1958. The following year the M1 London to Birmingham motorway would be opened. As automobile ownership rose rapidly post-war and personal transport became the norm the motorway network would expand rapidly as had happened with the railways in the previous century. This required the construction of a great number of viaducts, over and underpasses, that had to allow for the characteristics of modern motorways with high-speed traffic. Bridges had now to adapt to the requirements of the road alignment rather than being its defining elements.

During the first half of the 20th century structural analysis continued to make progress in leaps and strides. In 1930 Hardy Cross published a seminal paper in which he outlined an iterative method for calculating statically indeterminate structures that enabled the swift analysis of complex structures with a high degree of static indeterminacy. The iterative nature of the method allowed the engineer to choose the degree of accuracy for the purpose at hand, and thus minimise calculation effort. The method would be used extensively until the late 1960's when computer analysis started to replace it.

The Pelham Bridge (Fig. 2.16) in Lincoln was built in 1958 to a design by WS Atkins which introduced several innovations. It was one of the earliest continuous composite bridges, with its four plate girder spans site welded with the splices tested ultrasonically. Since at the time Britain did not have a standard for composite bridges the design of the channel shear connectors was based on results of investigations conducted at the University of Illinois, USA. It was also the first bridge to make use of steel-rubber laminated bearings which are commonly used today (Hayward, 2015).



Fig. 2.16 – Pelham Bridge (from *geograph.co.uk*)

During the 1960's two landmark suspension bridges would be built in Britain: the 1964 Forth Road Bridge with a span of 1007m and the 1966 Severn Bridge with a 986m span. Both bridges were designed by Mott, Hay and Anderson with Freeman, Fox and Partners (Larena, 2004). The Forth Road Bridge was a classic design typical of American suspension bridges with vertical hangers and a deep truss stiffening girder deck. The Severn Bridge (Fig. 2.17) introduced innovative features until then seldom used in a bridge of this scale such as the aerofoil streamlined orthotropic steel box girder deck and the inclined hangers with Stockbridge tuned mass dampers (Severn River Crossing PLC, 2015).



Fig. 2.17 – First Severn Crossing (from *severnbridge.co.uk*)

Also completed in 1966 the Tay Estuary Road Bridge (Fig. 2.18) was at the time the longest river crossing in Britain, with a total length of 2250m. It was the first major box girder bridge in Britain. The superstructure consisted of a series of simply supported spans of 55m each, with two twin decks made of a single closed box section 3.65m wide by 3m deep with a 0.30m concrete slab carriageway. Only the central spans (70-76-76-70m) over the navigational channel were made continuous. In the design composite action was considered only for regions of sagging moment, with the steel box section alone catering for the resistance to hogging moments over the central piers (Larena, 2004).



Fig. 2.18 – Tay Estuary Road Bridge (from *songofthepaddle.co.uk*)

In 1968 Freeman, Fox and Partners designed the first two-tier road bridge in Britain, the Tinsley Viaduct (Fig. 2.19). The 1036m long viaduct carries the M1 motorway on the upper deck, and the A631 trunk road and services on the lower deck. The decks are comprised of twin longitudinal closed steel box sections with transverse cantilevering cross girders at 3m spacing. Construction of the two deck levels was simultaneous, with assembly of each deck in three longitudinal sections by means of overhead cranes travelling on the upper deck. The deck sections were cantilevered over the full span,

with the deflections retrieved at the pier with the new deck section being then hoisted in place (Larena, 2004).



Fig. 2.19 – Tinsley Viaduct (from *sabre-roads.co.uk*)

By this time the British steel industry was producing quality high yield steel plates and welding techniques were improving rapidly, setting the conditions to render steel and composite construction more competitive. With the publication in 1967 of *CP117 – Composite Construction in Structural Steel and Concrete, Part 2: Beams for Bridges*, the first standard specific to composite bridges, engineers were provided with rules and guidelines for the analysis and design of these structures.

One of the first modern composite bridge structures with full moment continuity over the piers was the M74 Raith Bridge (Fig 2.20) over the Clyde River, built in 1969. With a span arrangement of 43-52-43m the bridge deck is a twin trapezoidal open top box section with transverse steel cross girders supporting a reinforced concrete slab. The deck was launched from the abutments to its final position, with the concrete slab being prestressed by support movements (Larena, 2004). Deck configurations of twin box girders with cantilever cross girders had become one of the favoured forms of construction for medium spans amongst designers and contractors.



Fig. 2.20 – Raith Bridge (*James Brown,* 2010)

In the late 1960's and early 1970's four major accidents with steel box girder bridges occurred in Europe and Australia, one of them being the collapse of the Cleddau Bridge near Milford Haven in Wales. Designed by the reputable firms of Sir Alexander Gibb and Freeman, Fox and Partners, the bridge was a steel box girder with a total length of 820m split between 77m and 149m approach spans and a 214m main span (77-149-214-149-77-77-77m). As was typical of this type of bridge the cantilever construction method was used (Fig. 2.21), with each new box section being connected to the previous completed section of the deck cantilevering over the river until the next pier was reached. Failure of a pier diaphragm due to buckling resulted in the collapse of a 61m section of the deck, killing four workers (Akesson, 2008).



Fig. 2.21 – Cantilever construction of the Cleddau Bridge (*Robert Matera-Byford*, 2009)

In light of these accidents the Department of Transportation appointed an independent committee of investigation chaired by Dr Merrison, then Vice-Chancellor of Bristol University, with the mission of considering the lessons learned from the accidents and establishing rules and procedures to be adopted in the design and construction steel box bridges.

As a result of the work of the Merrison committee BE6/73 was published in October 1973. The report prescribed new design rules for steel box girder bridges and became the basis for steel box and plate girder design until the publication of BS5400. The new workmanship standards introduced restrict tolerances on the fabrication of welded stiffened thin plates, with the consequent rise in the ratio of workmanship to material costs leading to the demise of the box section in favour of plate girders (Bridle, 2009).

An interesting and innovative approach was proposed by G. Maunsell and Partners for the design of the Saltings Viaduct (Fig. 2.22) in South Wales, built in 1973. The viaduct is a continuous structure with a plan radius of 1000m with typical spans of 31.10m. The deck comprises four square closed steel boxes 1.20m deep with a reinforced concrete deck slab without any external diaphragms. Given their small size the box sections are able to do without longitudinal stiffeners, and were provided only with three steel plate internal diaphragms per span.



Fig. 2.22 – Saltings Viaduct (from *SWTRA*)

To address the evolution of the state-of the-art in bridge engineering a new set of standards came into effect in 1979 with the publication of *BS 5400: Steel, Concrete and Composite Bridges. Part 5: Design of composite bridges*. This was a modern code based on partial safety factor limit state design that addressed both serviceability criteria and ultimate resistance.

During the 1980's computer aided design became the norm within engineering consultancies. The matrix analysis of structures by the displacement method was well-established since the 1950´s and the development of the Finite Element Method would be the next step in the evolution of computer analysis of structures. During the decade the works of J. Argyris at Stuttgart University, R. Clough at U.C. Berkeley and O. Zienkiewicz at Swansea University among others would establish its theoretical background and demonstrate its application to the solution of engineering problems (Larena, 2004).

The 1978 Friarton Bridge (Fig. 2.23) on the Tay Estuary is a modern example of the closed box section girders typical of British practice designed to the limit state approach of the new regulations. The approach viaducts have typical spans of 75.0m leading up to the river crossing, where the span arrangement is 114.0-174.0-114.0m. Each of the twin decks is comprised of a single cell closed box with a depth varying from 2.70m in the approach spans to 7.50m over the river piers. The transverse crossbeams cantilevering 1.80m out from the box support the lightweight concrete slab with a total width of 10.40m. The approach spans were constructed with the aid of temporary piers, whereas in the main river span the choice was to use segmental cantilever construction. This solution proved to be more economical than a competing prestressed concrete balanced cantilever (Larena, 2004).



Fig. 2.23 – Friarton Bridge (from *geograph.org.uk*)

The opening of the Humber Bridge (Fig. 2.24) in 1981 gave Britain a world record for longest span. Designed by Freeman, Fox and Partners this suspension bridge carries the A15 motorway across the large tidal estuary at the confluence of rivers Ouse and Trent with a main span of 1410m.

This bridge introduced several innovative features. For the first time hollow reinforced concrete towers built with slipforms were adopted in a major suspension bridge, with these being 155m tall. The steel box section of the deck was streamlined following wind tunnel testing at the National Maritime Institute to investigate the structure's aerodynamic behaviour (Labrum, 1994). The adoption of inclined hangers, although not a novelty in itself (the firm had previously adopted them on the Severn Bridge), is unusual in long span suspension bridges. It offers the benefit of added stiffness to the structure with little material cost at the expense of a more complicated construction.

During the 1980´s and 90's steel fabrication became increasingly automated, which together with more potent construction equipment optimized and sped up composite construction, rendering steel and composite structures very competitive for medium spans. Twin girder and open top trapezoidal box section decks became prevalent over multi girder solutions for medium spans, with trapezoidal boxes being especially suited when dealing with curved alignments or when in urban settings due to improved aesthetical qualities.



Fig. 2.24 – Humber Bridge under construction (from *geograph.org.uk*)

The Dartford Crossing was a major engineering works scheme in the late 1980's which aimed to provide a crossing of the Thames River to the east of Greater London. A key part of the scheme is the Queen Elizabeth II Bridge (Fig. 2.25), a cable stayed structure with a main span of 450m. It was the longest cable stayed span in the world at time of completion in 1991. Designed by German engineer Helmut Homberg the bridge has a total length of 812m divided between two back spans of 181m and a central span of 450m, with a minimum clearance of 57.5m above high water level. The deck comprises composite girders supported by 56 pairs of stay cables anchored on two steel masts 84m tall, supported by concrete piers 53m high below deck (Labrum, 1994). Its world record was short-lived as in 1992 the 856m span of Michel Virlogeux's Normandy Bridge almost doubled it.



Fig. 2.25 – Queen Elizabeth II Bridge (from *sevenoakschronicle.co.uk*)

In 1997 the Hume Bridge (Fig. 2.26) in Manchester was opened. It was one of the first landmark structures designed involving the collaboration between architects and engineers, in this instance Wilkinson Eyre Architects and Arup. This approach would become customary of design competitions in the UK from the late 1990's onwards.

The bridge is a two pinned 52m span parabolic arch with a 25m rise with inclined hangers supporting a composite deck. Its main feature is the arch spanning diagonally from side to side of the deck. The arch is meant to stand as a gateway to the city as part of a larger regeneration project, so the bridge's sculptural form was as important to the client as the connection it provides.

The arch's positioning and its hanger inclinations result in large unbalanced lateral loads that generate transverse bending of the arch rib as well as additional forces on the bearings as the deck tends to twist out-of-plane. Whilst an iconic structure, its behaviour is neither ideal nor straightforward and demanded careful analysis throughout detailed design to achieve a cost effective solution (Warren, 2009).



Fig. 2.26 – Hulme Bridge (from *wikipedia.org*)

Completed in 2004 the River Usk Bridge (Fig. 2.27) in Newport, Wales, is an excellent example of a modern tied-arch bridge. With a span 187m the bridge provides a crossing for the A48 trunk road over the River Usk close to its confluence with the Severn estuary. The bridge was designed by AECOM and constructed by specialist steelwork contractor Mabey Bridge.

The deck is of the twin girder type with cantilevered cross girders, with a precast reinforced concrete slab providing the carriageway. The arch sections are rectangular boxes unstiffened longitudinally for ease of fabrication. The bridge was constructed with the aid a 1200 tonnes mobile crane and two temporary towers at approximately the third points of the span. The steel deck was first launched over

temporary piers, on top of which the temporary towers were then assembled. The arch ribs were split in three sections, with the outer sections being lifted in place by crane and the central portion raised to its final position by means of strandjacking (Fig. 2.28).

With future maintenance and whole life cycle costs being of concern, the bridge design included several innovative features. All the external steelwork surfaces were painted with a high performance epoxy based system and the box sections of the arch members were fabricated from weathering steel left unpainted internally, avoiding future maintenance painting in confined spaces. The use of full depth precast slab panels contributed to speed up construction while enabling an adequate control of cracking of the concrete slab (steelconstruction.org, 2005).



Fig. 2.27 – River Usk Bridge (from *newsteelconstruction.com*)



Fig. 2.28 – River Usk Bridge under construction (from *mabeybridge.com*)

The listed structures were deemed to be noteworthy examples of design and construction but obviously represent a small sample of the bridgeworks that have taken place in Britain in the last couple of decades.

2.2. COMPOSITE BRIDGES WITHIN ROAD NETWORKS IN WALES

The historical overview of steel bridges in Britain of the previous section accounted for the evolution in the design and construction of these structures spanning over a century since the Forth Railway Bridge. During this period steel competed firstly with masonry, then reinforced concrete, and from post-war onwards with prestressed concrete in the construction of road and rail bridges.

In order to ascertain the relative weight of steel and composite road bridge construction within the universe of bridges in service a statistical appraisal was made of existing road bridges in Wales, which is expected to be representative of the trends in Britain.

The relevant data was provided by Welsh Government and relates to bridge structures under its direct management, thus excluding bridges whose asset holders are local councils. Structures from the sample data provided of which either construction date, construction type or span length were unknown were not considered in the subsequent statistical appraisal. The total number of structures considered from the initial sample is of 934 road bridges.

2.2.1. EXISTING BRIDGE DISTRIBUTION BY CONSTRUCTION TYPE

The existing bridges were classified in six categories according to construction type, so as to evaluate their relative proportion to the total number of bridges. The following categories were defined: masonry (MA), reinforced concrete (RC), precast concrete (PC), post-tensioned concrete (PT), steel (ST) and composite (COMP).

From the distribution obtained it is clear that reinforced concrete accounts for almost half the existing bridges in service, and concrete construction as a whole (reinforced, precast and post-tensioned) represents close to 80% of the total number of bridges, with steel and composite structures making up about 12% of the total (Fig. 2.29).

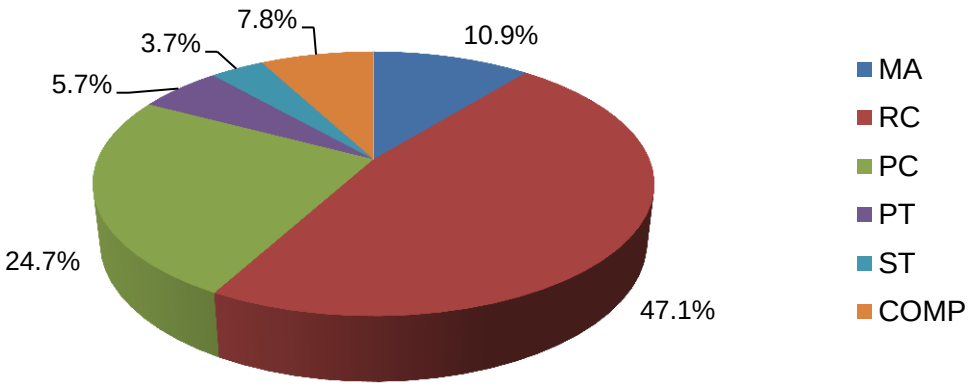


Fig. 2.29 – Existing bridge distribution by construction type

Bearing in mind that composite construction is the most recent of the construction type categories, the fact that it is accountable for close to 8% of the bridges in service is in itself significant. The masonry bridges in service are typically short span structures with over 100 years of service life. While it is impressive that they have endured the test of time and still represent 11% of the total bridges, they are

today a liability demanding inspection and maintenance programs and most are likely to be decommissioned in the future.

2.2.2. Existing Bridge Distribution by Span Range

Analysing the distribution according to span range it is evident that small spans up to 20m account for almost 73% of the total bridges, with medium spans up to 60m amounting to 26% and long spans being only marginal with 1% of the total (Fig. 2.30). The pattern found in the distribution was expected, as over and underbridges on trunk roads that make up the bulk of the existing bridge structures will typically fall within the small span range. Medium spans will be required to cross either water courses or motorways (especially where there are constraints to pier locations on central reserves) whereas long spans are costly pieces of infrastructure which are only justified when a major fixed link of a transportation network is required.

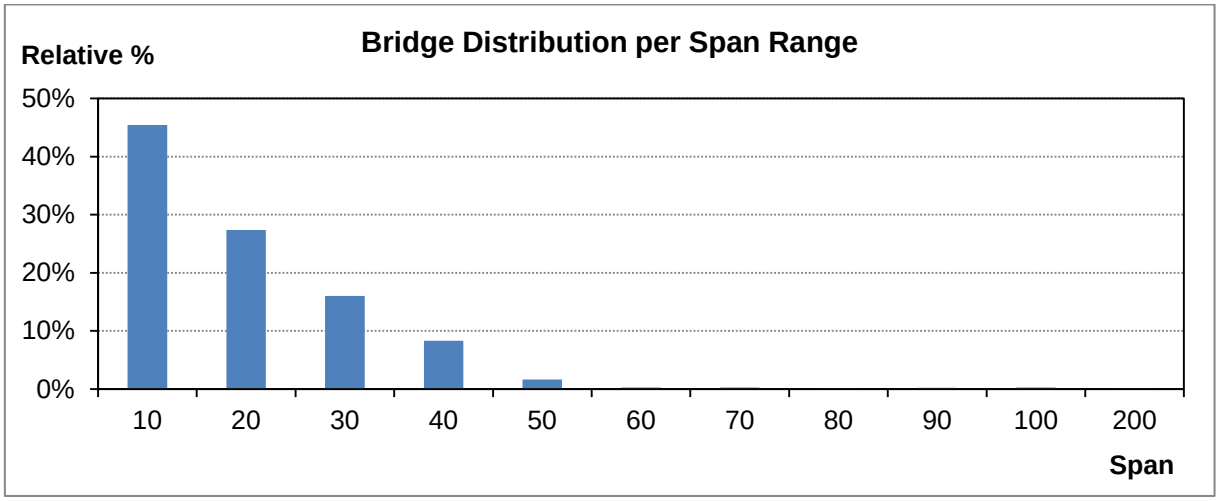


Fig. 2.30 – Existing bridge distribution by span range

2.2.3. Existing Bridge Distribution by Construction Date

The distribution of bridges according to construction date provides some interesting information, namely the fact that during the 1970's there were as many bridges built as the total number of existing bridges up to that decade. The construction rate of new bridges peaked during the 1980's and in the 1990's the number of existing bridges again doubled. New build construction gradually began losing momentum during the decade and continued until the late 2000's, after which it dropped to levels comparable only to those of the first half of the 20th century (Fig. 2.31).

The observed distribution reflects changing social and economic patterns, as well as government policies that defined British infrastructure needs and steered how these would be addressed. The 1960's marked the beginning of the motorway era in Britain, with the rise of available income allowing for growing numbers of car ownership and a preference for personal over public transport. In Wales, only in 1965 did the Government announce it had decided to construct an extension of the M4 from Tredegar (west of Newport, close to the English border) to Bridgend to expand the motorway network through South Wales. The Welsh section of the M4 Motorway would only be completed in

1993, and with the construction of the Second Severn Crossing finalized in 1996 the motorway was diverted to its present day route (ukmotorwayarchive.org, 2009).

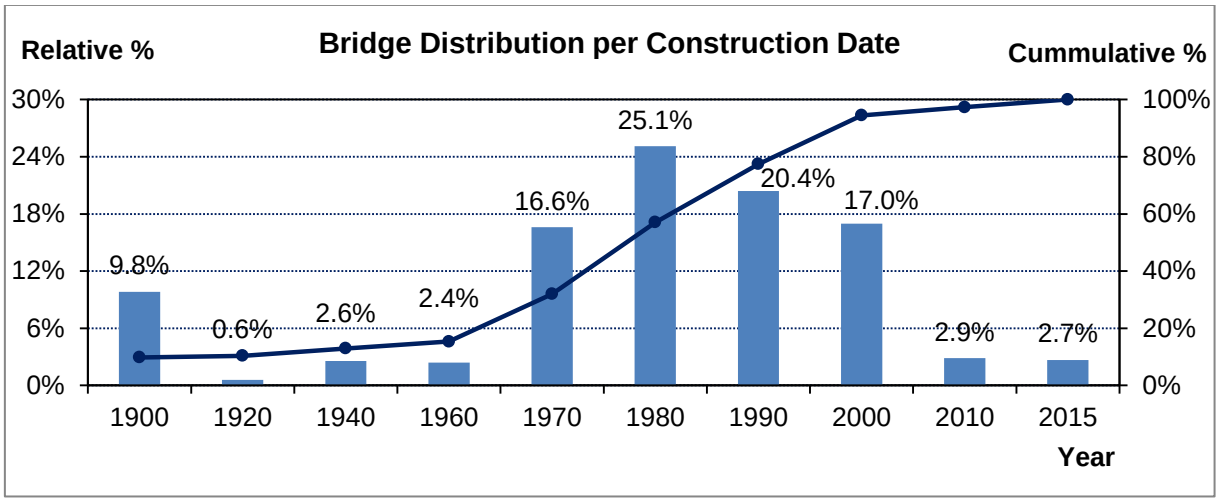


Fig. 2.31 – Existing bridge distribution by construction date

The construction rate that occurred from the 1970's through to the early 2000's reflects the growth of the Welsh motorways and trunk roads, which was expected to decrease as the needs for infrastructure were met. The abrupt drop registered in the 2010's is consequence of the construction industry as whole and public works in particular being extremely hard hit by the financial crisis of 2008, which saw funding for new schemes being halted. While the construction rate of new bridges is expected to rise in the near future, the levels of the aforementioned period are not likely to be replicated.

2.2.4. Construction Type in Relation to Span Range

By relating bridge construction type to span it becomes evident for which span range each construction type is most competitive. For spans of up to 30m reinforced concrete and precast concrete bridges are the dominant types, but from 40m onwards post-tensioned concrete and composite construction become increasingly important and are clearly dominant in the 70 to 100m span ranges (Fig. 2.32).

The observed distribution reflects the technological development and field of application of the different bridge construction types as well as that of existing construction equipment. The prevalence of precast concrete for spans up to 30m is due to the fact that precast "I" and "W" beams are particularly well suited for this range, whereas from 40 to 60m precast elements became too large and heavy and the use of launching gantries becomes economical (especially for long viaducts). For spans in excess of 60m concrete bridge construction tends to shift from span-by-span on launching gantries to balanced cantilever construction. This form of construction can be either precast segmental or cast in-situ and is usually most competitive for longer spans in the 90 to 140m range.

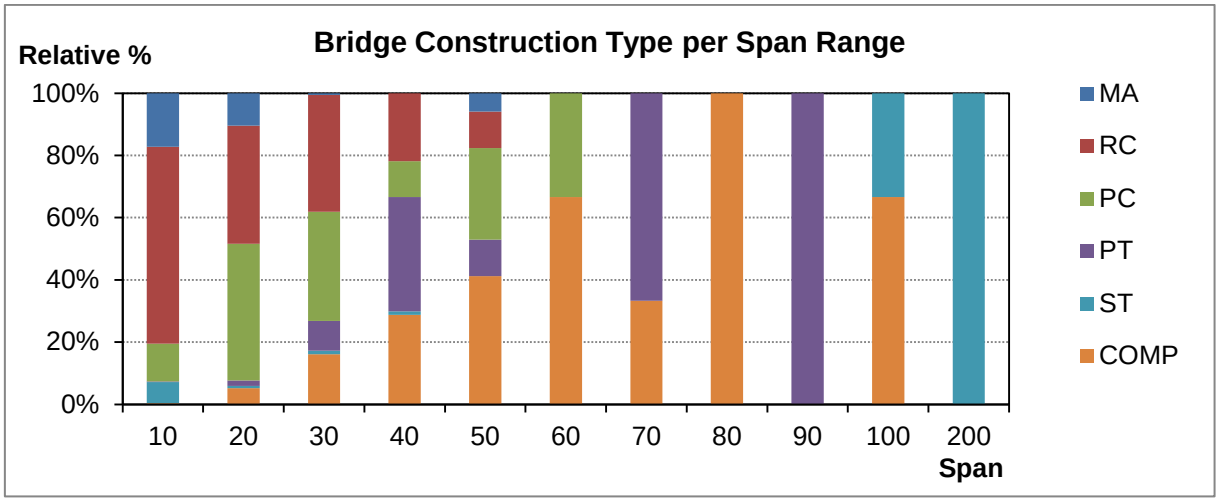


Fig. 2.32 – Bridge construction type in relation to span range

Composite construction is versatile in the sense that it is competitive over a wide span range, be it from modest spans of just 30m to long spans up to 100m in which it amounts to 44% of the built works.

For short spans composite construction offers similar benefits to precast construction (quality fabrication off site, reduced works on site, reduced construction time) but with beam elements that are lighter and can be erected with smaller cranes. The higher cost of fabricated steel girders can then be offset by lower mobilization costs for erection equipment, depending on the specific constraints of each project.

For longer spans the use of site splices and temporary propping allows the spans to be comprised of smaller fabricated elements, lighter and hence easier to transport and handle that are then assembled on site. Whereas typically mobile cranes are used for the erection of steel girders launching of the steelwork is also possible, and it is particularly well suited for long viaducts with straight or constant plan curvature.

Given the growing importance of speed of construction in meeting with short programmes and the know-how and proven track record of British steelwork contractors it is expected that composite construction will remain a dominant construction type for medium span bridges.

2.3. TYPICAL COMPOSITE BRIDGE DECKS FROM UK PRACTICE

The growing urbanisation and increasing traffic density throughout Britain from the 1980's onwards brought new restrictions and requirements for transportation systems to address Bridge designers often have to cope with curved, tapered or skewed structures with severe construction depth constraints. Since disruption to existing traffic is to be avoided, the choice of construction methods and speed of construction are likely to influence heavily the design. These trends have contributed to a shift for greater off site fabrication, which favoured the use of structural steelwork (Hayward, 2002a).

The last thirty years have brought about several technological developments which together with conjunctural factors have contributed to make steel bridge construction more competitive in relation to concrete alternatives:

- Increased automation in steel fabrication has greatly improved its efficiency;
- The use of permanent formwork systems and partial or full depth precasting of the deck slab have improved quality and speed of construction;
- Improved protection systems with fewer paint coats or dispensing them altogether by adopting weathering steel;
- The use of site welding or high strength friction grip bolting to achieve continuous splices;
- The enhanced lifting capacity of new generation mobile cranes;
- The relative stability of steel prices and wide availability of suppliers.

The typical cross-sections currently used by British designers reflect the overall tendency for simplicity of fabrication that has characterized the increased automation of the fabrication process as well as the preferences of designers and steelwork contractors stemming from a background of over fifty years of composite bridge construction.

2.3.1. MULTI GIRDER BRIDGE DECK CROSS SECTIONS

Preferably used for small and medium spans up to 30m these cross sections comprise a number of similar size plate girders at equal spacing with a constant depth reinforced concrete slab spanning transversely between the longitudinal girders (Fig. 2.33). Typical construction depth excluding surfacing is within 1/20 to 1/30 of the span and the girder transverse spacing between 2.5 to 3.5m.

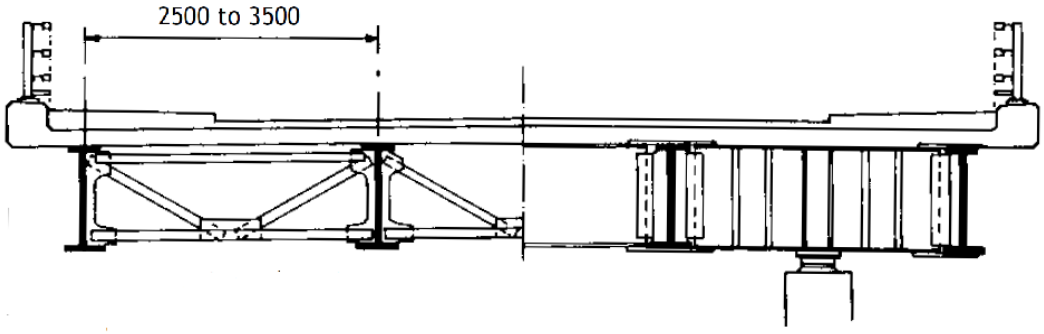


Fig. 2.33 – Multi girder deck cross section (from *Steel Detailers Manual*, Blackwell Science, 2002)

It is customary of British practice to select an even number of girders to allow for the erection of braced pairs. The required bracing for stability during construction and stabilizing of the bottom flange adjacent to the support sections in service can be provided either by channel sections pairing the longitudinal beams at about mid height or triangulated bracing systems usually made of angle sections. Similar types are adopted for support bracings at pier and abutment locations, albeit more robust for flange stability and transfer of horizontal loads to the bearings (Hayward, 2002a).

Construction of the reinforced concrete deck slab almost always makes use of permanent formwork. This is usually in the form of precast concrete planks or fiberglass reinforced panels that span transversely between girders. Consideration has to be given on how to cast the cantilever section of the slab, for which precast solutions are available or cantilever formwork can be fitted to the edge girders. The later represents added time and risks to the works on site.

Multi girder decks also offer a good solution where there are constraints to construction depth. An adequate selection of girder spacing will allow for slender sections to bridge the gap. They are also well suited when dealing with skew crossings, with intermediate support bracings arranged on the line of the skew for moderate skew angles (less than 25º) and square to the girders for large skew angles. Intermediate bracings will almost always be arranged square to the main girders regardless of skew angle (Iles, 2010).

2.3.2. TWIN GIRDER BRIDGE DECK CROSS SECTIONS

For spans in excess of 40m twin plate girder decks become prevalent over multi girder solutions. Having fewer girders to fabricate and erect, together with the savings in web material, makes this configuration very competitive for medium spans. The same trend is observed elsewhere in Europe, but some particular design aspects are characteristic of UK practice.

In continental Europe the preferred French and German practice is to design twin beam cross-sections with a single transverse cross girder bracing the longitudinal "I" beams at mid height to free up space for under-deck movable formwork for the in-situ casting of the reinforced concrete slab.

In British practice the most common arrangement for twin beam cross-sections is the ladder deck (Fig. 2.34), with cross girders at a spacing of about 3.0m levelled with the top flanges of the main girders and a 0.25-0.30m constant thickness deck slab spanning longitudinally between them (Larena, 2004). Again, preference is given to ease of fabrication by adopting permanent formwork spanning between cross girders and minimizing site works by dispensing with formwork travellers.

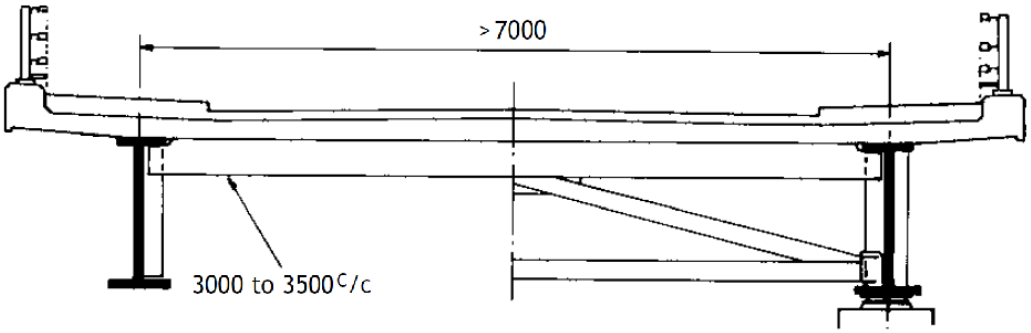


Fig. 2.34 – Twin girder deck with transverse girders cross section (from *Steel Detailers Manual*, Blackwell Science, 2002)

Construction depths within a range of 1/15 to 1/25 of the main span length and girder spacing between 5.5 to 18m are typical of these structures, with girder depth towards the deeper end of the range with increasing girder spacing for wider decks. Both the main longitudinal girders and the cross girders are provided with shear connectors and develop composite action to make efficient use of materials. For cross sections with main girders less than 10m apart it may be possible to use rolled sections for the cross girders, whereas for larger spacing plate girders are likely to be required. These are usually designed as simply supported, as the restraint to end moments by the longitudinal girders is in most cases very small.

The required bracing for stability during construction is achieved by U-frame action, with the cross girders providing restraint to the lateral torsional buckling of the main girders. With the exception of launched bridge decks temporary plan bracings between main girders are usually not required. The cross girders are almost always unbraced except for very long members.

When in service the cross girders must provide stability to the compressed bottom flanges of the main girders in hogging moment regions, which is again achieved by inverted U-frame action between cross girders and the transverse stiffeners. If the cross girder is significantly shallower than the longitudinal girders knee bracing or haunches can be adopted, but these add to fabrication costs and tend to be avoided in favour of deeper cross girders. Cantilevering of the cross girders to provide continuous support to the reinforced concrete slab is feasible, but usually not a preferred option also due to added fabrication cost. At abutment and pier supports deep cross girders are typically used to cope with larger restraint forces, but attention is made to keep these shorter than the main girders so that there is no conflict between the flanges and avoid complicated connection details (Iles, 2010).

Construction of the reinforced concrete deck slab makes use of precast concrete planks spanning longitudinally between cross girders. Where the cross girders are cantilevered, precast planks can be used over the full width of the bridge deck, otherwise cantilever formwork fitted to the main girders will need to be used.

Ladder deck type bridges deal can accommodate skew angles at intermediate supports with relative ease. Since cross girders will always be square to the main longitudinal girders at support locations one of the ends of the cross girder will coincide with a bearing stiffener whereas the other is connected to an intermediate stiffener, with the skew angle dictating an irregular spacing of the cross girders in the vicinity of the supports. At end supports usually an end trimmer girder is adopted, with trimmed cross girders of varying lengths spanning between one of the main girders and the end trimmer girder.

2.3.3. Multiple Compact Box Bridge Deck Cross Sections

Multiple box sections are suitable for medium spans with significant plan curvatures which introduce high torsional effects on the main girders or in the case of viaducts in urban settings where aesthetic criteria for improved appearance govern the design (Hayward, 2002a).

Typical span ranges for this type of bridge decks is usually between 45 and 100m, and construction depth is similar to that of plate girders with values ranging from 1/20 to 1/25 of the main span length usual for constant height box sections. A deck accommodating a dual carriageway will usually comprise three to four box sections at spacing of about 2.5 to 3.5m between outer webs of the boxes, which is compatible with constant thickness reinforced concrete slabs about 0.25m deep (Fig. 2.35). A possible alternative solution for wide carriageways is to adopt twin box girders with cross girders, with the deck slab spanning longitudinally between cross girders. Such an arrangement is not common for spans less than 100m.

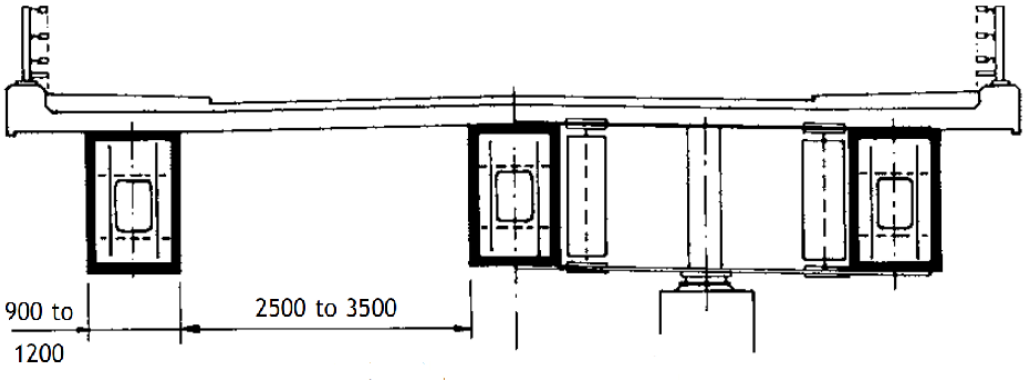


Fig. 2.35 – Multiple closed box deck cross section (from *Steel Detailers Manual*, Blackwell Science, 2002)

Despite having higher initial cost this form of construction may prove beneficial in terms of whole life cycle costs if full use is made of its advantages (Iles, 1994):

- Economic span lengths are larger than for concrete construction;
- Span long sections can be erected by mobile crane without intermediate bracing given the boxes inherent stability
- Box stability may also allow for a reduced number of bearings to be used;
- The total external area to be painted is less than that of a similar size plate girder deck, with the clean surfaces offering no water traps safeguarding against corrosion;
- Access for internal inspection and maintenance needs to be provided, and the required access routes and manhole dimensions may influence the cross section configuration.

Fabrication of box sections has not been automated to the same degree as that of plate girders and requires more man hours of assembly by traditional methods, rendering them more expensive to fabricate. Flanges and webs are made up of pre-welded stiffened plate panels, with diaphragms at regular intervals (usually not exceeding three times the section depth) required for the box section to retain its shape during fabrication. Internal welding will be required at least for diaphragms at support sections, which presents a health and safety hazard (Hayward, 2002a).

Unlike elsewhere in Europe, namely France and Germany, where this type of box section is usually made up of longitudinally stiffened plates, it is customary of UK practice for small boxes with flange widths less than 1.2m to make without longitudinal stiffeners altogether by thickening the flange plates. Again preference is given for ease of fabrication over material economy, with complicated details for internal diaphragms that must allow for longitudinal stiffeners to slot through being avoided.

2.3.4. Open Top Trapezoidal Box Bridge Deck Cross Sections

Also typical of UK practice from the 1990's onwards is the use of trapezoidal open top box sections with inclined webs. This type of solution is used often when curved alignments demand a section with high torsional stiffness or in urban viaducts for its aesthetical qualities (Hendy and Iles, 2010).

Similarly to closed compact box sections the typical span range is between 45 and 100m, with construction depth ranging from 1/20 to 1/25 of the main span length. For dual carriageway decks two boxes are usually adopted, with the resulting spacing between the webs of the boxes being about 2.5 to

3.5m enabling the choice of a constant thickness reinforced concrete deck slab, usually about 250mm deep (Fig. 2.36).

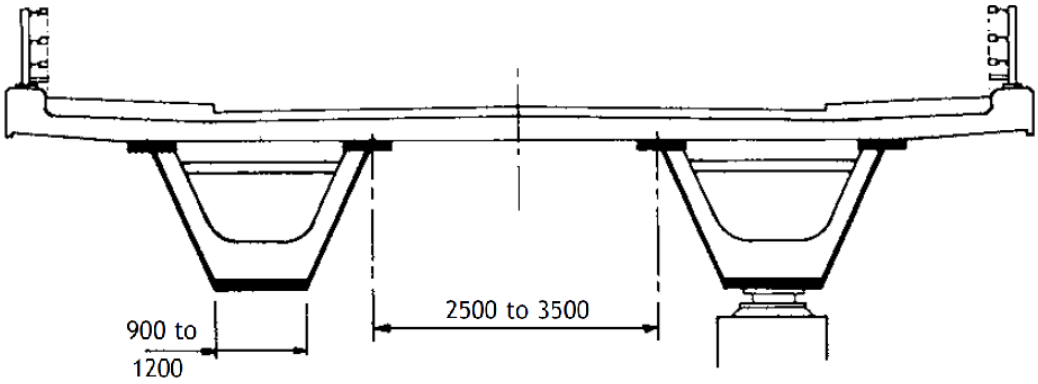


Fig. 2.36 – Open top trapezoidal box deck cross section (from *Steel Detailers Manual*, Blackwell Science, 2002)

This type of cross section presents most of the characteristics of closed box sections, but attention should be made to particular aspects. Unlike closed box sections, plan bracing to the open top is required during the construction stage to avoid excessive distortion of the cross section. This is usually provided in the form of angle section diagonals between intermediate transverse stiffeners. The adoption of inclined webs results in a wider spacing of the top flanges of the box and reduces the transverse span of the reinforced concrete deck slab. This enables the use of a lesser number of longitudinal girders by comparison with compact box sections. Inclined webs also reduce the width of the bottom flange, which is advantageous for the hogging moment regions since it leads to a lighter longitudinal stiffening of the compressed flange and allows for ease of fabrication (Fig. 2.37).



Fig. 2.37 – Open top box section with and without longitudinal stiffening (from *Guidance Notes on Best Practice in Steel Bridge Construction*, SCI, 2010)

Despite current UK practice favouring minimal stiffening and heavier plates for ease of fabrication it has been noted that the provisions of EN1993-1-5 regarding stiffened plates lead to greater resistance

than the rules from BS 5400-3, hence it is foreseeable that a shift back to thinner stiffened plates may take place in the near future (Hendy and Iles, 2010).

The trend for minimising maintenance and whole life cycle costs has led to box sections being preferably fabricated from weathering steel whenever possible, thus avoiding the need for protective painting of the inside of the box even when the outside is painted for aesthetics reasons.

2.4. ECONOMY AND FABRICATION COSTS

In present day the fabrication of steel plate girders has become a very streamlined process for experienced steel fabricators. The fabrication of an I-girder bridge can be divided into 4 general steps:

- Supply to the workshop of steel plates from the steel plant;
- Fabrication of the plate girders and partial assembly in the workshop;
- Transport to the construction site from the workshop;
- Final assembly on site prior to erection of the structure.

For an inexperienced designer it may be tempting to assume that economy of design will be the result of minimising steel weight, but experienced steel fabricators will be aware that this is often not the case. Whereas the built-up of a plate girder is nowadays an automated process and the required continuous long weld runs are usually performed by submerged arc welding in "T and I" machines, the fitting and welding of transverse stiffeners is still done manually. The handling required for turning the girder for welding on the opposite side also remains one of the most time consuming parts of the work.

The data in Table 2.1 shows the typical distribution of the required work hours and added steel weight for each step of the workshop fabrication process of an I-girder bridge. The disproportionate amount of time required by the transverse stiffeners (31%) is evident when compared to the total hours required for the cutting, butt-welding and built-up of the plate girder (51%).

Table 2.1 - Typical distribution of work hours to girder weight for UK steel fabrication.

Steps of the Fabrication Process	Time Consumption (% of total work hours)	Steel Weight (% of total girder weight)
Fabrication of the Plate Girders		
• Cutting of plate elements	27%	-
• Butt welding	13%	-
• Built-up of the plate girder	11%	85%
• Transverse stiffeners	31%	6%
• Headed stud connectors	4%	-
• Dispatch	2%	-
Fabrication of the cross bracing	6%	6%
Miscellaneous / Others	6%	3%

When the minimal additional weight that transverse stiffeners represent is also taken into consideration the added cost of stiffening is shown to be even very high indeed. The required work hours per weight unit to fit and weld the transverse stiffeners are close to ten-fold when compared to that of the built-up of the plate girder.

Due to the high unit cost that stiffening represents the choice is often made in current practice to design girders with thicker web plates and increase transverse stiffener spacing in order to reduce its weight on the total cost. An exception is made in the case of twin-girder bridges with transverse girders, where transverse stiffeners are provided at the connection of each cross girder with the main girders. In this instance, since transverse stiffeners are present at close spacings it is logical to optimise the web plate thickness to the practicable minimum.

3
GLOBAL ANALYSIS OF COMPOSITE DECKS

3.1. OVERVIEW OF DESIGN ACTIONS

The analysis of a bridge deck requires two fundamental components:a model of the structure replicating its geometry and stiffness, and the actions the effects of which the bridge must withstand. Some actions are well defined and quantifiable with little uncertainty, such as the dead and superimposed loads, while others can only be assessed with a stochastic approach and quantified based on likelyhood of occurrence, as is the case of wind, temperature and traffic actions.

In accordance with EN1990 §4.1.1 actions are classified by their variation in time, with distinction made between:

- Permanent actions (G), such as the self-weight of the structure, road surfacing or fixed equipment;
- Prestressing actions (P), either by controlled forces or deformations imposed on the structure;
- Variable actions (Q), like wind loads, temperature ranges and traffic loads;
- Accidental actions (A), such as earthquakes and vehicle impact.

It is defined in §4.1.2 that an action must be represented by its characteristic value, which can either be a mean value, an upper or lower bound value, or a nominal value. In the case of permanent actions such as the self-weight of a bridge deck, where its variability may be neglected, the action should be represented by a mean value. As for variable actions, their characteristic value represents either an upper bound or a lower bound value, relating to an intended probability of either not being exceeded or of not being achieved.

For the quantification of design actions the prescriptions of "Eurocode 1: Actions on structures" and its UK National Annexes will need to be adhered to. The relevant parts of Eurocode 1 to be used in defining appropriate characteristic values of actions for the design of bridges in the UK are:

- BS EN1991-1-1 "Eurocode 1: Actions on structures – Part 1-1: General actions - Densities, self-weight, imposed loads for buildings", for the definition of dead loads from the self-weight of the structure and superimposed loads acounting for the weight of non-structural but permanent elements;
- BS EN1991-1-4 "Eurocode 1: Actions on structures – Part 1-4: General actions – Wind actions", for the quantification of forces applied to the structure by wind;
- BS EN1991-1-5 "Eurocode 1: Actions on structures – Part 1-5: General actions – Thermal actions", for the definition of uniform temperature components and vertical temperature components sustained by the structure;

- BS EN1991-1-7 "Eurocode 1: Actions on structures – Part 1-7: General actions – Accidental actions", for the forces to consider due to impacts to either the substructure or superstructure from road vehicles travelling on carriageways going under the structure;
- BS EN1991-2 "Eurocode 1: Actions on structures – Part 2: Traffic loads on bridges", for the load models to apply to the superstructure to represent the effects of motorway traffic.

The action effects arising from the bridge's self-weight together with the thermal actions and traffic actions are likely to govern the design of the deck. Wind and accidental actions are usually of relevance mostly in the design of bracing elements of the deck and substructure elements such as columns and foundations. Since the aim of this dissertation is to provide an overview on the analysis and design of composite plate girder bridge decks, the effects of wind and accidental actions will not be developed further.

3.1.1. Dead Loads – Self-Weight of Structure

The characteristic values of the dead loads from the steel and concrete of which the bridge deck is comprised are obtained from the nominal cross sectional area of the steel plate girders and reinforced concrete slab and their respective mean unit masses, as stated in EN1990 §4.2.1.

In accordance with Table A.1 of EN1991-1-1 the nominal density for normal weight concrete is 24.0kN/m^3, increased by 1N/m^3 for normal percentages of reinforcing steel. The nominal density of steel is given in Table A.4 as ranging from 77.0 to 78.5kN/m^3, with the lower bound value of 77.0kN/m^3 generally being assumed for structural steelwork.

Elements that make up the deck such as transverse stiffeners and intermediate bracings are often not included in analysis. They are usually considered as a uniformly distributed load with an intensity of about 5% of the plate girder weight.

For continuous multi-girder bridge decks with span to depth ratios ranging from 20 to 30 and transverse girder spacing between 2.5 to 3.5m the average structural steelwork consumption lies typically between 85-110kg/m^2 for short spans of about 20m, increasing gradually to 145-180kg/m^2 for 40m spans, and in the region of 220-260kg/m^2 for spans above 60m (Hayward, 2002b).

Twin girder decks of the ladder deck type with similar span to depth ratios and longitudinal girder spacing between 6.0 to 18.0m can be expected to yield an average steelwork consumption of 150kg/m^2 for modest spans up to 30m increasing to about 215-240kg/m^2 for 60m spans (Vayas, 2014). Typically ladder decks are most economical in comparison to multi-girder decks at the high end of the spectrum, when both the main girder spacing and span are maximized.

Semi-empirical formulae can be found in specialist literature for obtaining an initial estimate of structural steel consumption for twin girder and ladder deck superstructures with good agreement. In the case of multi girder bridge decks, where the number of plate girders used for a given deck width is also a variable, these empirical expressions often lack consistency.

An estimate of the steel consumption for ladder decks can be obtained by the following expression (Vayas, 2014):

$$G = 65 + 0.9 \cdot L_{eq}^{1.2} \cdot \left(1.43 - \frac{b_c}{30}\right) + 0.22 \cdot L_{eq} + 2 \cdot b_c \quad \left[kg/m^2\right] \tag{3.1}$$

Where

L_{eq} - is the reference span length.

$L_{eq} = 1.4 \cdot L$ for simply supported spans

$L_{eq} = (2 \cdot L_i + L_{i+1})/3, L_i > L_{i+1}$ for continuous spans

b_c - is the total deck width.

3.1.2. Superimposed Dead Loads - Self-Weight of Non-Structural Elements

The superimposed dead loads on the bridge deck account for the weight of the non-structural elements that are a permanent part of the deck cross-section (Fig. 3.1) and provide a carriageway suited for the requirements of modern highway traffic. Typically the superimposed dead loads will consist of:

- A surfacing layer with a minimum depth of approximately 100mm;
- A waterproofing membrane layer;
- Fill to verges and/or footways and cyclepaths;
- Vehicle restraint systems on central reserves and edges of the carriageway;
- Parapets along on the outer edges of the deck.

Any utilities carried by the bridge deck such as water and gas mains are also considered to be superimposed dead loads.

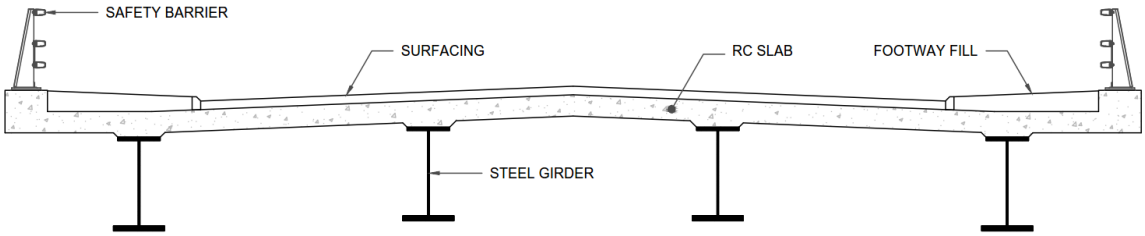


Fig. 3.1 – Typical cross section of a single carriageway road bridge.

The quantification of superimposed loads is based on their nominal dimensions and mean unit masses as for the dead loads of structural elements, with nominal densities of typical bridge deck materials given on Table A.6 of EN1991-1-1. The mean density of hot rolled asphalt is given as 23.0kN/m^3.

Additional provisions for bridges are given in EN1991-1-1 §5.2.3 addressing the variability of self-weight of non-structural elements, with additional guidance in Table NA.1 of the UK National Annex regarding the deviation to consider from the nominal values:

- For the self-weight of waterproofing, surfacing and other coatings, a deviation of ±40% if a post-execution coating is included in the nominal value and between +55% and -40% if not, as per §5.2.3(3);
- For the self-weight of cables, pipes and service ducts, a deviation of ±20%, as per §5.2.3(4);
- For the self-weight of other elements such as safety barriers, parapets and other bridge furniture the characteristic values should be taken as equal to the nominal value, as per §5.2.3(5).

3.1.3. THERMAL ACTIONS – TEMPERATURE DIFFERENCE COMPONENTS

The consideration of the effects of temperature differences are of importance for composite bridges, in particular when cooling of the reinforced concrete deck slab takes place relative to the steel girders, in which instance they will add to the effects of shrinkage (Rueda, 2009).

Two approaches are given in EN1991-1-5 §6.1.4 for dealing with the effects of temperature difference components, with a vertical linear component being proposed in Approach 1 and a non-linear component in Approach 2. However, in accordance with §NA.2.8 of the UK National Annex in general Approach 1 should not be used, with the vertical temperature components with non-linear effects of Approach 2 being adhered to.

Temperature difference profiles for composite decks are given in Fig. 6.2b of §6.1.4.2, with both a heating and a cooling profile being provided for a normal (Fig. 3.2) and a simplified (Fig. 3.3) calculation procedure. It is noted that the simplified procedure gives an upper bound of the thermal effects.

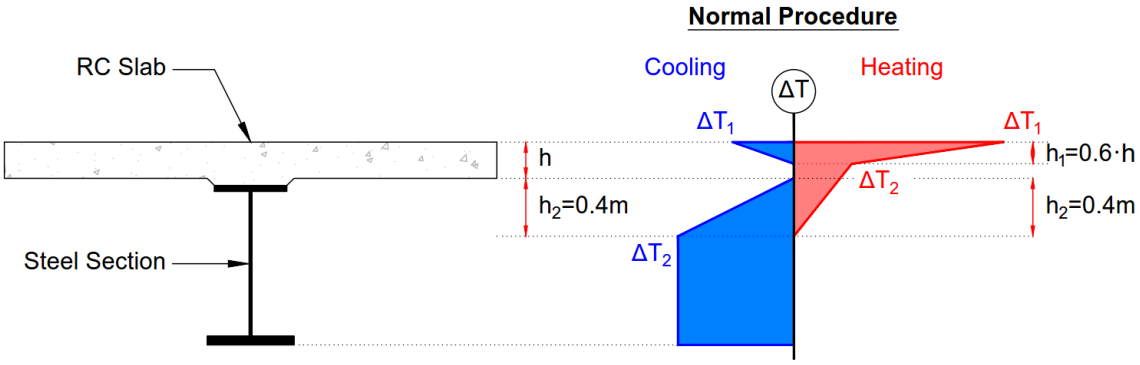


Fig. 3.2 – Normal procedure for the definition of the temperature difference component.

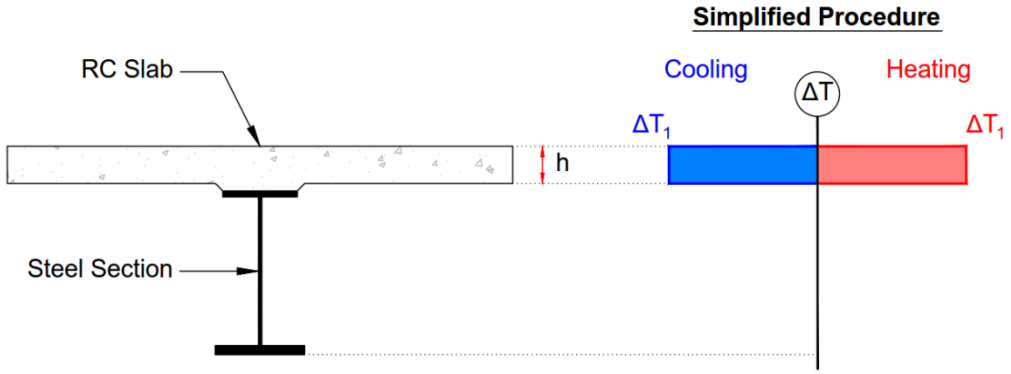


Fig. 3.3 – Simplified procedure for the definition of the temperature difference component.

If the simplified procedure is followed the effects of the temperature difference components are assimilated to those of a temperature difference due to heating or cooling of the concrete slab in relation to the steel girders of $\Delta T_1 = \pm 10^{\circ}C$.

While the proposed simplified procedure is of greater ease of application and is generally adopted in current design practice comment should be made in regards to the adoption of equal absolute values for both positive and negative temperature ranges. Heating of the deck by direct solar radiation can produce a large temperature gradient between the warmer concrete slab and the shaded steel girders which remain at ambient temperature. Conversely, cooling of the deck by snow or other atmospheric weather effects is unlikely to result in a lower temperature of the concrete slab than that of the steel girders due to the concrete's inherent thermal mass. In fact, this is corroborated by the normal procedure cooling temperature profile, where the steel section is assigned a lower temperature than the deck slab (Rueda, 2009).

3.1.4. ROAD TRAFFIC ACTIONS ON BRIDGES

3.1.4.1. Models of Road Traffic Actions

The load models applicable to bridges representing road traffic consisting of cars, lorries and special vehicles that give rise to vertical and horizontal forces to be considered for persistent and transient design situations are the subject of Section 4 of EN1991-2. Therein the following models for road traffic loads are defined:

- Models LM1 to LM4 of vertical loads for ultimate and serviceability limit state verification except fatigue;
- Models of horizontal braking, acceleration and centrifugal forces;
- Models FLM1 to FLM5 of vertical loads for fatigue verification;
- Models for accidental design situations such as collisions from vehicles either under or on the bridge;
- Actions on pedestrian parapets;
- Models for vertical and horizontal loads on abutments and walls adjacent to bridges.

As for the models for vertical loads given in Section 4 to be considered in the analysis and design of bridge decks, these consist of:

- Model LM1, which is a general model comprised of a uniform distributed load together with concentrated loads from a tandem system;
- Model LM2, consisting of a single axle with two wheels intended for the local verification of short structural members;
- Model LM3, where sets of special vehicles are used to account for the effects of Special Types General Order vehicles and Special Order vehicles;
- Model LM4, representing the effects of crowd loading on bridge decks.

The general load model LM1 provided by the code does not describe operational loads, but rather has been calibrated such that their effects represent those of actual traffic in European countries in the year 2000. In the definition of road traffic actions characteristic values were adopted with a probability of exceedence of 5% in 50 years. This corresponds to a return period of 1000 years and the intention was to limit the probability of any irreversible limit state to be exceeded during the reference period (Calgaro, 2010).

The main load model applicable to all bridges is model LM1, with the special vehicles to consider in model LM3 defined by the National Annexes and specified individually for each project by the relevant authority in accordance with road route requirements.

3.1.4.2. Division of the Carriageway and Load Application

For the application of the road traffic load models the basic concept is the division of the carriageway into a number of notional lanes, which are a function of the carriageway width *w*. The carriageway width *w* should be taken as the distance between the inner limits of vehicle restraints or between kerbs, if present (Fig. 3.4). In EN1991-2 §4.2.3(1) a minimum height of 100mm for a kerb to be taken into account is proposed, but the UK National Annex sets a minimum of 75mm for a kerb defining a carriageway in §NA.2.10. When the carriageway width is divided in two parts separated by a physical barrier, distinction needs to be made to whether a temporary or permanent restraint system is used. If a temporary restraint system is used, then *w* should be taken as the whole of the carriageway including the central reservation. Otherwise, when a permanent restraint system is in place, then a value for *w* should be considered for each separate part.

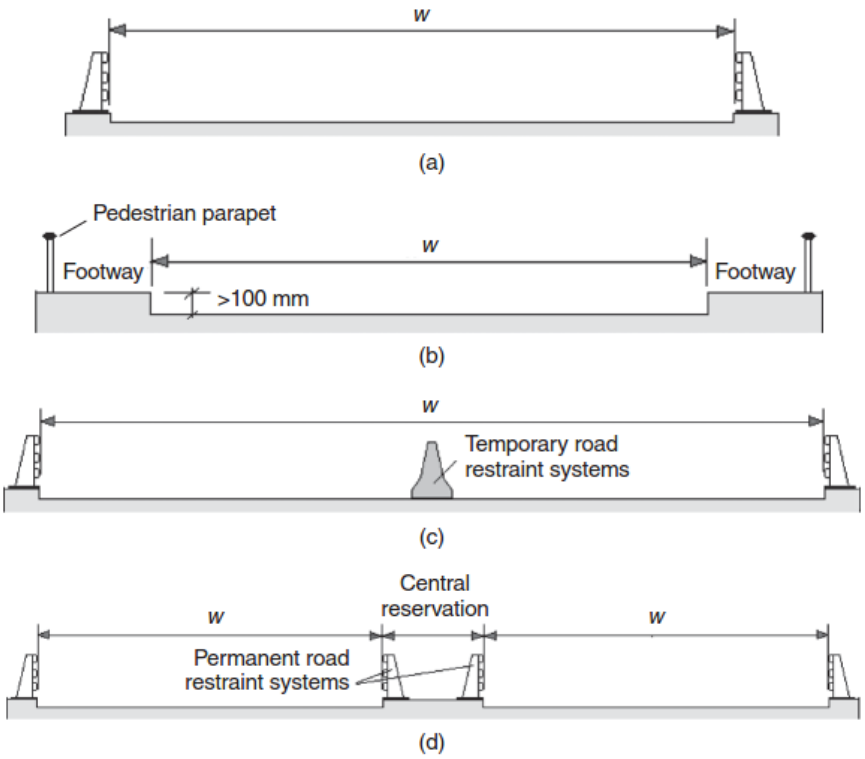


Fig. 3.4 – Examples of carriageway widths *w* to consider (from *Designers Guide to Eurocode 1*, Thomas Telford, 2010)

According to §4.2.3 the full carriageway width *w* is to be divided in the greatest possible integer number of notional lanes n_l with a notional lane width w_l each as per Table 4.1 of EN1991-2. It is noted that the customary lane width is 3.0m except for carriageway widths *w* between 5.4 and 6.0m where the notional lane width w_l is taken as half the carriageway width. As a result of the carriageway

being divided in an integer number of notional lanes of fixed width, there will usually be a remaining width equal to difference of the carriageway width and the sum of the widths of all notional lanes.

Table 3.1 - Number and width notional lanes

Carriageway width, w	Number of notional lanes, n_l	Width of a notional lane, w_l	Width of the remaining area
$w < 5.4$m	$n_l = 1$	3.0m	$w - 3.0$m
5.4m $< w <$ 6.0m	$n_l = 2$	$\frac{w}{2}$	0
6.0m $\leq w$	$n_l = \text{int}\left(\frac{w}{3}\right)$	3.0m	$w - 3 \times n_l$

The principles and rules for the location and numbering of notional lanes for design are given in §4.2.4, as follows:

- Location of the lanes should not be related to their numbering,
- The number of lanes, their location, and numbering, to be taken into account for each verification should be chosen so that the effects obtained are the most adverse;
- For fatigue verifications the lane numbering should be selected based on the traffic expected in normal conditions;
- For each verification, the lane giving the most unfavorable effect is numbered as Lane 1, the second most unfavorable Lane 2, and likewise for all the lanes of the carriageway;
- When a carriageway is comprised of two separate parts on a single bridge deck only one numbering should be used for the whole carriageway;
- Otherwise, when a carriageway consists of two separate parts on two independent decks, then separate numbering should be used for each deck.

It should be noted that with the exception of fatigue verifications the notional lanes and their numbering do not correspond to any actual physical lanes on the carriageway. The numbering of the notional lanes is such as to yield the most adverse effect on the element of the deck under consideration. Both the lane positions and their numbering are interchangeable (Fig. 3.5, Fig.3.6).

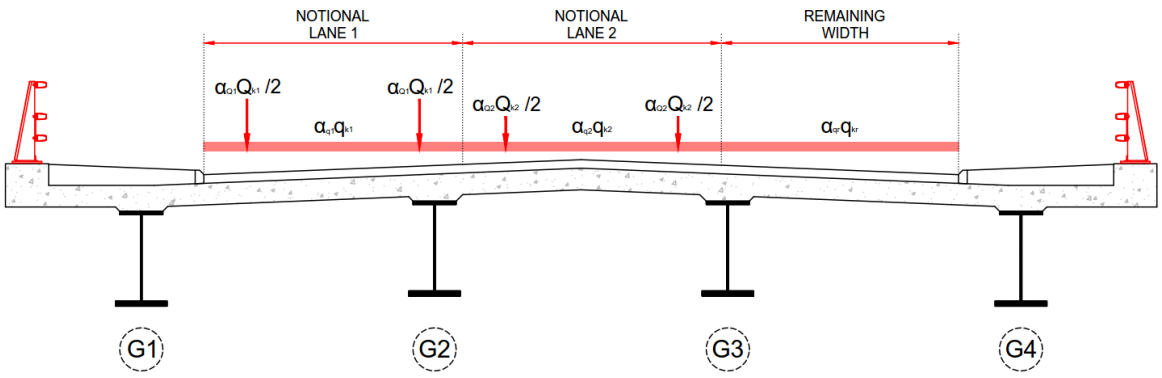


Fig. 3.5 – Possible notional lane definition for worst effects from LM1 on girder G1.

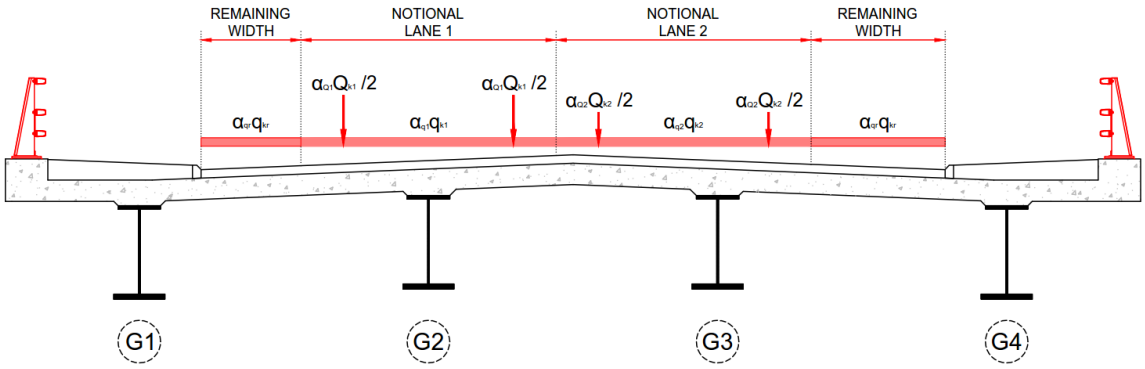


Fig. 3.6 – Possible notional lane definition for worst effects from LM1 on girder G2.

With their transverse position in the carriageway defined, the load models will need be applied longitudinally to yield the most adverse effect for each of the verifications required. It is often the case in the design of bridge decks that different load positions relate to maximum effects for bending and shear.

3.1.4.3. Load Model 1

As previously stated, LM1 is the main load model applicable to all bridges, and it is intended to cover flowing, congested or traffic jam situations with a high percentage of heavy good vehicles, with allowance for dynamic effects. It comprises a uniformly distributed load system q_k together with tandem systems that consist of double-axle concentrated loads Q_k whose characteristic values are given in §4.3.2.

These characteristic values are to be combined with adjustment factors α specified in the National Annexes that reflect the expected traffic and different route classes. The UK National Annex sets the values for adjustment factors to be considered in Table NA.1.

Table 3.2 - Load Model 1 characteristic values and UK National Annex adjustment factors.

Notional Lane Location	UDL System q_{ik} (kN/m^2)	Adjustment Factor α_{qi}	Tandem System TS, Q_{ik} (kN)	Adjustment Factor, α_{Qi}
Lane 1	9.0	$\alpha_{q1} = 0.61$	300	$\alpha_{Q1} = 1.0$
Lane 2	2.5	$\alpha_{q2} = 2.2$	200	$\alpha_{Q2} = 1.0$
Lane 3	2.5	$\alpha_{q3} = 2.2$	100	$\alpha_{Q3} = 1.0$
Other Lanes	2.5	$\alpha_{qn} = 2.2$	0	-
Remaining Area	2.5	$\alpha_{qr} = 2.2$	0	-

The loads from the uniformly distributed system and the tandem system should be applied to each notional lane and to the remaining area (Fig. 3.7) in observation of the following rules:

- Only one tandem system should be accounted per notional lane;
- Only complete tandem systems should be considered;
- For the assessment of global effects each tandem system should be considered as travelling along lane centrelines;
- Each axle of the tandem system accounts for two identical wheel loads $0.5\alpha_Q Q_k$;
- The contact area of each wheel is a 0.4m square;
- The remaining area is loaded only with the uniformly distributed system.

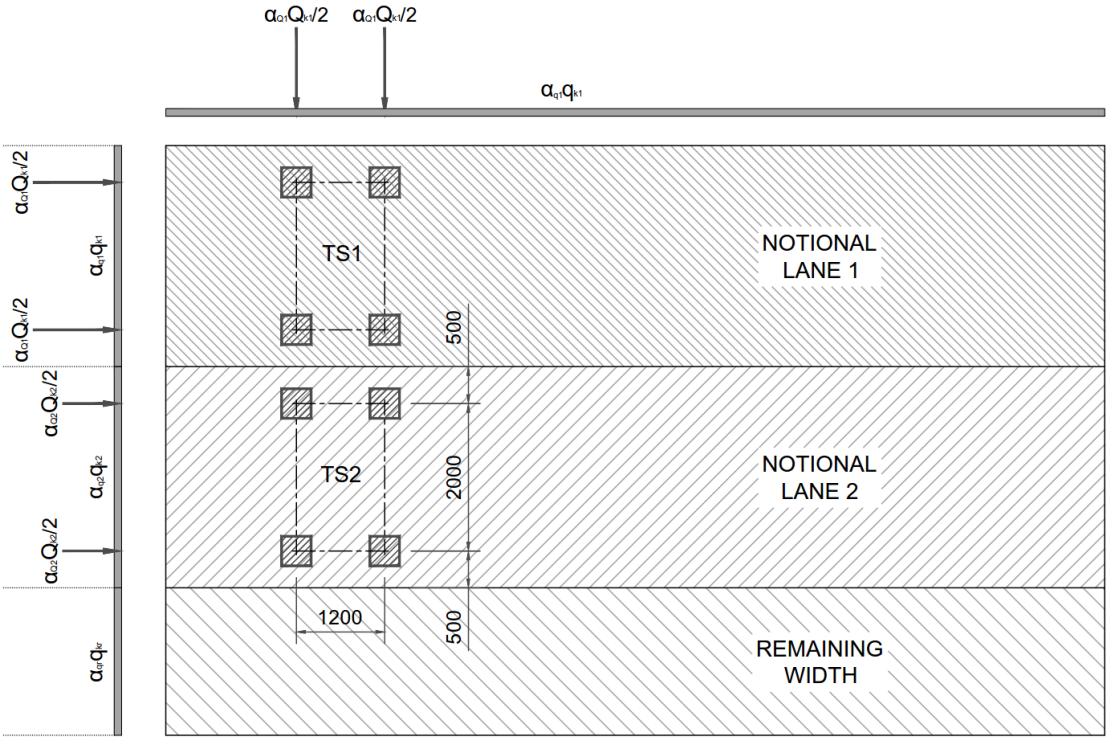


Fig. 3.7 – Longitudinal and plan application of Load Model LM1 as per UKNA of EN1990.

It is noted that no modification is made to the tandem system axle loads, with a maximum of three notional lanes loaded with a single tandem system per lane. It should be bourne in mind that only complete tandem systems should be taken into account, depending on whether its global effects are favorable or unfavorable (Calgaro, 2010).

As for the uniform distributed system, the proposed adjustment factors α_{qi} render this loading uniform for all notional lanes and remaining area, with a single value of 5.5kN/m^2. Since the uniformly distributed loads should be applied only to the unfavorable areas of the influence surface for the effect and member under consideration, these can be applied to widths lesser than that of a notional lane, and hence using a single value for its intensity allows for ease of application of the load model (Calgaro, 2010).

While LM 1 was defined and calibrated so that it is applicable to both general and local verifications, the application rules differ slightly in regards to the assessment of global or local effects. Whereas for the quantification of global effects the tandem systems travel centered in the notional lanes, for local

verifications these can be placed eccentrically within the lane. Also, tandem systems applied to neighbouring lanes are allowed to come closer to within 0.5m of wheel centrelines.

3.1.4.4. Load Model 2

In order to account for local effects of various types of vehicles not covered by the main model EN1991-2 provides an additional model in §4.3.3 suited for the verification of short structural members. Load Model 2 is comprised of a single axle load $\beta_Q Q_{ak}$ equal to 400kN, which includes the effects of dynamic amplification. The load is equally distributed by the two wheels, with the contact surface of each wheel load taken as a rectangle of 0.35m in lenght by a 0.60m width (Fig. 3.8).

The UK National Annex makes no change to the adjustment factor β_Q, which is to be taken as equal to α_{Q1}.The contact surface of each wheel load is altered by §NA.2.15 to a square of sides 0.40m, which is identical to the contact area of the wheels of the tandem systems in Load Model 1.

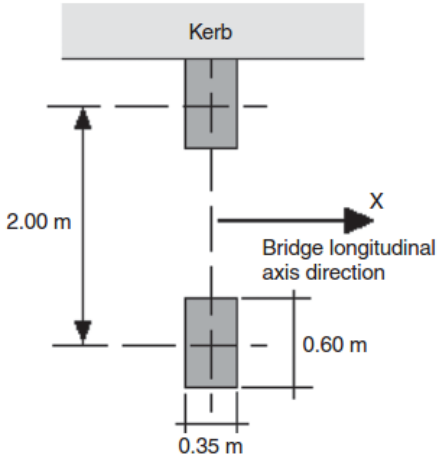


Fig. 3.8 – Load Model LM2 consider (from *Designers Guide to Eurocode 1*, Thomas Telford, 2010)

The purpose of this load model is to correct the effects of Load Model 1 for short influence lines in the assessment of load effects for short structural members (Calgaro, 2010). While usually not relevant for the calculation of the global effects on main longitudinal girders it can be the governing live load on short spanning elements such as the reinforced concrete deck slab spanning between cross girders.

3.1.4.5. Load Model 3

In order to account for the effects of exceptional loads sets of special vehicles are defined in the UK National Annex to EN1991-2. The relevant vehicles to be considered in the design of a given structure are to be defined individually for each project in accordance with client requirements.

The definition of the vehicle models to consider and their conditions of use are given in §NA.2.16. It is noted in this clause that the proposed load models do not describe actual vehicles, but rather have been calibrated so that the effects of the nominal axle weights multiplied by a dynamic amplification factor represent the effects that could actually be induced by vehicles in accordance with the Special Types General Order (STGO's) and Special Order (SO) Regulations.

To simulate the vertical effects of STGO vehicles with nominal axle weights not exceeding 16.5 tonnes three SV model vehicles with two wheel axle configurations are given in §NA.2.16.1: SV80, SV100 and SV196. Their basic axle loads, plan and axle configuration, as well as wheel contact area are shown in Fig. NA.1 of EN1991-2 (Fig. 3.9).

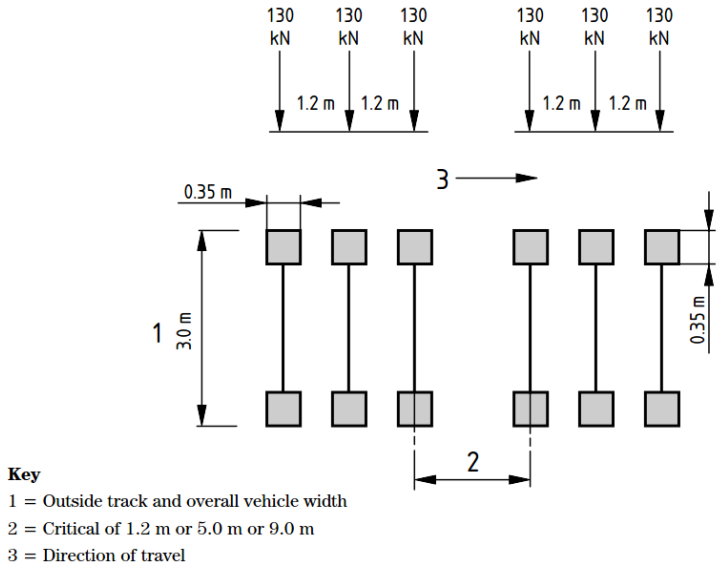


Fig. 3.9 – Configuration of SV80 vehicle (from *UK National Annex to EN 1991-2:2003*, BSI, 2008)

For the vertical effects of Special Order vehicles with maximum total trailer weights up to 600 tonnes four models are given in §NA.2.16.2: SOV-250, SOV-350, SOV-450 and SOV-600. The typical longitudinal configuration of the SOV vehicles consisting of trailer units with two tractors and two bogies can be seen in Fig. NA.2 of EN1991-2 (Fig. 3.10), with the lateral wheel arrangements for the trailer axles of all SOV's shown in Fig. NA.3.

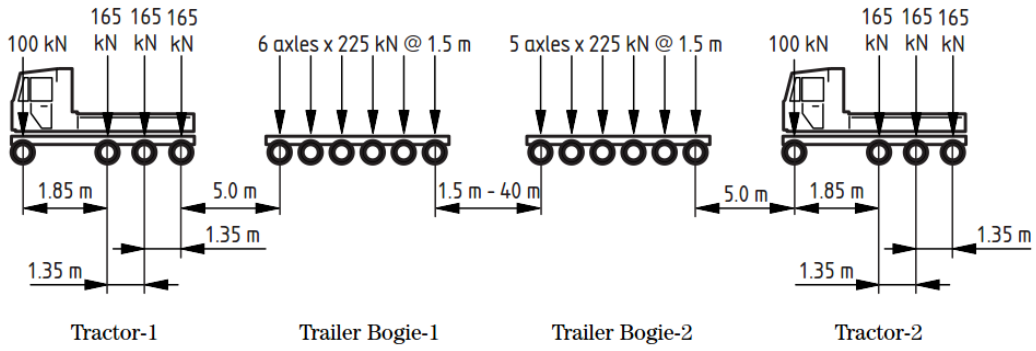


Fig. 3.10 – Configuration of SOV-250 vehicle (from *UK National Annex to EN 1991-2:2003*, BSI, 2008)

The dynamic amplification factors to be applied to the axle loads of both SV and SOV vehicles to determine their total load effects are dependent on the basic axle loads, and are listed in Table NA.2 given in §NA.2.16.3.

Consideration must be given to the simultaneous application of the LM 3 vehicles representing the exceptional load with normal traffic represented by LM 1, with rules for their combined application given in §NA.2.16.4 as follows:

- Only a single SV or SOV vehicle should be considered on any one deck at any time;
- The accompanying Load Model 1 should be considered at the frequent values (Ψ_1=0.75), and applied to each notional lane and the remaining area of the carriageway.

Like any other live load, the SV and SOV vehicles should be positioned longitudinally and transversely according to the influence surface so as to obtain the most adverse effect for any particular verification of a member of the structure. The vehicle can be placed either wholly within a notional lane or straddling over adjacent notional lanes, but with its side always paralel to the kerb lines. Only complete vehicles must be considered and be applied only when their global effects are adverse.

The SV and SOV vehicles are considered to displace the LM 1 loading on the notional lanes in which they are positioned. Hence no loading should be applied within a 5.0m distance of the outermost axles of the SV or SOV vehicle considered. When the vehicles lay partially within a notional lane two scenarios present themselves depending on whether or not the distance from the vehicle's side to the edge of the notional lane is less than 2.5m. In the first instance no loading is to be applied within the 5.0m distance of the SV or SOV vehicle axles, whereas for edge distances greater than 2.5m, then the uniformly distributed system of LM 1 should be applied over the remaining width of the notional lane

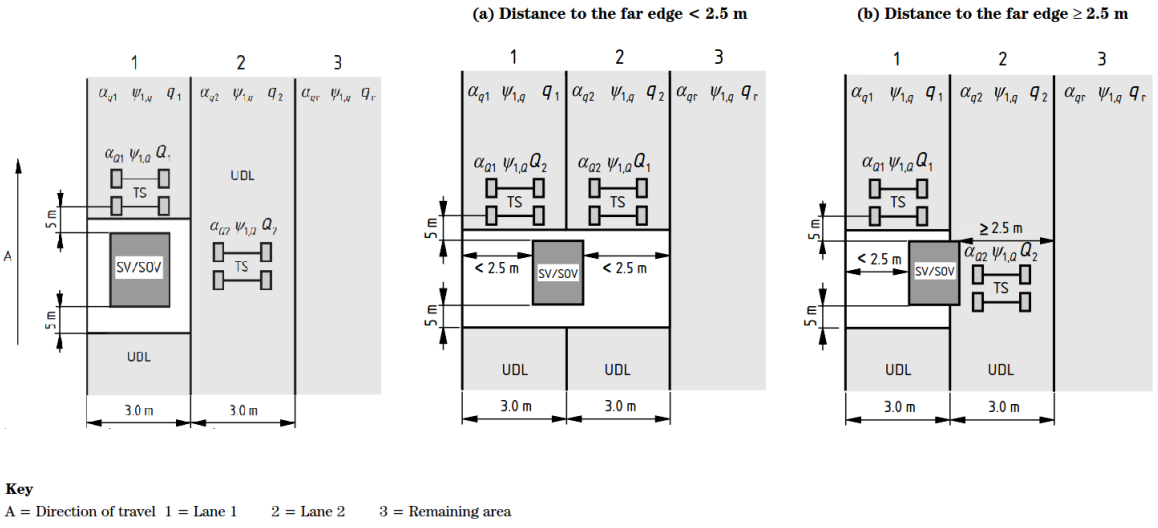


Fig. 3.11 – Application of SV or SOV vehicle with Load Model 1 (from *UK National Annex to EN 1991-2:2003*, BSI, 2008)

3.1.4.6. Load Model 4

In instances where crowd loading is deemed to be of relevance or is specified by the client, the provisions of EN1991-2 §4.3.5 should be adhered to. This load model reflects the effects of a moving crowd and includes uncorrelated dynamic amplification, being assimilated to a uniform distributed load of 5.0kN/m^2 (Calgaro, 2010).

Since the model represents the effects of a crowd it should be applied to the whole width of the bridge deck with central reservations included where relevant, and not just the carriageway width as for other traffic loads. This model is intended to address the use of bridges in urban areas as venues for cultural and sporting events. It is equivalent to the intensity of the uniform load corresponding to the physical maximum weight imposed by six to seven persons per square metre. As for all live loads, this model is to be applied to the relevant parts of the influence surface so as to obtain the most adverse effects.

3.1.4.7. Loading on Footways and Cycletracks

Load models applicable to footways, cycle tracks and footbridges are given in Section 5 of EN1991-2 for the determination of the effects due to pedestrian and cycle traffic. Three mutually exclusive load models are defined in §5.3.2, consisting of a uniformly distributed load q_{fk}, a concentrated load Q_{fwk}, and a load representing service vehicles Q_{serv}.

For road bridges that also provide for footways and cycle tracks only the uniformly distributed load q_{fk} need be considered in accordance with the prescriptions of §5.1(2), with all other variables actions being intended for consideration in footbridges only. The characteristic value of the uniformly distributed load q_{fk} is defined as 5.0kN/m^2.

3.1.4.8. Groups of Traffic Loads

In accordance with §4.5.1 the vertical and horizontal traffic loads together with pedestrian loads on footways and cycletracks should be grouped to take into account their simultaneous application to a bridge deck, and considered as a single multi-component characteristic action. The load groups thus defined are mutually exclusive and should be used as characteristic actions for combination with non-traffic loads.

The UK National Annex provides the definition of the traffic load groups to be considered in Table NA.3 of §NA.2.21. Other representative values of the multi-component action are given in §4.5.2 regarding frequent values to be used for checking serviceability criteria.

Only three load groups are proposed: gr1a, gr1b and gr3. The load groups include vertical forces only, with group gr1a being comprised of Load Model 1, group gr1b of Load Model 2, and gr3 of the footway and cycle track uniformly distributed load, with all of the above traffic loads taken at frequent values.

The aim of defining load groups as single multi-component characteristic actions is to limit the number of potential permutations to be investigated, and thus avoid the need to consider an unreasonably large number of combinations of actions in the design.

Table 3.3 - Characteristic values of the multi-component action of group traffic loads.

Load Type		Carriageway						Footway
		Vertical Forces				Horizontal Forces		Vertical
Reference		§4.3.2	§4.3.3	Annex A	§4.3.5	§4.4.1	§4.4.2	§5.3.2.1
Load System		LM1	LM2	LM3	LM4	Braking	Centrifugal	UDL
Load Groups	gr1a	Charact.						0.6 Char.
	gr1b		Charact.					
	gr2	Frequent				Charact.	Charact.	
	gr3							Charact.
	gr4				Charact.			Charact.
	gr5	Frequent		Charact.				
	gr6			Charact.		Charact.	Charact.	

3.2. COMBINATIONS OF ACTIONS FOR ROAD BRIDGES

3.2.1. LIMIT STATE DESIGN TO THE PARTIAL FACTOR METHOD

The design of bridge structures to the Eurocodes is based on the principles of limit state design, which makes a distinction between two categories of limit states: ultimate limit states and serviceability limit states. A generic outline of the principles governing limit state design is given in Section 3 of EN1990.

In accordance with EN1990 §3.1 each limit state to be considered must relate to a design situation, which can be of a persistent, transient or accidental nature. The design situations are to be chosen specifically to take into account the particular circumstances under which a structure is to fulfill its functions. The different types of design situations are classified in §3.2 as:

- Persistent design situations, regarding conditions of normal use over the service life of the structure;
- Transient design situations, referring to temporary conditions occuring during construction or repair of the structure;
- Accidental design situations, taking into account the structure's exposure to exceptional conditions such as vehicle impact;
- Seismic design situations.

Ultimate limit states are described as limit states that concern the safety of people and/or of the structure itself. In broad terms this is to be understood as limit states which were they surpassed would result in a partial or total collapse of the structure, which could occur by means of loss of stability or a rupture failure of any part of the structure. Serviceability limit states are of a different nature, being concerned with the functioning of the structure under its normal conditions of use, especially in regards to the comfort of users and the appearance of the construction works, expressed here as allowable deflections and control of cracking.

The application of the Eurocodes philosophy of partial safety factor limit state design requires partial safety factors to be applied to both the effects of actions and the material resistances, and that in all relevant design situations considered no limit state is exceeded where the design values of actions

outweigh the design resistances or the performance criteria of the limit state being verified. The basic rules for the combination of actions to be considered in the verification of both ultimate and serviceability limit states are given in Section 6 of EN1990, with the UK National Annex setting national parameters where applicable.

3.2.2. ULTIMATE LIMIT STATE COMBINATIONS

There are several ultimate limit states that must be considered when designing a structure, depending on its type, intended purpose, construction method, and site conditions, among others. Limit states such as equilibrium (EQU), internal failure of the structure (STR), failure or excessive deformation of the foundation ground (GEO), fatigue failure (FAT), buoyancy or uplift by water pressure (UPL), heave and piping caused by hydraulic gradients (HYD), should all be considered where relevant.

For ultimate limit state verifications the following inequality must be observed:

$$E_d < R_d \tag{3.2}$$

Where

E_d - design value of the effects of actions

R_d - design value of the corresponding resistances

In regards to the design of a bridge deck the relevant limit state to consider is the internal failure of its structural members (STR), governed by the strength and stiffness of the structural components. When considering this limit state it must be verified that the effects of actions do not exceed the corresponding design material resistances defined in the relevant parts of the Eurocodes, which for composite bridges are EN1992, EN1993 and EN1994.

According to EN1990 §6.4.3 for each critical loadcase the design values of the effects of actions should be determined by combining the values of actions considered to occur simultaneously. Each combination shall include the design value of the leading variable action together with the most onerous combination of accompanying variable actions.

The general form for combinations of actions regarding persistent or transient design situations, acidental design situations, and seismic design situations are given in §6.4.3.2 to §6.4.3.4, and are expressed as follows:

For persistent or transient design situations,

$$\sum_{j\geq 1} \gamma_{G,j} \cdot G_{k,j} \quad "+" \quad \gamma_P \cdot P \quad "+" \quad \gamma_{Q,1} \cdot Q_{k,1} \quad "+" \quad \sum_{i>1} \gamma_{Q,i} \cdot \psi_{0,i} \cdot Q_{k,i} \tag{3.3}$$

For accidental design situations,

$$\sum_{j\geq 1} G_{k,j} \quad "+" \quad P \quad "+" \quad A_d \quad "+" \quad (\psi_{1,1} \text{ or } \psi_{2,1}) \cdot Q_{k,1} \quad "+" \quad \sum_{i>1} \psi_{2,i} \cdot Q_{k,i} \tag{3.4}$$

For seismic design situations,

$$\sum_{j\geq 1} G_{k,j} \quad "+" \quad P \quad "+" \quad A_{Ed} \quad "+" \quad \sum_{i\geq 1} \psi_{2,i} \cdot Q_{k,i} \tag{3.5}$$

Where

"+" - implies “to be combined with”

Σ - implies “the combined effect of”

G_k - is the characteristic value of the permanent actions

P - is the characteristic value of a prestressing action

$Q_{k,1}$ - is the characteristic value of the leading variable action

$Q_{k,i}$ - are the characteristic values of the accompanying variable actions

A_d - is the design value of the accidental action

A_{Ed} - is the design value of the seismic action

$\gamma_G, \gamma_P, \gamma_Q$ - are partial factors for permanent, prestressing and variable actions

ψ_0, ψ_1, ψ_2 - are combination factors for variable actions

The UK National Annex provides additional notes on the combination rules for road bridges in §NA.2.3.3. Attention is draw to the fact that while the rules for combining special vehicles (SV’s and SOV’s of LM 3) with normal traffic are explained in the UK National Annex to EN1991-2 the values of the ψ and γ factors to consider are given in the National Annex to EN1990. Reference is also made to the consideration of snow loading, which can generally be disregarded in the UK, which is also the case of combinations of wind and thermal actions except for special cases where they will be determined for the individual project.

3.2.3. SERVICEABILITY LIMIT STATE COMBINATIONS

The limitation of deflections, the control of crack widths, and the check of stress limitations in conditions of normal use of the structure are among the serviceability limit states to be considered. The serviceability criteria must be defined in relation tho the requirements of the relevant parts of the Eurocodes, with EN1992 setting criteria for crack widths and EN1993 together with EN1994 prescribing steel stress limits. The verification of limit states concerning deformation and vibration of road bridges after completion is seldom required, with EN1990 §2.4.2 recommending these criteria to

be defined where relevant. For the assessment of deformation recommendation can be found in specialist literature for the frequent combination of actions to be used (Calgaro, 2010).

For serviceability limit state verifications the following inequality must be observed:

$$E_d < C_d \tag{3.6}$$

Where

E_d - design value of the actions or their effects

C_d - design value of the limiting serviceability criterion

In accordance with §6.5.3 the combinations of actions to be taken into account should be appropriate for the serviceability criteria under verification. Similarly as for ultimate limit state combinations actions considered to occur simultaneously are combined together, with each combination including leading and accompanying variable actions. The general form of the combinations is as follows:

For characteristic combinations,

$$\sum_{j\geq 1} G_{k,j} \quad "+" \quad P \quad "+" \quad Q_{k,1} \quad "+" \quad \sum_{i>1} \psi_{0,i} \cdot Q_{k,i} \tag{3.7}$$

For frequent combinations,

$$\sum_{j\geq 1} G_{k,j} \quad "+" \quad P \quad "+" \quad \psi_{1,1} \cdot Q_{k,1} \quad "+" \quad \sum_{i>1} \psi_{2,i} \cdot Q_{k,i} \tag{3.8}$$

For quasi permanent combinations,

$$\sum_{j\geq 1} G_{k,j} \quad "+" \quad P \quad "+" \quad \sum_{i\geq 1} \psi_{2,i} \cdot Q_{k,i} \tag{3.9}$$

Where

"+" - implies “to be combined with”

Σ - implies “the combined effect of”

G_k - is the characteristic value of the permanent actions

P - is the characteristic value of a prestressing action

$Q_{k,1}$ - is the characteristic value of the leading variable action

$Q_{k,j}$ - are the characteristic values of the accompanying variable actions

ψ_0, ψ_1, ψ_2 - are the combination, frequent and quasi-permanent factors for variable actions

3.2.4. PARTIAL SAFETY FACTORS FOR ACTIONS

Recommended values for the partial safety factors γ for the definition of the design values of actions for ultimate limit state combinations as well for the combination factors ψ are given in Annex A2 *"Application for bridges"* of EN1990. National choice is allowed for these factors, with the values to be adopted for bridge design in the UK given in §NA.2.3 of the National Annex.

As previously stated, the relevant limit state to consider in the design of a bridge deck is the internal failure of its structural members (STR). In §A.2.3.1(4) it is recommended that for the design of members not involving geotechnical actions the design values in Table A2.4(B) should be used, meaning that for non-integral structures only Set B of the STR/GEO design approach need be considered. These values are subsequently modified by the National Annex, with the UK values of the design actions given in Table NA.A2.4(B).

Table 3.4 - Partial factors for design values of actions (STR/GEO) Set B (from EN1990)

Persistent and Transient Design Situation (from Table NA.A2.4(B) of EN1990)	Effects of Actions	
	Unfavourable	Favourable
Permanent Actions:	$\gamma_{Gj,sup}$	$\gamma_{Gj,inf}$
Concrete self-weight	1.35	0.95
Steel self-weight	1.20	0.95
Superimposed dead load	1.20	0.95
Road surfacing	1.20	0.95
Weight of soil	1.35	0.95
Self-weight of other materials (EN1991-1-1, Tables A.1 to A.6)	1.35	0.95
Settlement (linear structural analysis)	1.20	0
Settlement (nonlinear structural analysis)	1.35	0
Shrinkage	1.00	1.00
Prestressing	1.00	1.00
Variable Actions:	γ_Q	-
Road traffic actions (gr1a, gr1b, gr2, gr5, gr6)	1.35	0
Pedestrian actions (gr3, gr4)	1.35	0
Wind actions	1.70	0
Thermal actions	1.55	0

It is noted in the original table that the single source principle applies, and hence the characteristic values from all permanent actions from one source should be multiplied by either $\gamma_{G,sup}$ or $\gamma_{G,inf}$ depending on whether the total resulting action from this source is favourable or unfavourable.

For the partial factor γ_{SH} to be considered for the effects of shrinkage a value of 1.0 is recommended in EN1992-1-1 §2.4.2.1(1). In the case of prestressing by controled imposed deformations the partial factor γ_P should be taken as 1.0 for both favourable and unfavourable effects, as recommended in EN1994-2 §2.4.1.1(1) and §NA.2.2. As for prestressing by tendons, EN1992-1-1 §2.4.2.2(1) states that the design value of prestress may be based on the mean value of the prestressing force, with the recommended value of γ_P for persistent and transient design situations being 1.0.

The combination values for the definition of the accompanying variable actions in persistent and transient ultimate limit state combinations as well as their frequent and quasi-permanent values for use in serviceability limit state combinations and accidental ultimate limit state combinations are given in Table NA.A2.1 of the UK National Annex.

Table 3.5 - Recommended values of ψ factors for road bridges (from EN1990)

Action	Group of Loads	Load Components	Ψ_0	Ψ_1	Ψ_2
Traffic loads	gr1a	TS	0.75	0.75	0
		UDL	0.75	0.75	0
		Footway and cycle track	0.40	0.40	0
	gr1b	Single axle	0	0.75	0
	gr2	Horizontal forces	0	0	0
	gr3	Pedestrian loads	0	0.40	0
	gr4	Crowd loading	0	-	0
	gr5	Vert. forces from SV and SOV's	0	-	0
	gr6	Horiz. forces from SV and SOV's	0	0	0
Wind forces	F_{wk}	Persistent design situations	0.50	0.20	0
		During execution	0.80	-	0
	F^*_w	During execution	1.00	-	0
Thermal actions	T_k		0.60	0.60	0.50
Snow loads	$Q_{Sn,k}$		0.80	-	-
Construction loads	Q_c		1.00	-	1.00

With the partial factors for design values of actions and the combination values of actions defined the combinations of actions can now be formulated attending to the combinations rules prescribed in EN1990. By inspection it will often be evident which leading variable action is likely to yield the most onerous effect for a particular member, but judgement is essential to avoid oversight.

Table 3.6 - Basic combinations at ULS (STR/GEO) for analysis of road bridges decks.

No.	G Permanent	S Shrinkage	Q Traffic Loads	T Temperature
1	1.35	1.00	1.35×gr1a	1.55×0.60
2	1.35	1.00	1.35×(gr1b, gr4, gr5)	1.55×0.60
3	1.35	1.00	1.35×0.75×gr1a	1.55

Table 3.7 – Basic combinations at SLS for analysis of road bridges decks.

No.	G Permanent	S Shrinkage	Q Traffic Loads	T Temperature
Characteristic Combinations (Stress limitation checks)				
1	1.00	1.00	1.00×gr1a	0.60
2	1.00	1.00	1.00×(gr1b, gr4, gr5)	0.60
3	1.00	1.00	0.75×gr1a	1.00
Frequent Combinations (Concrete crack widths with bonded tendons)				
1	1.00	1.00	0.75×(gr1a, gr1b)	0.50
2	1.00	1.00	0.40×gr3	0.50
3	1.00	1.00	0	0.60
Quasi Permanent Combinations (Long-term effects and concrete crack widths)				
1	1.00	1.00	0	0.50

3.3. TIME DEPENDENT PROPERTIES OF CONCRETE

3.3.1. SHRINKAGE OF CONCRETE

Shrinkage is a time dependent property of concrete which would result in a shortening of the reinforced concrete slab of composite bridge decks if it was not restrained by the steelwork. In the case of reinforced concrete structures the total shrinkage strain comprises a combination of autogenous and drying shrinkage components but composite structures will also require the consideration of thermal shrinkage during construction stages (Rueda, 2009).

Regarding the definition of concrete properties Eurocode 4 makes reference in EN1994-2 §3.1 to the provisions of Eurocode 2, where properties of normal weight concrete are given in EN1992-1-1 §3.1. The quantification of the shrinkage strains is covered in EN1992-1-1 §3.1.4, where the total shrinkage strain ε_{cs} is given as:

$$\varepsilon_{cs} = \varepsilon_{ca} + \varepsilon_{cd} \tag{3.10}$$

The autogenous shrinkage strain ε_{ca} is caused by the cement hydration process that occurs during the curing of the concrete when a reduction in its initial volume takes place. This is a linear function of concrete strength and develops rapidly within the early days after casting, with about 50% of the strain accounted for in the first 15 days (Fig. 3.12).

$$\varepsilon_{ca}(t) = \beta_{as}(t) \cdot \varepsilon_{ca}(\infty) \tag{3.11}$$

Where

$\varepsilon_{ca}(\infty)$ - is the autogenous shrinkage strain at time infinity.

$$\varepsilon_{ca}(\infty) = 2.5 \cdot (f_{ck} - 10) \cdot 10^{-6}$$

f_{ck} - is the concrete characteristic compressive strength at 28 days.

$\beta_{as}(t)$ - is a coefficient describing the evolution of autogenous shrinkage over time.

$$\beta_{as}(t) = 1 - \exp(-0.2 \cdot t^{0.5})$$

t - is the concrete age in days at the time being considered.

The drying shrinkage strain ε_{cd} occurs slowly with time as consequence of the progressive evaporation of water of the hardened concrete (Fig. 3.12). At a concrete age of 28 days roughly 15% of the total drying shrinkage is likely to have occurred, with about 80% developing within the first two years (Rueda, 2009).

$$\varepsilon_{cd}(t) = \beta_{ds}(t, t_s) \cdot k_h \cdot \varepsilon_{cd,0} \tag{3.12}$$

Where

$\beta_{ds}(t, t_s)$ - is a coefficient describing the evolution of drying shrinkage over time.

$$\beta_{ds}(t, t_s) = \frac{(t - t_s)}{(t - t_s) + 0.04\sqrt{h_0^3}}$$

t - is the concrete age in days at the time being considered.

t_s - is the concrete age in days at the beginning of drying shrinkage, which in accordance with EN1994-1-1 §5.4.2.2(4) should generally be assumed as 1 day.

h_0 - notional size of the concrete slab.

$$h_0 = 2 \cdot A_c / u$$

Ac - cross sectional area of the concrete member.

u - is the perimeter exposed to drying. In bridge decks where there is a waterproofing system applied to the top of the deck slab only the exposed soffit perimeter should be considered.

k_h - is a coefficient accounting for the notional thickness of the concrete slab h_0 given in Table 3.3 of EN1992-1-1.

$\varepsilon_{cd,0}$ - is the basic drying shrinkage strain, determined in accordance with EN1992-1-1 §B.2.

The typical long term values for the total shrinkage strain ε_{cs} lie usually between 25×10^{-5} and 30×10^{-5}, of which approximately 75% is accounted for by the drying shrinkage strain ε_{cd} and the remaining 25 % by the autogenous shrinkage strain ε_{ca} (Fig. 3.12) (Rueda, 2009).

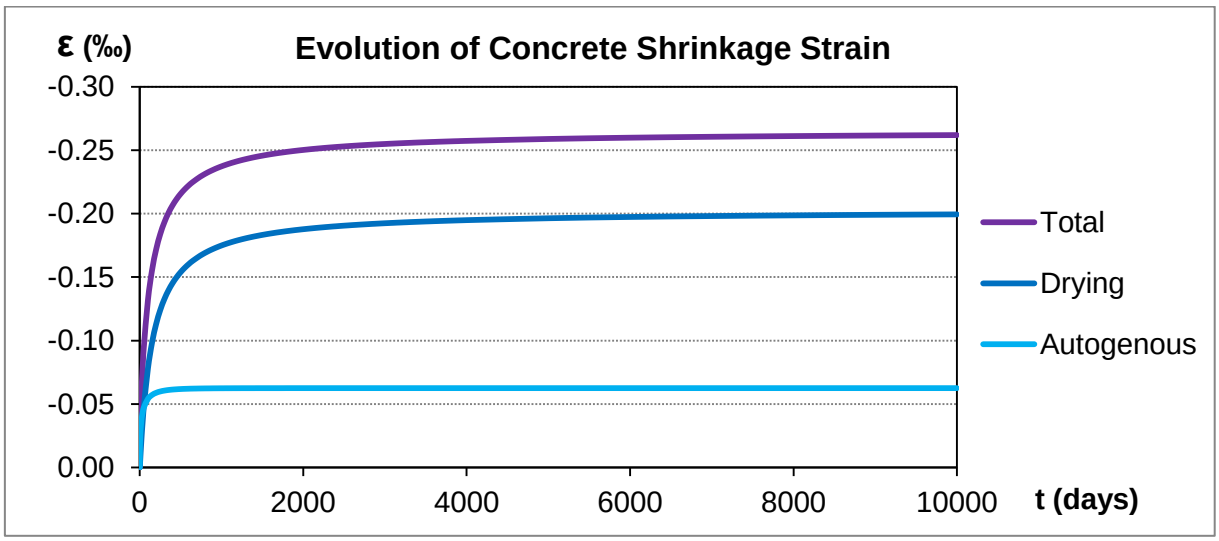


Fig. 3.12 – Time dependant evolution of concrete shrinkage strain (h_0=250mm, t_s=1d, RH=80%)

It is recommended in EN1994-2 §7.4.1(5) that where composite action becomes effective as the concrete hardens the effects of the heat of hydration of cement and of the corresponding thermal shrinkage strain be taken into account for the serviceability limit state in the construction stage. It is further recommended in §7.4.1(6) that in the absence of specific measures to mitigate heat of hydration of cement its effects be replicated by temperature difference of 20K between the steel and concrete. The effects of thermal shrinkage are considered in the determination of cracked regions for global analysis and in the checking of permissible crack widths at traffic opening (Davaine et al, 2007).

$$\varepsilon_{th} = \alpha \cdot \Delta T \tag{3.13}$$

Where

α - is the coefficient of linear thermal expansion, taken as 10×10^{-6} as per EN1994-2 §5.4.2.5(2).

ΔT - is the temperature between steel and concrete, taken as 20°C.

When calculating the sectional forces on the composite bridge deck due to the effects of concrete shrinkage two design situations will need to be considered:

- At traffic opening immediately after the end of construction for a shrinkage strain given by $\varepsilon_{cs}(t) = \varepsilon_{ca}(t) + \varepsilon_{cd}(t) + \varepsilon_{th}$, with the derived sectional forces to be included in the serviceability limit state checks;
- At the end of the service life for a shrinkage strain $\varepsilon_{cs}(\infty) = \varepsilon_{ca}(\infty) + \varepsilon_{cd}(\infty)$, to be considered in both serviceability and ultimate limit state checks.

3.3.2. CONCRETE CREEP

Creep is a rheological property of concrete where under a sustained compressive stress the concrete member experiences the development with time of a non-recoverable strain in addition to the corresponding elastic deformation. The magnitude of this additional strain is influenced by ambient humidity, section size of the member, composition and age at first loading of the concrete, as well as the magnitude of the applied load.

As for shrinkage, Eurocode 4 refers back to the provisions of EN 1992-1-1 regarding concrete properties. The creep deformation of concrete $\varepsilon_{cc}(t,t_0)$ at age t for a constant compressive stress σ_c applied at concrete age t_0 is given in EN1992-1-1 §3.1.4(3) as follows:

$$\varepsilon_{cc}(t,t_0) = \varphi(t,t_0) \cdot (\sigma_c / E_c) \tag{3.14}$$

The purpose of the creep coefficient is to relate the creep deformation to the elastic deformation of concrete, and translate how much the latter will be magnified over time under sustained stress. The basic equations for determining the creep coefficient $\phi(t,t_0)$ are given in EN1992-1-1 §B.1.

$$\varphi(t,t_0) = \varphi_0 \cdot \beta_c(t,t_0) \tag{3.15}$$

Where

φ_0 - is the notional creep coefficient.

$\beta_c(t,t_0)$ - is a coefficient describing the development of creep over time.

$$\beta_c(t,t_0) = \left[\frac{t - t_0}{(\beta_H + t - t_0)} \right]^{0.3}$$

t - is the concrete age in days at the time being considered.

t_0 - is the concrete age at first loading in days.

β_H - is a coefficient that accounts for the relative humidity *RH* and notional size h_0.

In the above equation the creep coefficient is expressed as a function of the notional creep coefficient ϕ_0 and coefficient $\beta_c(t,t_0)$. When estimating the long term effects of creep at time infinity, as is usual for design purposes, the equation will yield $\phi(\infty,t_0)= \phi_0$. Values of the creep coefficient will typically lie between 1.5 to 2.5.

A set of equations for determining the notional creep coefficient taking into account the influence of relative humidity, concrete strength and concrete age at loading is provided in EN1992-1-1 §B.1.

$$\varphi_0 = \varphi_{RH} \cdot \beta(f_{cm}) \cdot \beta(t_0) \tag{3.16}$$

Where

φ_{RH} - is a factor to allow for the influence of the relative humidity *RH* of the ambient environment.

$$\varphi_{RH} = 1 + \frac{1 - RH/100}{0.1 \cdot \sqrt[3]{h_0}} \quad , f_{cm} \le 35MPa$$

$$\varphi_{RH} = \left[1 + \frac{1 - RH/100}{0.1 \cdot \sqrt[3]{h_0}} \cdot \alpha_1 \right] \cdot \alpha_2 \quad , f_{cm} \le 35MPa$$

$\beta(f_{cm})$ - is a factor accounting for the effect of mean concrete strength on the creep strain.

$$\beta(f_{cm}) = \frac{16.8}{\sqrt{f_{cm}}}$$

$\beta(t_0)$ - is a factor that takes into consideration the concrete age at loading.

$$\beta(t_0) = \frac{1}{\left(0.1 + t_0^{0.20}\right)}$$

$\alpha_{1/2/3}$ - are coefficients that consider the influence of concrete strength f_{cm}.

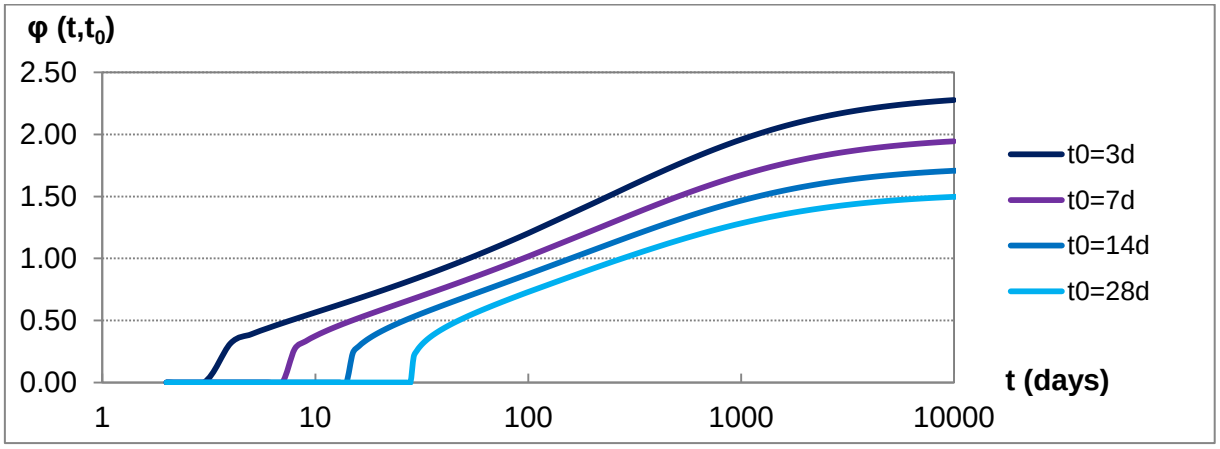


Fig. 3.13 – Development of creep coefficient over time (h_0=250mm, f_{ck}=35MPa, RH=80%)

In the concluding section the time dependent properties of concrete that are creep and shrinkage were described and the methodologies prescribed by EN1992-1-1 for determining the creep coefficient and shrinkage strain were presented. An overview of the factors influencing the magnitude and development of creep and shrinkage over time has shown how ambient factors (such as relative humidity), material properties of concrete (like concrete strength) as well as the age of the concrete at loading, all affect the final creep coefficient and shrinkage strain.

3.4. Structural Analysis of Composite Decks

3.4.1. Structural Modelling for Analysis

The general principles regarding the structural analysis of bridges are addressed in Section 5 of EN1990, with additional recommendations for dealing with aspects inherent to steel and composite structures given in EN1993 and EN1994.

The fundamental premises on structural modelling as stated in EN1990 §5.1 are that calculations must be carried out using appropriate models capable of predicting the structural behaviour to an adequate degree of accuracy based on established engineering theory and practice. Furthermore, EN1993-2 §5.1.1 and EN1994-2 §5.1.1 add that the calculation model should reflect the anticipated behaviour of members, cross-sections, joints and bearings, with §5.1.2 and §5.1.3 emphasizing the need for consideration of the type of joint and ground-structure interaction.

In multi-span continuous girder bridges, where a continuous joint model is assumed in the analysis, the behaviour of the joint may be assumed to have no effect on the distribution of internal forces and moments. The effects of soil-structure interaction should be considered where the deformation characteristics of the supports are relevant. In this instance the stiffness of the supports should account for the deformation characteristics of bearings, piers and foundation (the support stiffness being equivalent to a set of springs connected in series).

The broad statement of principles and rules of EN1994-2 §5.1 gives the designer freedom in the choice of model used for structural analysis. Classical or matrix analysis by the theory of structures either by hand calculation or computer programs, or use of the finite element method (FEM) with the structure discretised by means of beam and/or shell elements, are all valid analysis approaches. Given the availability of powerful structural analysis software based on the finite element method this has become the standard in current day practice.

A plan grillage model where the bridge deck is idealised as a number of longitudinal beam elements interconnected rigidly at the nodes with transverse beam elements. This is one of the simplest forms of finite element model and is used extensively in the UK (Fig. 3.14). The longitudinal elements model the main composite girder and are assigned the corresponding section properties, with the transverse elements being assigned the properties of only the slab. Models for the bare steel and the partially composite construction stages are required, as well as models for short-term and long-term deck behaviour.

An assessment of the effective width of the composite girder's concrete flange is necessary, since the shear lag effect is not captured by the model. The analysis outputs of such models are sectional forces (axial force, shear and bending moment) that can be checked in a straightforward manner against the corresponding resistances. For the design of bracing elements local models will be necessary as these elements are not included in the global model.

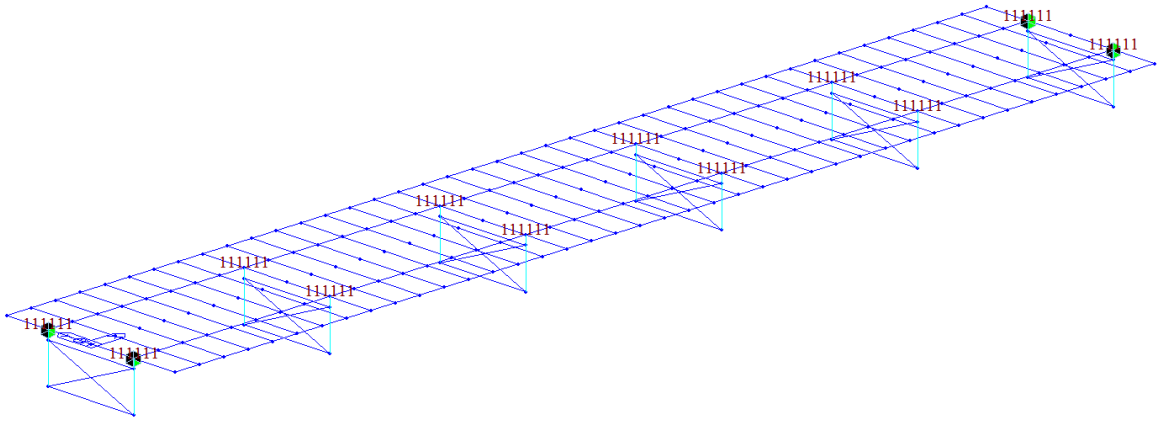


Fig. 3.14 – Example of finite element grillage model

Hybrid models can also be adopted, where longitudinal beam elements representing the steel sections of the composite girders are offset from a surface of shell elements modelling the concrete slab of the deck are also a possibility (Fig. 3.15). The offset beam elements are rigidly connected to the deck's shell elements by means of very stiff dummy beam members or displacement constraints, depending on the capabilities of the software used. Both methods replicate the composite behaviour of the real structure. Modelling of the deck with shell elements improves the longitudinal and transverse distribution of concentrated loads as opposed to only transverse distribution in grillage models. Moreover, the shear lag effects are captured by the model provided a fine enough mesh is used for the shell elements and no additional consideration for effective width of the concrete flange is necessary.

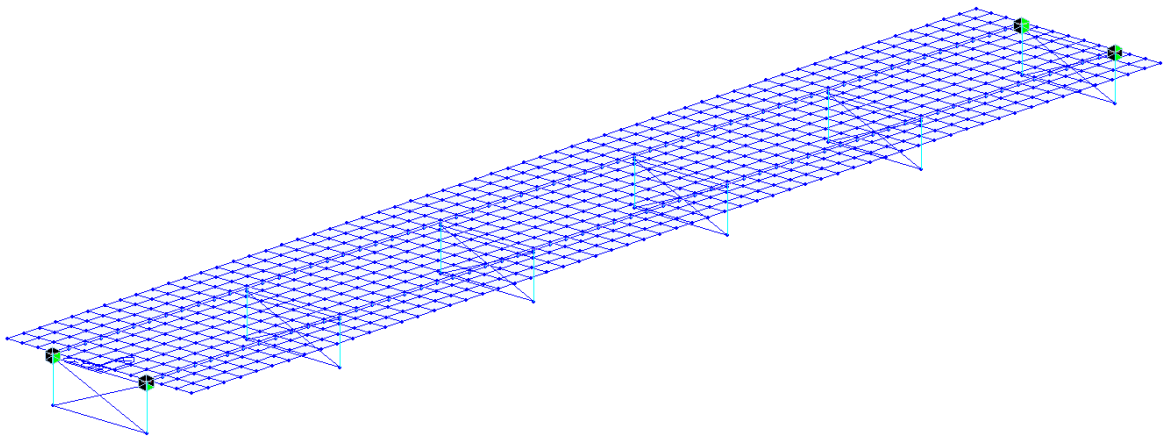


Fig. 3.15 – Example of finite element hybrid model

Extraction of analysis output is not straightforward, as results for the beam element will be internal forces referring the element's elastic neutral axis and for the shell elements stresses at mid-plane of the slab. To obtain the resulting shear forces and bending moments acting on the composite section it is necessary to compute the stress resultants of the shell elements, take the sectional forces acting on the

offset beam element and calculate the equivalent set of forces at the centroid of the composite section. The derived sectional forces will be used in the resistance checks. Several software packages already currently include post-processing capabilities that allow the user to obtain forces and moments from stress resultants for a section slice of the model, thus facilitating the above approach.

The option for an analysis model where both the girder's steel section as well as the concrete deck slab are modelled with shell elements provides the most detailed and accurate form of modelling (Fig. 3.16), albeit at the expense of computation time and post-processing of the results. For example, it gives the possibility of a realistic assessment of critical loads for lateral torsional buckling modes, which neither of the previous approaches is capable of. Furthermore, no additional local models for bracing elements are required, as these can be easily introduced in the model and the action effects obtained directly.

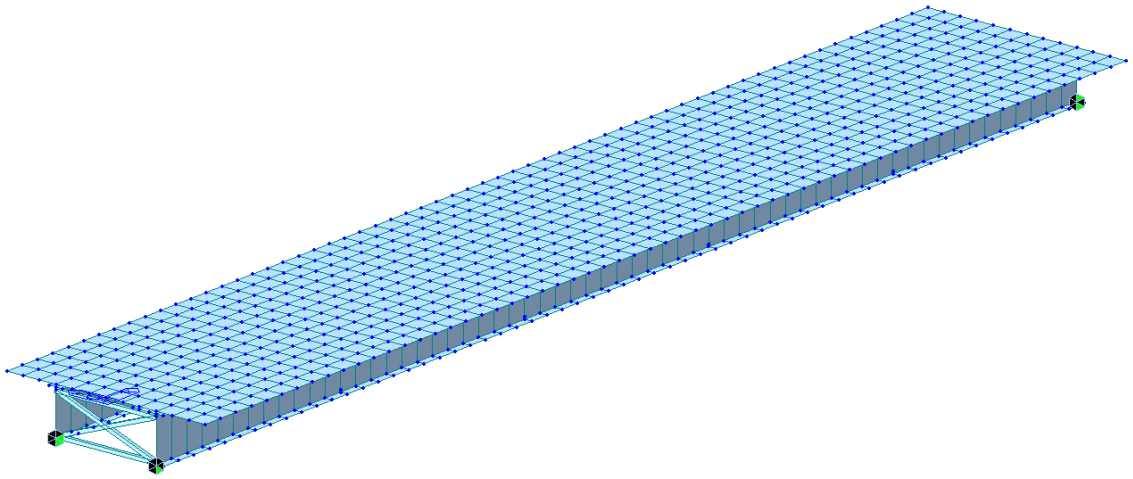


Fig. 3.16 – Example of finite element shell model

The flexural and shear resistance models proposed in EN1994-2, such as the plastic resistance moment of composite cross-sections and the post-critical shear buckling resistance of web panels, are materially nonlinear resistance models to which the stresses obtained from a linear elastic analysis of a shell model cannot be compared directly. The benefits of such models for design purposes is limited if the software does not possess adequate post-processing tools. Similarly to the hybrid model, the section forces acting on the composite section must be obtained by integration of the stresses acting on a slice through the shell elements that make up the girder's steel section and concrete deck slab.

3.4.2. Structural Stability

The need for consideration of the effects of the deformed geometry of the structure in the calculation of action effects depends on whether or not second-order effects significantly increase first-order effects or modify the structural behaviour. EN1994-2 §5.2.1 provides the familiar criteria from EN1993 allowing for the use of first-order analysis provided the increase in internal forces and moments by deformations is less than 10%, a condition assumed to be fulfilled when the load factor for the lowest elastic critical buckling mode is at least 10 ($\alpha_{cr} \geq 10$).

In the case of girder bridges where the bridge deck members are acting in flexure only, the deformed geometry of the structure has no influence on the distribution of internal forces and moments and therefore a first-order analysis is suitable (Davaine et al, 2007). On the contrary, for frame and arch bridge structures, the compressive forces acting on the deck, piers and arch members give rise to P-Δ effects when considering the deformed geometry of the structure, which may need to be taken into account.

Regarding methods of analysis applicable for bridges for the assessment of second-order effects EN1994-2 §5.2.2 cross-references EN1993-2 §5.2.2 where a practical method of moment amplification of first-order effects is proposed:

$$M_{II} = M_{I} \cdot \frac{1}{1 - \frac{1}{\alpha_{cr}}} \tag{3.17}$$

Where

M_{II} - is the second-order bending moment.

M_{I} - is the first-order bending moment.

α_{cr} - is the load factor the lowest global elastic critical buckling mode.

It is noted that this method is applicable for critical load factors α_{cr} not lower than 3.0 ($3 \leq \alpha_{cr} \leq 10$), at which point a more accurate method for second-order analysis should be used. If the lower bound load factor of 3.0 is considered the equation yields second-order effects equivalent to an onerous 50% of the first-order action effects. By limiting the method's applicability EN1993-2 effectively mandates the designer to make use of second-order analysis (nonlinear geometric) for a realistic assessment of the effects of the deformed geometry of structures that are fairly sensitive to instability phenomena.

The evolutionary nature of composite cross-sections means that bare steel sections are present during construction and subject to the weight of fresh concrete and construction loads, with the composite section effective only for superimposed and traffic loads. Structural stability needs to be checked for all the relevant stages from construction to service conditions.

In girder bridges this means attention should be given to global lateral torsional buckling during construction stages attending to the prescribed erection method and construction sequence, and to the stability of the compressed bottom flanges of girders in hogging moment regions over the piers in service conditions (Rueda, 2009). Verification of safety against lateral torsional buckling is covered by member resistance checks with guidance in EN1994-2 §6.4.

3.4.3. Effective Width of Flanges for Shear Lag

The shear lag effect in wide flanges is a consequence of the in-plane flexibility of the flanges which gives rise to a non-uniform distribution of longitudinal bending stresses. The stress adjacent to the web will exceed the value obtained according to Euler-Bernoulli beam bending theory, whereas the stress in the flange remote from the web will be lower than anticipated.

To allow for the effects of shear lag EN1994-2 proposes the use of a fictitious effective width. In this approach an effective flange width of less than the actual flange width is considered, so that the uniform stress calculated using engineering bending theory is equivalent to the real peak stress adjacent to the web (Fig. 3.17) (Hendy and Johnson, 2006).

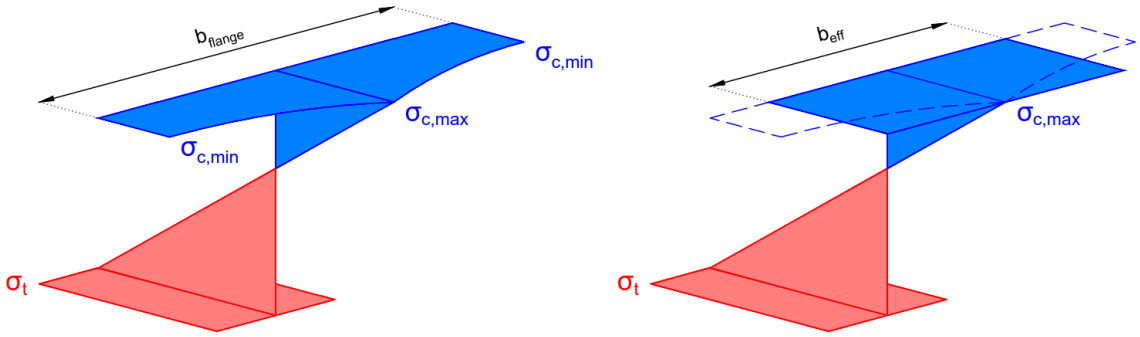


Fig. 3.17 – Bending stress distribution in wide flanges due to shear lag effect.

In accordance with EN1994-2 §5.4.1.2 a constant effective width may be assumed over the whole of each span when linear elastic global analysis is used, with the corresponding value at mid-span being considered. For the quantification of the effective width at mid-span or an internal support the following expression is provided:

$$b_{eff} = b_0 + \sum b_{ei} \tag{3.18}$$

Similarly, for the quantification of the effective width at an end support:

$$b_{eff} = b_0 + \sum \beta_i \cdot b_{ei} \tag{3.19}$$

With:

$$\beta_i = \left(0.55 + 0.025 \cdot L_e / b_{ei}\right) \leq 1.0 \tag{3.20}$$

Where:

b_0 - is the distance between the centres of the flange outstand shear connectors.

b_{ei} - is the effective width of the concrete flange on each side of the web.

The effective widths b_{ei} are taken as $L_e/8$, with the length L_e being the approximate distance between points of null bending moment, but not exceeding the geometric width b_i taken as the distance from the outstand shear connector to the midpoint between adjacent webs. In the case of a free edge b_i will be the edge distance itself.

In the analysis of continuous beams the design is usually governed by moment envelopes from several load arrangements, hence a somewhat lenient assessment of the equivalent span length L_e between contraflexure points is admissible. Guidance on the equivalent spans L_e to consider in most scenarios is given in §5.4.1.2(7) (Fig.3.18).

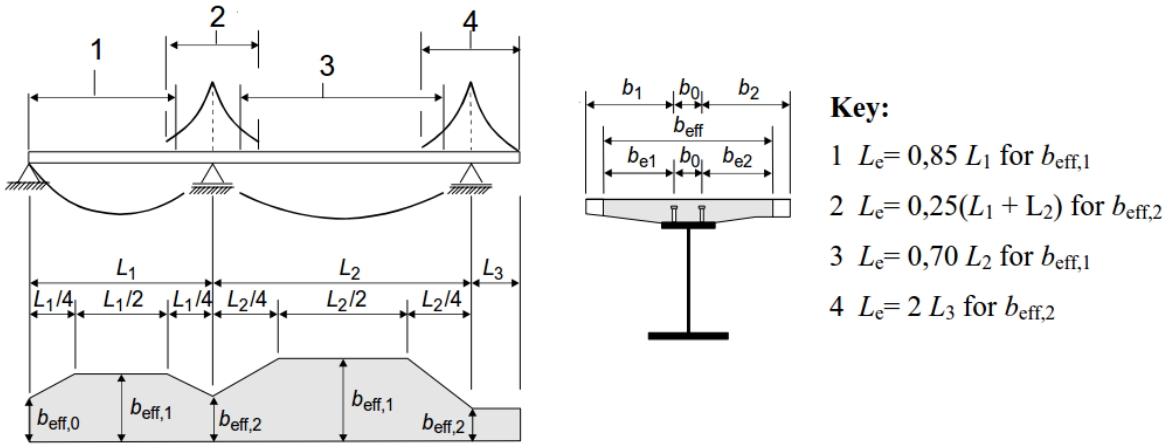


Fig. 3.18 – Equivalent span Le for continuous girders (from *EN1994-2, BSI, 2010*).

Unlike EN1992-1-1 and EN1993-1-5 there is no reference in EN1994-2 regarding the validity of the range of application of the effective spans given in *Fig. 3.18*. It is prudent to adhere to the recommendations of the concrete and steel codes which limit the applicability of the equivalent spans L_e to span arrangements where adjacent spans do not differ more than 50% and cantilevers not exceeding half the adjacent span length. For other span ratios the equivalent spans should be assessed based on the moment distribution from an initial analysis (Hendy and Johnson, 2006).

The effective width approach is related to the type of analysis model chosen by the designer and it applies to grillage models comprising line beam elements only. In models where the concrete flange is modelled with shell elements the shear lag effects are account directly (Fig. 3.19) and hence the flange must be assigned its actual width.

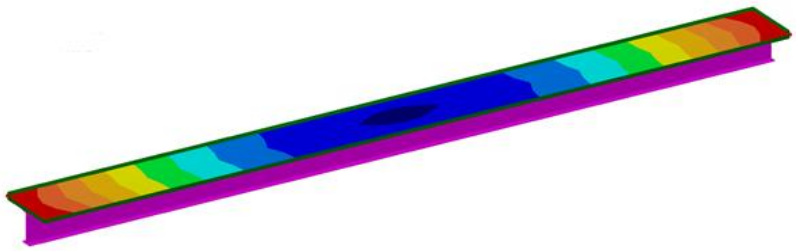


Fig. 3.19 – Non-uniform longitudinal stress at mid-plane of the concrete flange of a hybrid model.

3.4.4. MODULAR RATIOS FOR CONCRETE

It is a requirement of EN1994-2 that the effects of creep and shrinkage of concrete are taken into account. An approach based on the use of different modular ratios n_L for concrete depending on the type of loading is proposed in EN1994-2 §5.4.2.2 for the definition of the composite section properties in steel units.

$$n_L = n_0 \cdot (1 + \psi_L \cdot \varphi_t) \tag{3.21}$$

Where

n_0 - is the modular ration E_a / E_{cm} for short-term loading.

φ_t - is the creep coefficient $\phi(t,t_0)$ at age t of concrete and age t_0 at loading.

ψ_L - is the creep multiplier depending on the type of loading.

The values adopted for the creep multiplier ψ_L according to the type of loading are:

- ψ_L =1.10 for permanent loads;
- ψ_L =0.55 for primary and secondary effects of shrinkage;
- ψ_L =1.50 for prestressing by imposed deformations.

The purpose of the creep multiplier ψ_L is to account for the changes in concrete compressive stress over time. For instance, the value for permanent loading on reinforced concrete is 1.0, but this is increased to 1.1 for composite structures as the structural steel does not creep. Shrinkage is also a time dependent effect of concrete and develops in parallel with creep. Since concrete is more susceptible to creep when young and the shrinkage strains are introduced gradually over time there is less creep than for uniform stresses caused by permanent loads, hence the reduced value of 0.55 of the creep multiplier. As for imposed deformations, their effects are significantly reduced by creep when the concrete is young (Hendy and Johnson, 2006).

For permanent loads on composite structures cast in several stages it is permitted to consider a single mean value t_0 for the age at loading of concrete. This assumption is particularly useful in the case of continuous bridge structures built span-by-span, where a concrete pour sequence has taken place instead of having all the concrete placed in one go, with adjacent spans having different ages when superimposed loads are applied to the deck (Hendy and Johnson, 2006).

The above approach applies directly to models where equivalent cross sections with properties defined in terms of steel units are used to assess the effects of actions on the real composite section. This is the case for grillage models where separate models are required for the different types of loading:

- A model of the bare steel girders for the construction stage;
- A model with section properties using the long-term modular ratio for permanent actions;
- A model with section properties defined with the modular ratio for shrinkage;
- A model with section properties using the short-term loading modular ratio for live loads.

The stresses on the cross sections fibres obtained by each of the models will then be superimposed when assessing action effects for the relevant load combinations for serviceability and ultimate limit states.

The same principle can be extended for use with hybrid or shell models by considering an effective concrete modulus given by:

$$E_{c,eff} = E_{cm}/(1+\psi_L \cdot \varphi_t) \tag{3.22}$$

It should be noted that §5.4.2.2(2) excludes the use of the above approach for quantifying the effects of creep and shrinkage for members with both flanges composite. This is however not consistent with §5.4.2.2(10) where the restriction is limited to members in double composite action with both flanges uncracked, in which case the effects of creep and shrinkage should be determined by more accurate methods (Hendy and Johnson, 2006).

3.4.5. Effects of Cracking of Concrete

Appropriate allowance must be made for the effects of concrete cracking on the distribution of internal forces and moments, as stated in EN1994-2 §5.4.2.3(1). This clause states that the loss of flexural stiffness due to cracking of the concrete deck slab alters the uncracked bending moment distribution. This generally leads to larger sagging moment while relieving the hogging moments over pier sections.

Two approaches are proposed for accounting for the effects of cracking of concrete, with a general method described in §5.4.2.3(2) and a simplified method in §5.4.2.3(3).

The general method described in §5.4.2.3(2) is a two stage approach. It initially requires calculating the envelope of the internal forces and moments for the characteristic combinations including long-term effects using the flexural stiffness of the uncracked sections E_aI_1, where I_1 is the second moment of area of the equivalent steel section calculated assuming that concrete in tension is uncracked. This stage is defined as "uncracked analysis".

Subsequently, in regions where the extreme fibre tensile stress in the concrete exceeds twice the concrete tensile strength f_{ctm} or f_{lctm} the flexural stiffness should be reduced to E_aI_2, where I_2 is the second moment of area of the equivalent steel section calculated neglecting concrete in tension but including reinforcement. The resulting stiffness distribution may then be used for re-analysis for both ultimate and serviceability limit states, thus obtaining a new distribution of internal forces. This stage is defined as "cracked analysis".

The simplified method described in §5.4.2.3(3) is applicable to continuous composite beams with the concrete flanges above the steel section and non-prestressed where all the ratios of continuous adjacent spans are at least 0.6. In this instance the effect of concrete cracking may be accounted for by adopting the flexural stiffness of the cracked section E_aI_2 over 15% of the span to each side of internal support sections and the uncracked flexural stiffness E_aI_1 elsewhere (Fig. 3.20).

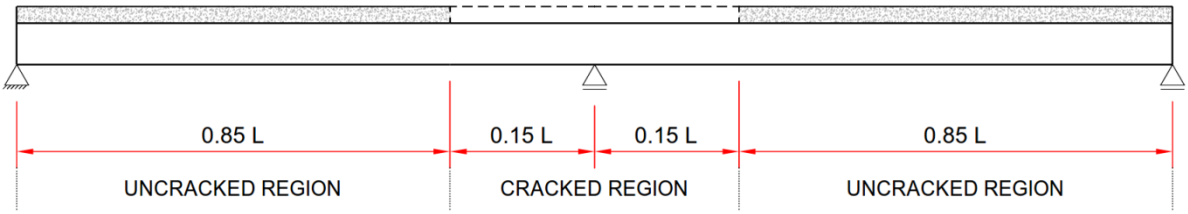


Fig. 3.20 – Cracked regions over an internal support as per the simplified method.

Regarding composite cross members §5.4.2.3(5) states that in multiple beam decks where transverse members are not subject to axial tensile forces they may be assumed to uncracked throughout. While this assumption stands valid for twin girder and ladder decks with cross girders spanning only between the main girders it cannot be extended to twin girder decks where cantilevering cross girders are adopted, since hogging moments develop in the transverse members and hence tensile stresses in the concrete slab. The general method described in §5.4.2.3(2) is also applicable to these transverse members (Hendy and Johnson, 2006).

The effects of concrete cracking on the longitudinal shear forces at the steel-concrete interfaces are the subject of §5.4.2.3(7) and §5.4.2.3(8). For the effects of cracking on the design longitudinal shear for the shear connection at ultimate limit states §5.4.2.3(7) makes reference to the §6.6.2, where it is recommended that the elastic properties of the uncracked cross section be generally adopted even in regions where concrete cracking has been assumed in global analysis. The basis for this recommendation is that by using the uncracked elastic section properties the longitudinal shear will be overestimated in cracked regions, and thus provides a simple and conservative way to avoid to explicitly considering the effects of tension stiffening or concrete over-strength in cracked regions (Hendy and Johnson, 2006). The same procedure is recommended in §5.4.2.3(8) in regards to serviceability limit states.

3.4.6. Primary and Secondary Effects of Concrete Shrinkage

As seen in section 1.2.1 shrinkage is a rheological property of concrete that consists of the development with time of a shortening deformation of the concrete member. The long-term values of the total shrinkage strain ε_{cs} are usually within 25×10^{-5} and 30×10^{-5}.

In an unrestrained concrete member the shrinkage strain will not induce any sectional forces in the member, as it will deform freely. However, in composite bridge decks shear connectors are provided to ensure there is no slip at the steel-concrete interface, enabling the hypothesis that plane sections remain plane in deformation and hence materialising composite behaviour of the structure. With no relative displacement permitted the concrete member thus becomes restrained, with the shrinkage strain giving rise to tensile locked-in stress in the member.

$$\sigma_{cs}(\infty) = \varepsilon_{cs}(\infty) \cdot \frac{E_a}{n_L} \tag{3.23}$$

Where

$\varepsilon_{cs}(\infty)$ - is the long term shrinkage strain.

E_a - is the modulus of elasticity of structural steel.

n_L - is the modular ratio for primary and secondary effects of shrinkage;

Considering that the modular ratio n_L for the effects of shrinkage is usually similar to that for long-term action effects such that for pre-dimensioning purposes a single value of between 15 to 20 is often considered for both, a range of values from 2.5 to 4.5MPa for the magnitude of the locked-in stress can be expected.

The internal locked-in stresses on the concrete slab act upon the composite section as a compressive force applied at the centroid of the slab, with the eccentricity to the elastic neutral axis of the composite section also resulting in a sagging moment applied to the section (Fig. 3.21).

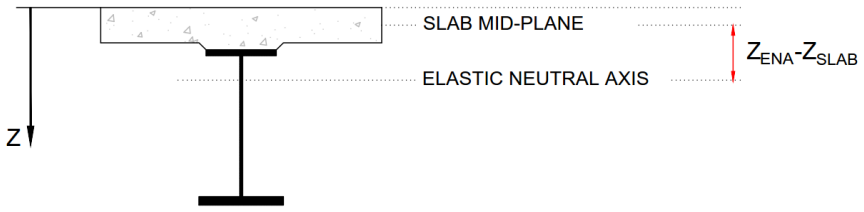


Fig. 3.21 – Eccentricity between slab mid-plane and centroid of composite section

$$N_{cs}(\infty) = \varepsilon_{cs}(\infty) \cdot \frac{E_a}{n_L} \cdot A_c \tag{3.24}$$

$$M_{cs}(\infty) = N_{cs}(\infty) \cdot (z_{ENA} - z_{SLAB}) \tag{3.25}$$

Where

$\varepsilon_{cs}(\infty)$ - is the long term shrinkage strain.

A_c - is the total area of the concrete flange.

z_{ENA} - is the level of the elastic neutral axis of the composite section.

z_{SLAB} - is the level of the centroid of the concrete slab.

In a statically determinate system (Fig. 3.22 and Fig. 3.23) with no external forces applied to the composite section the support reactions will forcibly be null, and hence the locked-in stresses in the concrete slab together with bending and direct stresses from the eccentric compression force must define a self-equilibrated state of stress (Fig. 3.24). It is noted that while the self-equilibrated stresses

result in a null net force applied to the section they induce a sagging curvature to the composite member. Also, since the vertical support reactions are nil the beam will not be subjected to any vertical shear force. The above effects are the primary effects of shrinkage.

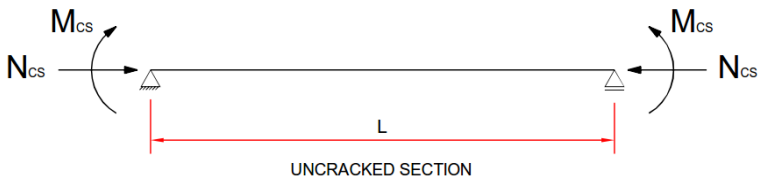


Fig. 3.22 – Structural analysis diagram of a simply supported composite beam.

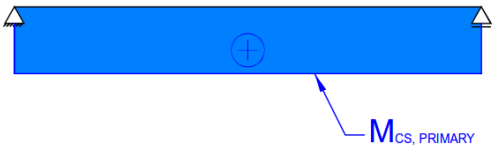


Fig. 3.23 – Bending moment due to shrinkage effects in a simply supported composite beam.

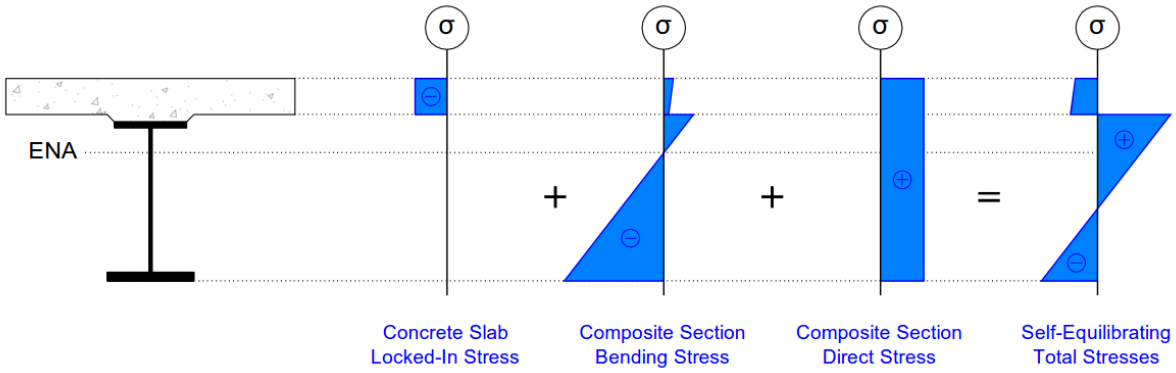


Fig. 3.24 – Uncracked section stresses due to primary shrinkage effects.

In a statically indeterminate system like a continuous beam (Fig. 3.25) the sagging curvature due to the primary shrinkage effects will be constrained at the internal supports where vertical displacement is impeded. At each support a vertical reaction is required to ensure compatibility of deformations. Again taking note that there are no external forces applied to the structure, the resulting support reactions must form a set of self-equilibrating forces. With no forces other than the support reactions being applied to the structure within the spans the bending moment diagram will be linear between supports (Fig. 3.26).

The bending moment diagram obtained by applying the compressive axial force and the concentrated moments to both ends of the continuous beam relates to the total effects of shrinkage. Since the

primary effects are the axial compression and the sagging moment due its eccentricity in order to obtain the effects due to the support reactions the primary effects will need to be deducted from the total effects previously calculated. The bending moments and shear forces associated with the support reactions are the secondary effects of shrinkage.

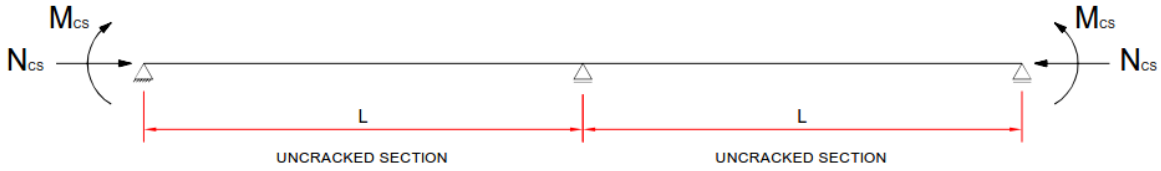


Fig. 3.25 – Structural analysis diagram of a continuous uncracked composite beam.

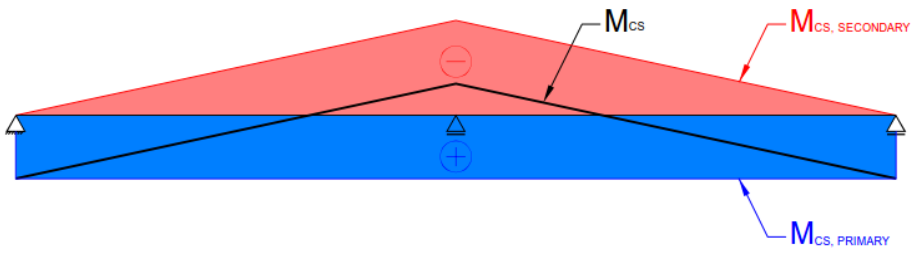


Fig. 3.26 – Bending moments due to shrinkage effects in a continuous uncracked composite beam.

The calculation of the total stresses on the composite section can then be undertaken by calculating the secondary stresses on the composite section and superimposing these with the previously calculated primary stresses (Fig. 3.27).

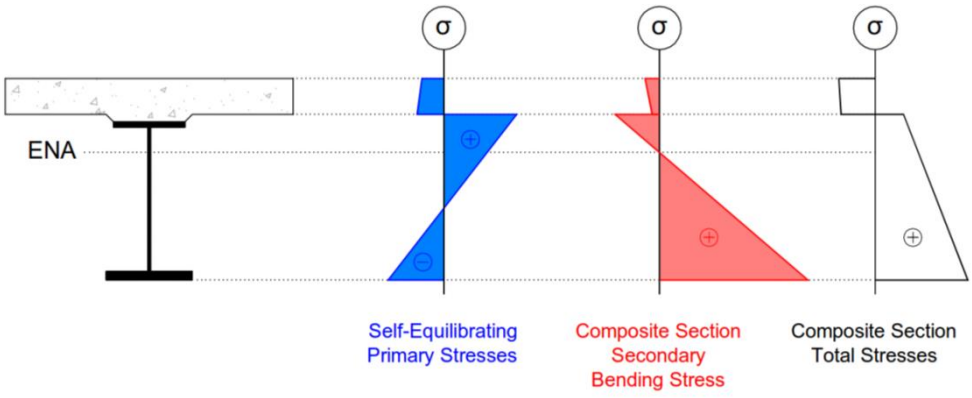


Fig. 3.27 – Uncracked section stresses due to primary and secondary shrinkage effects.

In continuous composite beams the concrete slab will typically be cracked over the support regions, with the exception of some very particular cases. In this instance EN1994-2§5.4.2.2(8) allows the primary effects of shrinkage to be neglected in the calculation of the secondary effects since the cracking of the concrete slab would have released the tensile shrinkage stress due to restraint. The total effects of shrinkage are then obtained by applying the compressive axial force and the concentrated moments to both ends of the uncracked regions (Fig. 3.28).

The resulting bending moment diagram will display a step at the transition between the uncracked and the cracked regions due to the presence of a concentrated moment applied within the span. The primary bending moment is only present in the uncracked regions and is null elsewhere, whereas the secondary bending moment due to the effects of the support reactions will extend along the whole length of the beam (Fig. 3.29). Since the secondary moments are due to the effects of the support reactions alone the resulting diagram will still be linear between supports, and can be obtained as before by deducting the primary effects from the total effects.

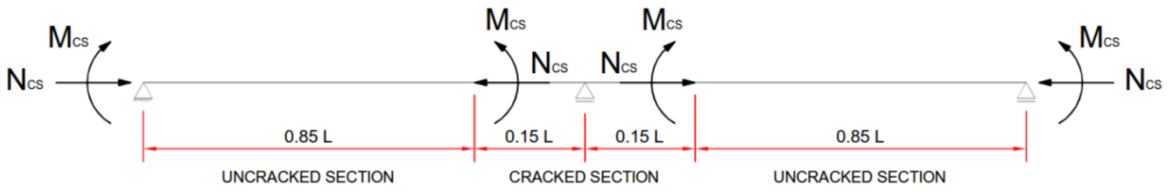


Fig. 3.28 – Structural analysis diagram of a continuous composite beam with cracked regions.

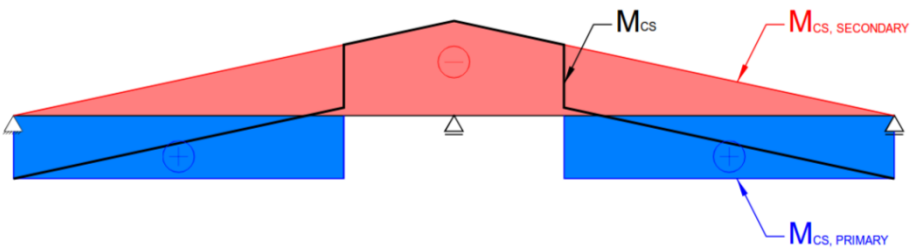


Fig. 3.29 – Bending moments due to shrinkage effects in a composite beam with cracked regions.

The stresses on the composite sections in cracked regions of the beam will present a pattern distinct from the one characteristic of uncracked sections. The section properties now relate to a cracked cross-section, where concrete in tension is neglected and only the contribution of the slab reinforcement is considered as per EN1994-2§1.5.2.12.

Since the primary effects of shrinkage are neglected in cracked regions the primary stresses will necessarily be null the section is subjected to secondary stresses only. With the secondary stresses now acting on the cracked composite section the stress distribution on the section will be discontinuous, with two lines representing the reinforcement stress at the centroid level of the top and bottom

longitudinal reinforcement layers and a linear stress distribution along the depth of the steel section (Fig. 3.30).

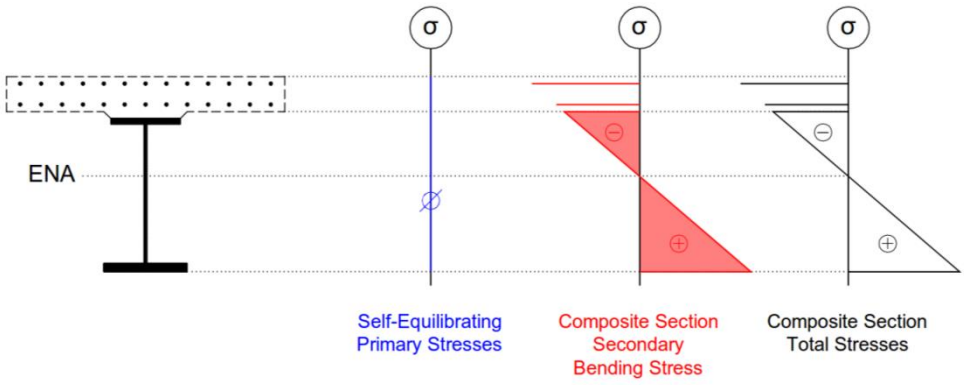


Fig. 3.30 – Cracked section stresses due to secondary shrinkage effects.

The primary and secondary shrinkage stresses obtained from the above procedure should be added to the cumulative stress history taking into account the construction sequence and the changes in cross sections from steel only to composite to obtain the final stress distribution to be combined with the stresses from live load envelopes and used in serviceability limit state permissible stress checks as per EN1994-2§7.2.2.

For ultimate limit state resistance checks EN1994-2 makes allowance in §5.4.2.2 (7) for neglecting the effects of creep and shrinkage for verifications other than fatigue provided that all cross sections are in either Class 1 or 2 and no allowance for lateral-torsional buckling is necessary. This last requirement relates to the compressed flange of the composite beam in hogging moment regions and implies that in service conditions the reduction factor for lateral torsional buckling χ_{LT} must be 1.0. Observation of this requirement may prove difficult to achieve given the over-resistance necessary for it to be applicable, which will be at least 25 times the characteristic resistance of the composite section.

$$\chi_{LT} = 1.0 \quad \Rightarrow \quad \bar{\lambda}_{LT} \leq 0.2 \tag{3.26}$$

$$\bar{\lambda}_{LT} \leq 0.2 \quad \Leftrightarrow \quad \sqrt{\frac{M_{R,k}}{M_{cr}}} \leq 0.2 \quad \Leftrightarrow \quad M_{R,k} \leq (0.2)^2 \cdot M_{cr} \quad \Leftrightarrow \quad M_{cr} \geq 25 \cdot M_{R,k} \tag{3.27}$$

Where

χ_{LT} - is the reduction factor for lateral torsional buckling.

$\bar{\lambda}_{LT}$ - is the non-dimensional slenderness.

$M_{R,k}$ - is the characteristic resistance moment of the composite section.

M_{cr} - is the critical moment of the composite section.

In the closing section the general principles of structural analysis of composite bridge decks together with possible approaches for their application to design were addressed. An overview of the actions to be considered as well as the applicable partial factors and combination factors for the definition of code combinations was presented. The importance of the consideration of the time-dependant properties of concrete in composite structures and the current rules in EN1994-2 for their quantification were developed upon. Finally, the possibilities regarding modelling of structures for analysis and a discussion of the range of applicability the models as well as their limitations were explained, together with effects that are particular to composite structures and need be considered in their design.

4
DESIGN OF COMPOSITE CROSS-SECTIONS

4.1. CLASSIFICATION OF CROSS-SECTIONS

The verification of the resistances of a composite cross-section must start with the classification of its individual steel parts. EN1994-2 §5.5.1(1) states that the classification system defined in EN1993-1-1 also applies to cross-sections of composite beams.

The purpose of the classification system advocated by EN1993-1-1 is to identify to which extent the cross-section resistance and its rotation capacity will be influenced by the local buckling of the cross-section components. The cross-section classification is thus a function of the stress distribution in the compressed elements of the cross-section at ultimate limit states (Rueda, 2009).

The governing principles of cross-section classification are explained in EN1993-1-1 §5.5. The classification of a cross section depends on the width to thickness ratio of its parts that are either totally or partially subject to compression. The cross-section class is that of its least favourable compression part. Four cross-section classes are defined:

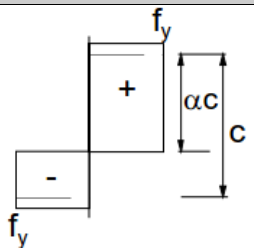
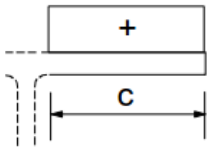
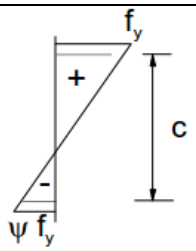
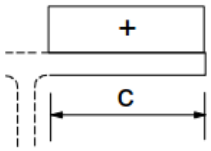
- Class 1 cross-sections (plastic), which possess a rotation capacity adequate for the formation of plastic hinges required for plastic analysis without reduction of resistance;
- Class 2 cross-sections (compact), whilst being capable of developing their plastic moment resistance have limited rotation capacity;
- Class 3 cross-sections (semi-compact), where the extreme compression fibre can reach the yield stress assuming an elastic stress distribution, but local buckling prevents the development of the plastic moment resistance;
- Class 4 cross-sections (slender), whose resistance is limited by local buckling which will occur at stresses below the yield stress of one or more of the cross section parts.

The maximum width-to-thickness ratios for compression parts that define the slenderness limits between classes are given in Table 5.2 of EN1993-1-1, with Sheet 1 applicable to internal compression parts and Sheet 2 to outstand flanges. An internal compression part is an element bordered on opposite edges by perpendicular elements, as is the case of the web of an I-girder. The outstand flange is the compressed flange of the I-girder, either top or bottom depending on the acting moment (Davaine et al, 2007).

4.1.1. DETERMINATION OF THE CROSS-SECTION CLASS

As per EN1994-2 §5.5.1(4), in order to determine the class of a cross-section part it should first be assumed that the section is able to develop its plastic resistance. The position of the plastic neutral axis is then used to determine the slenderness limit of each cross-section part for Class 1 and 2. The width-to-thickness ratio of the parts are then compared with their slenderness limits, thus checking the initial assumption on the usage of plastic resistance. When a cross section part fails the plastic resistance criteria the elastic stress distribution at ultimate limit state should then be used to determine the slenderness limit between Class 3 and 4. If the width-to-thickness ratio of a cross section part exceeds this limit it will be classified as Class 4 (Davaine et al, 2007).

Table 4.1 - Maximum width-to-thickness ratios for compression parts as per Table 5.2 of EN1993-1-1.

Section Part Classification	Internal Compression Parts (subject to bending and compression)	Outstand Flanges (subject to compression)
Stress Distribution		
Class 1	when $\alpha > 0.5$: $c/t \le \frac{396 \cdot \varepsilon}{13 \cdot \alpha - 1}$ when $\alpha \le 0.5$: $c/t \le \frac{36 \cdot \varepsilon}{\alpha}$	$c/t \le 9 \cdot \varepsilon$
Class 2	when $\alpha > 0.5$: $c/t \le \frac{456 \cdot \varepsilon}{13 \cdot \alpha - 1}$ when $\alpha \le 0.5$: $c/t \le \frac{41.5 \cdot \varepsilon}{\alpha}$	$c/t \le 10 \cdot \varepsilon$
Stress Distribution		
Class 3	when $\psi > -1$: $c/t \le \frac{42 \cdot \varepsilon}{0.67 + 0.33 \cdot \psi}$ when $\psi \le -1$: $c/t \le 62 \cdot \varepsilon \cdot (1 - \psi) \cdot \sqrt{-\psi}$	$c/t \le 14 \cdot \varepsilon$
Notes:	i.) $\varepsilon = \sqrt{235/f_y}$ ii.) $\psi \le -1$ applies where compression stress $\sigma < f_y$	

It is also stated in EN1994-2 §5.5.1(4) that the elastic stress distribution should account for the construction sequence as well as the effects of creep and shrinkage, and that design values of material strengths should be used. To account for the construction sequence implies that the stress distribution used for classification of the cross-section should reflect the superposition of stresses in the bare steel section during construction stages with the stresses in the composite section in service conditions. Provided that the composite section properties were calculated using the modular ratios defined in EN1994-2 §5.4.2.2(2) the effects of creep will have indirectly been taken into account.

The steel sections used in composite plate girders are typically monosymmetric, with unequal top and bottom flanges. As a consequence, the net sectional forces on a web plate derived from its longitudinal stress distribution are comprised of a bending moment and an axial force. For this reason internal compression parts usually need to be classified as parts subject to bending and compression, as indicated in the right-hand column of Sheet 1 of Table 5.2 of EN1993-1-1. As for the compressed flange of the steel section, it will typically be classified as a part subject to compression only.

A set of additional clauses applicable to the classification of composite cross-sections is given in EN1994-2 §5.5.2. In the case of a steel flange in compression that is connected to a concrete flange by shear studs local buckling can be assumed to be restrained, provided the connectors spacing is in accordance with EN1994-2 §6.6.5.5. For cross-sections where both flanges are of Class 1 or 2 with the web in Class 3 it is permitted to treat the section as an effective Class 2 cross-section, with an effective web being considered as per EN1993-1-1 §6.2.2.4. This clause gives the designer the interesting possibility of using the plastic bending resistance even for semi-compact cross-sections.

In classifying cross-sections of composite bridge decks it is often the case that its Class will vary from construction stages to service condition. The steel only sections during construction are typically Class 3 or even 4. When composite in service conditions the restraint of the concrete slab to the top flange in sagging moment regions means these cross-sections are easily within Class 1 or 2, with a very small portion of the web in compression or even fully in tension. Conversely, cross-sections in hogging moment regions typically present a fairly important part of the web in compression and are more often of Class 3 or 4 (Davaine et al, 2007).

4.1.2. Effective Section of Class 4 Cross-Sections

For Class 4 cross-sections EN1993-1-1 §5.5.2(2) states that the effects of local buckling on reduction of resistances may be accounted for by the use of effective widths as per EN1993-1-5 §4.4. The flanges of plate girders are typically compact parts either in Class 1 or 2, so that an effective width will only need to be considered for the part of the web in compression in bending.

In accordance with §4.4(1) the effective area of the compression zone $A_{c,eff}$ of a plate should be obtained from the gross area of the compression zone by a reduction factor ρ for plate buckling as follows:

$$A_{c,eff} = \rho \cdot A_c \tag{4.1}$$

Where

ρ - is the reduction factor for plate buckling

A_c - is the area of the compression zone

For internal compression elements such as the webs of plate girders the plate buckling reduction factor is given by:

$$\begin{cases} \rho = 1.0 \quad \text{for } \bar{\lambda}_p \le 0.5 + \sqrt{0.085 - 0.055 \cdot \psi} \\ \rho = \dfrac{\bar{\lambda}_p - 0.055 \cdot (3 + \psi)}{\bar{\lambda}_p^2} \quad \text{for } \bar{\lambda}_p > 0.5 + \sqrt{0.085 - 0.055 \cdot \psi} \end{cases} \tag{4.2}$$

With

$$\bar{\lambda}_p = \sqrt{\frac{f_y}{\sigma_{cr}}} = \frac{\bar{b}/t}{28.4 \cdot \varepsilon \cdot \sqrt{k_\sigma}} \tag{4.3}$$

Where

ψ - is the ratio between the tensile and compressive stresses at the extreme fibres of the plate

$\bar{b}$ - is the appropriate panel width to consider, which may be taken as the web depth h_w

t - is the panel thickness, which in this case is the web thickness t_w

k_σ - is the plate buckling factor corresponding to the stress ratio ψ and the boundary conditions

The plate buckling factor k_σ for internal compression elements is obtained from the expressions given in Table 4.1 of EN1993-1-5. For the webs of plate girders subject to bending and compression the stress distribution over the depth of the plate will vary linearly from a maximum compressive stress to a minimum tensile stress. For this reason it is usual that only negative values of the stress ratio ψ need be considered in the calculation of the buckling reduction factor.

$$\begin{cases} k_\sigma = 7.81 - 6.29 \cdot \psi + 9.78 \cdot \psi^2 \quad \text{for} \quad 0 > \psi > -1 \\ k_\sigma = 5.98 \cdot (1 - \psi^2) \quad \text{for} \quad -1 \ge \psi > -3 \end{cases} \tag{4.4}$$

With the reduction factor for plate buckling ρ defined the effective depth b_{eff} of the compression zone can then be determined:

$$b_{eff} = \rho \cdot b_c = \rho \cdot \frac{h_w}{1 - \psi} \tag{4.5}$$

The calculated effective web depth will then be split in two compression areas: one extending from the root of the web at the compression flange down into the web panel with a depth b_{e1}, and another one extending from the elastic neutral axis into the compressed portion of the web with a depth b_{e2} (Fig.4.1). The depth of these compression areas is given by:

$$\begin{cases} b_{e1} = 0.4 \cdot b_{eff} \\ b_{e2} = 0.6 \cdot b_{eff} \end{cases} \tag{4.6}$$

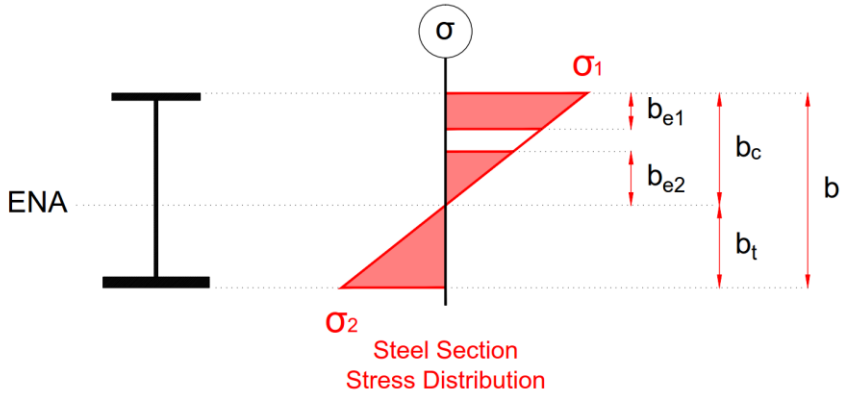


Fig. 4.1 – Effective web of Class 4 cross-section.

In composite bridges the cross-section classification at a given location may vary between different construction stages. In this event, EN1994-2 §6.2.1.5(7) recommends that the sum of the stresses from different construction stages calculated based on gross sections is used for calculating the effective steel cross-section at the time considered.

4.2. CROSS-SECTION VERIFICATION FOR ULTIMATE LIMIT STATES

The verification of composite cross-section beam resistances has a broad scope that is addressed in the Eurocode suite of standards by EN1992, EN1993 and EN1994 in the case of beam bridges. The resistance checks for ultimate limit states should cover:

- Bending resistance as per EN1994-2 §6.2.1;
- Resistance to vertical shear:
  - Plastic resistance to vertical shear as per EN1993-1-1 §6.2.6.
  - Shear buckling resistance as per EN1993-1-5 §5.
  - Bending and vertical shear interaction as per EN1994-2 §6.2.2.4.
- Lateral torsional buckling of composite beams as per EN1994-2 §6.4.
- Resistance to longitudinal shear:
  - Longitudinal shear at steel-concrete interface as per EN1994-2 §6.6.2.
  - Resistance of headed stud connectors as per EN1994-2 §6.6.3.
- Resistance to fatigue as per EN1994-2 §6.8.

The effective widths to consider in the cross-section verification are determined in accordance with EN1994-2 §5.4.1.2. Unlike in the global analysis of a bridge structure where a single representative value of the effective width may be taken for the whole span, for the cross sectional checks an effective width appropriate for the section under consideration should be used as stated in §6.1.2(1) (Hendy and Johnson, 2006). The distribution of effective widths between support and span regions is given in Fig. 5.1 of EN1994-2.

4.2.1. CROSS-SECTION BENDING RESISTANCE

The bending resistance of composite beams is addressed in §6.2.1 of EN1994-2 where three approaches are given for the calculation of bending resistances, namely: rigid-plastic theory, non-linear theory and elastic analysis.

The use of rigid-plastic theory is limited to Class 1 and 2 cross-sections and where prestressing by tendons is not used. The latter prescription is due to the need of assessing the tendon stress which may be below yield, hence a non-linear resistance calculation is deemed more adequate (Hendy and Johnson, 2006).

Non-linear theory and elastic analysis are applicable to any cross-section class. It may be assumed that the cross-section remains plane in deformation provided that the design is in accordance with the general principles of EN1994-2 §6.6, the implication being that longitudinal slip between steel and concrete is negligible.

A common principle for all the above approaches for calculating the bending resistance of composite beams is that the tensile strength of concrete shall always be neglected.

4.2.1.1. Plastic Resistance Moment

The assumptions to be made for the assessment of the bending resistance of a composite beam in accordance with rigid-plastic theory are stated in EN1994-2 §6.2.1.2.

It is assumed that there is full interaction of the cross-section elements (steel, reinforcement and concrete), meaning that there is no slip at the steel-concrete interface. The effective areas of the structural steel section parts are assumed to be stressed to their design yield strength f_{yd} both in tension

and compression, as well as the effective areas of longitudinal reinforcement which are stressed to their yield strength f_{sd}. For concrete in compression a constant stress block of $0.85 \cdot f_{cd}$ is assumed over the entire depth from the plastic neutral axis to the outermost compressed fibre of the concrete section.

The position of the plastic neutral axis is determined by equilibrium considering the forces acting on each element of the cross section: the parts of the steel section (web and flanges), the longitudinal reinforcement within the effective width of the slab, and the effective concrete flange. The resulting plastic resistance moment $M_{pl,Rd}$ is then obtained from the summation of the forces of each section part times their respective lever arms. The contribution of the reinforcement in compression in a concrete slab is usually ignored.

For cross-sections under sagging bending moment the plastic neutral axis often lies within the slab depth, with the steel section fully in tension (Fig. 4.2). In the case of hogging bending moment the plastic neutral axis will typically be located within the web of the steel section (Fig. 4.3).

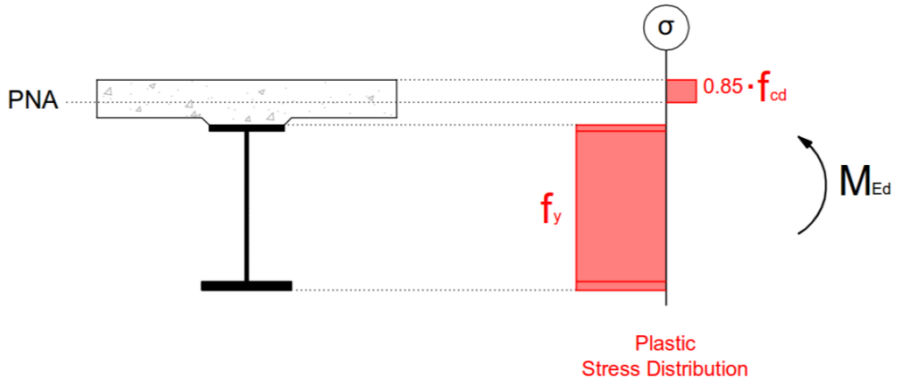


Fig. 4.2 – Stress distribution for plastic sagging resistance moment.

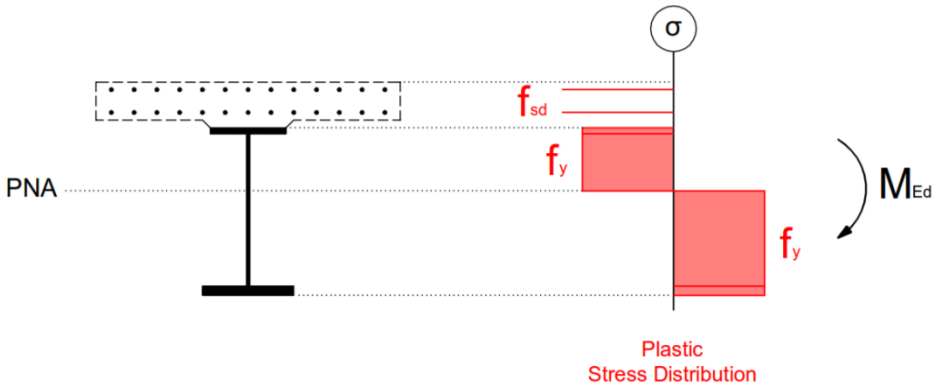


Fig. 4.3 – Stress distribution for plastic hogging resistance moment.

It should be noted that EN1994-2 allows the consideration of a constant stress block over the entire depth x of the concrete in compression, as opposed to the $0.8 \cdot x$ depth used in EN1992-1-1. The stress block from EN1992-1-1 was deemed inconvenient for use with composite cross-sections because the

region near the neutral axis assumed to be unstressed may include a steel flange, with the algebraic expressions for bending resistance becoming needlessly complicated (Hendy and Johnson, 2006).

As mentioned in the previous section, there is scope in EN1994-2 §5.5.2(3) for a cross-section with flanges in Class 1 or 2 and a web in Class 3 to be treated as an effective Class 2 cross-section. Reference is made to EN1993-1-1 §6.2.2.4 for the definition of the effective web. The clause states that the compressed portion of the web should be replaced by two parts with a depth of $20 \cdot \varepsilon \cdot t_w$, one adjacent to the compression flange the other to the plastic neutral axis (Fig. 4.4). The position of the plastic neutral axis will need to be determined from equilibrium of the forces acting on the effective cross-section (Davaine et al, 2007).

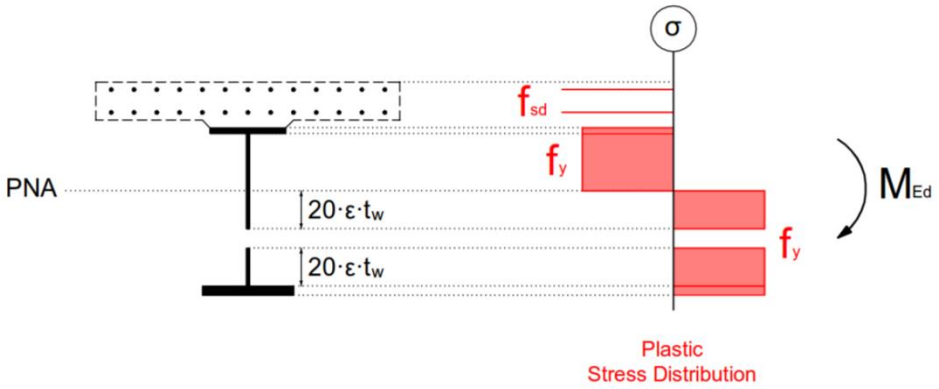


Fig. 4.4 – Stress distribution on effective section for plastic hogging resistance moment.

An important additional rule regarding the use of plastic bending resistance is given in EN1994-2 §6.2.1.3(2). The clause states that for Class 1 or 2 cross-sections in sagging bending the acting moment M_{Ed} should not exceed $0.9 \cdot M_{pl,Rd}$ where the support cross-section is in Class 3 or 4 and the ratio of the spans adjacent to the support is less than 0.6.

The basis for this limitation is the fact that the use of plastic resistances in bending implies the shedding of bending moments, typically from span regions to adjacent support sections. The acting moment M_{Ed} obtained from linear elastic global analysis takes no account of the resulting redistribution of bending moments, hence it would be possible that a Class 3 or 4 section at an internal support might be overstressed from moments shed from the Class 1 or 2 span section. For a span ratio of 0.6 the loadcase leading to the maximum sagging moment in the span is close to that of the maximum hogging moment at the support, and consequently the effects of moment redistribution could be harmful. Such a scenario is avoided by limiting resistance to $0.9 \cdot M_{pl,Rd}$ (Davaine et al, 2007).

4.2.1.2. Non-Linear Resistance Moment

The use of a non-linear resistance model for the calculation of the bending resistance of composite sections can be extended to any cross-section regardless of its classification, as stated in EN1994-2 §6.2.1.1(2). The specific rules applicable to this resistance model are given in EN1994-2 §6.2.1.4.

When using this model for determining the bending resistance of a cross-section the stress-strain relationships of its constitutive materials must be used:

- For concrete, the stress-strain parabola-rectangle diagram given in EN1992-1-1 §3.1.7;
- For reinforcement, the bi-linear diagram given in EN1992-1-1 §3.2.7;
- For structural steel, the bi-linear diagram given in EN1993-1-1 §5.4.3(4).

As can be seen on Fig.4.5 all three diagrams of the materials are characterised by non-linear stress-strain relationships.

The parabola-rectangle diagram of concrete is defined by the concrete design compressive strength f_{cd}, the strain at which maximum strength is reached ε_{c2} and the ultimate strain ε_{cu2}, which in accordance with Table 3.1 of EN1992-1-1 are 2‰ and 3.5‰ respectively.

The bi-linear diagram of reinforcement steel is defined by an initial linear branch where the slope corresponds to the modulus of elasticty of steel E_s up to the design yield strength of reinforcement f_{sd}, followed by a strain-hardening branch up to the ultimate strain ε_{ud}. The values of the ultimate strain ε_{uk}.and the corresponding maximum stress $k{\cdot}f_{sd}$ depend on the reinforcement class, and are given in Annex C of EN1992-1-1.

The bi-linear diagram of structural steel is that of an elastic-perfectly plastic material, where an inclined branch with the slope of the modulus of elasticity E_a up to the design yield strength f_y is followed by a horizontal plateau of constant stress until the ultimate strain ε_u is reached.

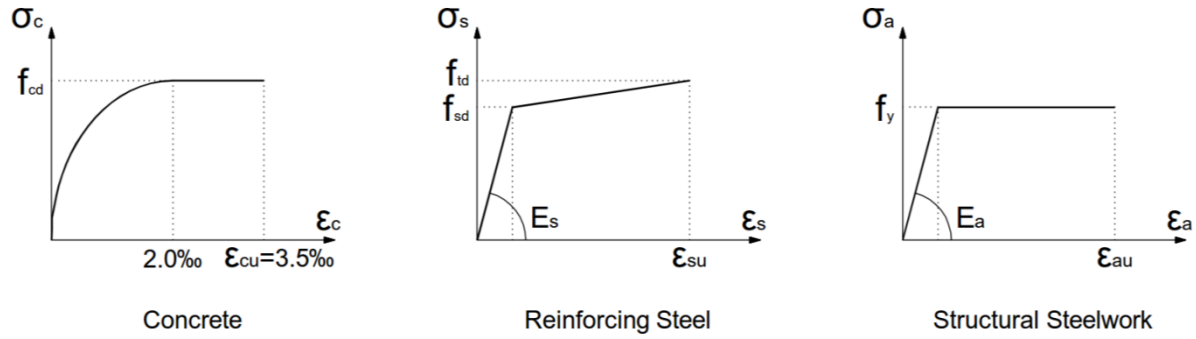


Fig. 4.5 – Stress-strain diagrams for non-linear resistance model.

The ultimate strain is not defined in EN1993-1-1, and the general view in specialist literature is that prudence is advised. The recommendations of BS5400, which were the previous UK bridge design standards, were that the strains in structural steelwork should be limited to the yield strain in the compressed portions of the cross-section and twice as much for the portions in tension (Rueda, 2009).

The calculation of the resistance of a cross-section by the non-linear resistance method is an iterative process, where an initial curvature and the position of the neutral axis need to be assumed. The resulting stresses are then used to calculate the forces in each part of the cross section and the section is checked for equilibrium. The position of the neutral axis is moved with each iteration until equilibrium is satisfied, at which point the bending resistance is calculated from the stress distribution obtained (Fig. 4.6). Given the iterative nature of this method it clearly lends itself to the use of software (Hendy and Johnson, 2006).

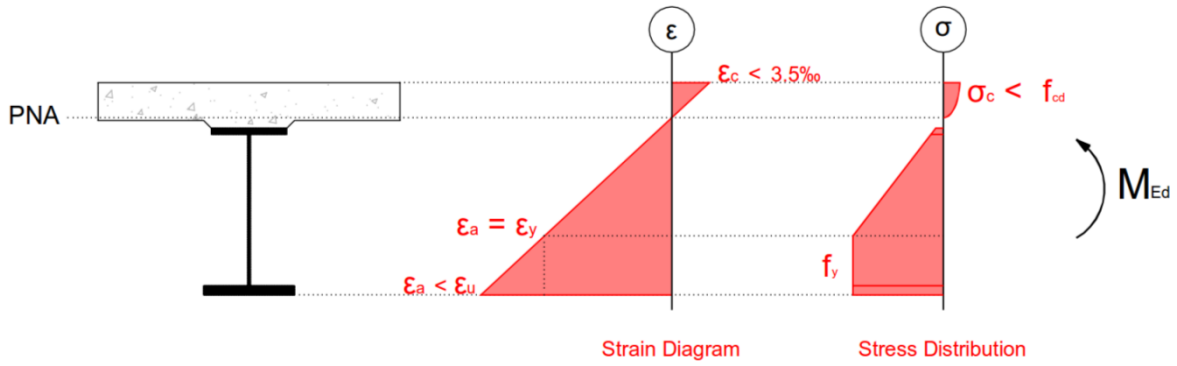


Fig. 4.6 – Stress distribution for elasto-plastic sagging resistance moment.

It should be noted that while the application of elasto-plastic model that characterises the non-linear bending resistance is permitted for all cross-section classes the strain limits used should be consistent with the section classification. For Class 3 cross-sections or Class 4 effective cross-sections the compressive strain in the structural steel should be limited to first yield (Hendy and Johnson, 2006).

The use of the elasto-plastic model is somewhat redundant for Class 1 and 2 cross-sections for which plastic resistance can be fully mobilised, hence its interest will lie in the enhanced capacity that can be achieved for Class 3 and Class 4 cross-sections. When yielding first occurs on the tension side of a Class 3 cross-section EN1993-1-1 §6.2.1(10) allows for the plastic reserves in the tension zone to be considered when determining its bending resistance, allowing for a more efficient use of the tension resistance of the steel section (Rueda, 2009).

A simplified method applicable to Class 1 and 2 cross-sections with the concrete flange in compresion, i.e. sagging bending moment, is given in §6.2.1.4(6). The proposed calculation procedure determines the non-linear resistance to bending as a function of the compressive force in the concrete slab using a set of simplified expressions.

4.2.1.3. Elastic Resistance Moment

The elastic resistance moment is applicable to cross-sections of any classification as per EN1994-2 §6.2.1.5. The cross-section stress distribution should be calculated by elastic theory considering the effective width of the concrete flange at the section being studied.

When calculating the elastic bending resistance of a cross-section the limiting stresses on the cross-section parts to consider are:

- For the concrete in compression, f_{cd};
- For the structural steel, either in tension or compression, f_y;
- For reinforcemente in tension or compression, f_{sd}.

The need to consider the stress build-up in the section taking account of the stresses due to actions on the bare steel section during construction stages and stresses from actions on the composite section is emphasized in §6.2.1.5(3) (Fig.4.7). The reason for this is that for unpropped construction, as is typical of composite bridge decks, the elastic bending resistance depends on the proportion of the total load applied before the member is composite. The available stress range for the load portion applied to the composite member will hence be lower than the design yield strength f_y.

Although not explicit, the above is actually covered in the previous section of EN1994-2 in relation to the simplified method for non-linear bending resistance given in §6.2.1.4(6) where the elastic resistance moment is defined as:

$$M_{el,Rd} = M_{a,Ed} + k \cdot M_{c,Ed} \tag{4.7}$$

Where

$M_{a,Ed}$ - is the design bending moment applied to the bare steel section

$M_{c,Ed}$ - is the design bending moment applied to the composite section

k - is the lowest factor such that a stress limit in a part of the section is reached

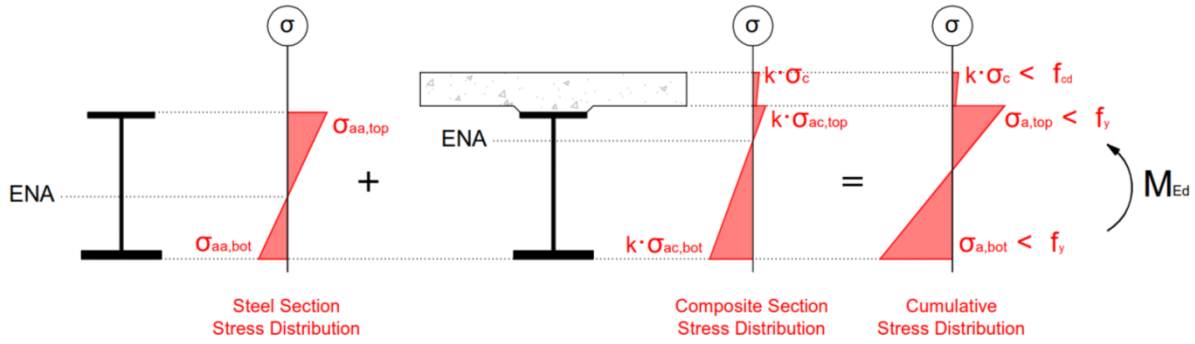


Fig. 4.7 – Cumulative stresses for calculation of the elastic resistance moment.

Since construction of composite bridge decks is usually unpropped, in most cases a stress limit will be reached in the steel section first. In such a scenario the bare steel section will have experienced significant stresses before the member is composite. The factor *k* so that a stress limit is reached in a fibre of the steel section is then:

$$k = \frac{f_y - \sigma_{a,Ed}}{\sigma_{c,Ed}} \tag{4.8}$$

Where

f_y - is the design strength of the part of the steel section under consideration

$\sigma_{a,Ed}$ - is the design stress in the fibres of the steel section from the portion of the load applied to the bare steel member.

$\sigma_{c,Ed}$ - is the design stress in the fibres of the steel section from the portion of the load applied to the composite member.

For Class 4 cross-sections two options are at the disposal of the designer for the calculation of the elastic bending resistance:

- The effective section method;
- The reduced stress method.

For standard cross-section geometries where its application is straightforward the effective section method is very efficient because it accounts not only for the post-critical reserve in the plate elements but also for load shedding between cross-section parts.

The general format of the reduced stress method offers advantages where geometrically complex cross-section shapes or non-uniform members are to be studied. While the method fully accounts for the post-critical reserve in plate elements it does not consider load-shedding between cross-section parts. It is the most versatile method, but at the expense of extensive use of computer analysis of local buckling of sub-panels of the cross-section in order to determine a permissible stress limit

If the effective section method is chosen EN1994-2 §6.2.1.5(7) recommends that the effective steel cross-sections at each stage of construction be obtained from the sum of the stresses considering gross cross-sections at each stage. The stresses on the effective cross-sections thus obtained should then be used in the cross-section verification.

Where the designer opts instead for the use of the reduced stress method gross section properties are used to determine resistance with a permissible stress lower than the yield strength of steel. The rules for the calculation of the stress reduction factors are given in Section 10 of EN1993-1-5.

4.2.2. Cross Section Resistance to Vertical Shear

The resistance to vertical shear as understood in EN1994-1 §6.2.2 applies to composite beams with rolled or welded steel sections with solid webs, stiffened or unstiffened, and without web encasement. The whole of the vertical shear is assumed to be carried by the steel section only, although §6.2.2.2(1) and §6.2.2.3(2) allow for the contribution of the concrete part to be considered. While the slab contribution may be significant where the steel section height is less than twice the concrete slab depth, it is customarily ignored in practice (Hendy and Johnson, 2006).

The design shear resistance of a web plate should be taken as the lesser of the plastic shear resistance and the shear buckling resistance. The consideration of either the plastic shear resistance or the shear buckling resistance depends on the web plate slenderness, which should be assessed against the slenderness limits given in EN1993-1-5 §5.1(2). Compact plates are deemed to be able to develop their plastic shear resistance, where the full depth of the web is assumed to reach the plastic shear stress $\tau_{pl} = f_y / \sqrt{3}$. In the case of slender web plates, their resistance will typically be limited by the onset of web buckling occurring for a critical shear stress τ_{cr} lower than the plastic shear stress τ_{pl}.

In order to assess whether or not a web plate is prone to shear buckling the depth-to-thickness ratio of the plate should be compared with the slenderness limits given in EN1993-1-5 §5.1(2):

$$\begin{cases} \dfrac{h_w}{t_w} > \dfrac{72}{\eta} \cdot \varepsilon \quad \text{, for unstiffened webs} \\ \dfrac{h_w}{t_w} > \dfrac{31}{\eta} \cdot \varepsilon \cdot \sqrt{k_\tau} \quad \text{, for stiffened webs} \end{cases} \tag{4.9}$$

Where

h_w - is the web plate depth

t_w - is the web plate thickness

$\varepsilon = \sqrt{235/f_y}$

η - is a factor to be taken as 1.0 for all steel grades as per EN1993-1-5 §NA.2.2

k_τ - is the shear buckling coefficient given in Annex A.3 of EN1993-1-5.

For plates with rigid transverse stiffeners and without longitudinal stiffeners the shear buckling coefficient will take the form:

$$\begin{cases} k_\tau = 5.34 + 4.00 \cdot (h_w/a)^2 & \text{, when } a/h_w \geq 1 \\ k_\tau = 4.00 + 5.34 \cdot (h_w/a)^2 & \text{, when } a/h_w < 1 \end{cases} \quad (4.10)$$

Where

h_w - is the web plate depth

a - is the distance between transverse stiffeners

4.2.2.1. Plastic Resistance to Vertical Shear

In accordance with EN1994-2 §6.2.2.2 the design plastic resistance to vertical shear of a web plate should determined as per EN1993-1-1 §6.2.6(2).

$$V_{pl,a,Rd} = \frac{A_v \cdot (f_y/\sqrt{3})}{\gamma_{M0}} = \frac{h_w \cdot t_w \cdot f_{yw}}{\sqrt{3} \cdot \gamma_{M0}} \quad (4.11)$$

Where

A_v - is the cross-sectional area of the web plate

h_w - is the depth of the web plate between flanges of the plate girder

t_w - is the thickness of the web plate

f_{yw} - is the design yield strength of the web plate

γ_{M0} - is the partial material factor of steel for resistance of cross-sections, taken as 1.00 as per Table 6.1 of EN1993-2.

4.2.2.2. Shear Buckling Resistance to Vertical Shear

In the case of slender web plates their shear resistance will usually be limited by web buckling due to shear stress. The study of the behaviour of plates under shear will need to address a state of pure shear stress and the post-critical tension field action.

Prior to buckling, i.e for shear stresses τ lower than the critical shear stress τ_{cr}, pure shear stresses occur in the plate. If these shear stresses are transformed into principal stresses they will correspond to a principal tensile stress σ_1 and a principal compressive stress σ_2 (Fig. 4.8). The principal stresses are of equal magnitude and inclined at 45° with the longitudinal girder axis (Beg et al, 2010).

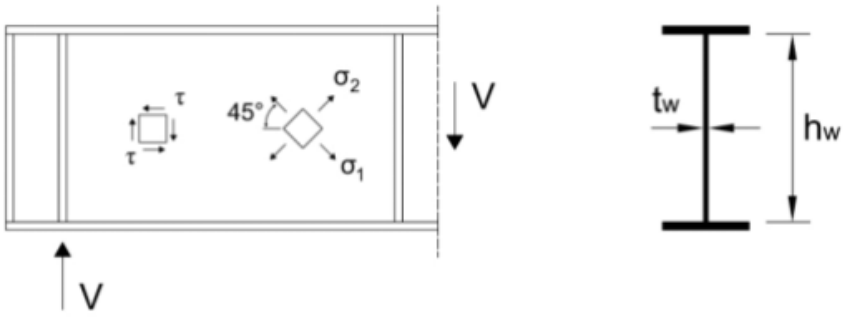


Fig. 4.8 – Pure shear stress state in a web plate (from *Design of Plated Structures*, ECCS, 2010)

As the shear stress τ increases beyond the critical stress τ_{cr} a shear buckle forms in the direction of the principal tensile stress σ_1. With the onset of buckling there cannot be an increase in the principal compressive stress σ_2, which is then limited to the critical stress τ_{cr}. However, the principal tensile stress σ_1 can still increase and hence principal stress values of different magnitude will occur, leading to a rotation of the stress field and the development of a membrane stress for equilibrium reasons (Fig. 4.9). This post-critical behaviour is denoted as "tension field action" (Beg et al, 2010).

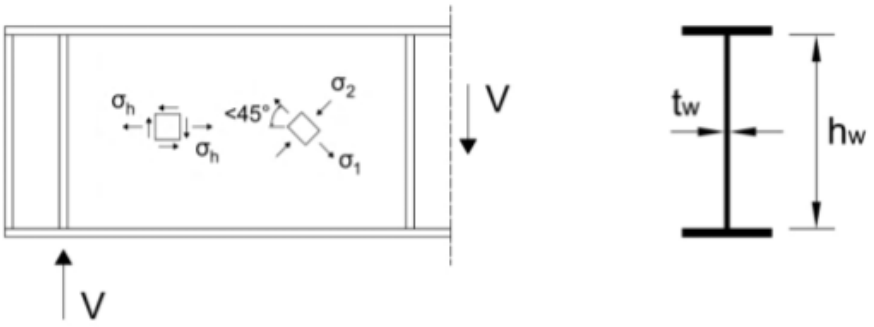


Fig. 4.9 – Post-critical stresses in a web plate (from *Design of Plated Structures*, ECCS, 2010)

The development of membrane stress is only possible if the boundary elements of the web panel provde anchorage to the tensile forces. For this reason transverse stiffeners will be required at the supports, where the flanges restrain the in-plane deformation of the stiffeners allowing the tension filed to be anchored (Fig. 4.10). The maximum axial force that can be carried will depend on the flexural stiffness of the transverse stiffener (Beg et al, 2010).

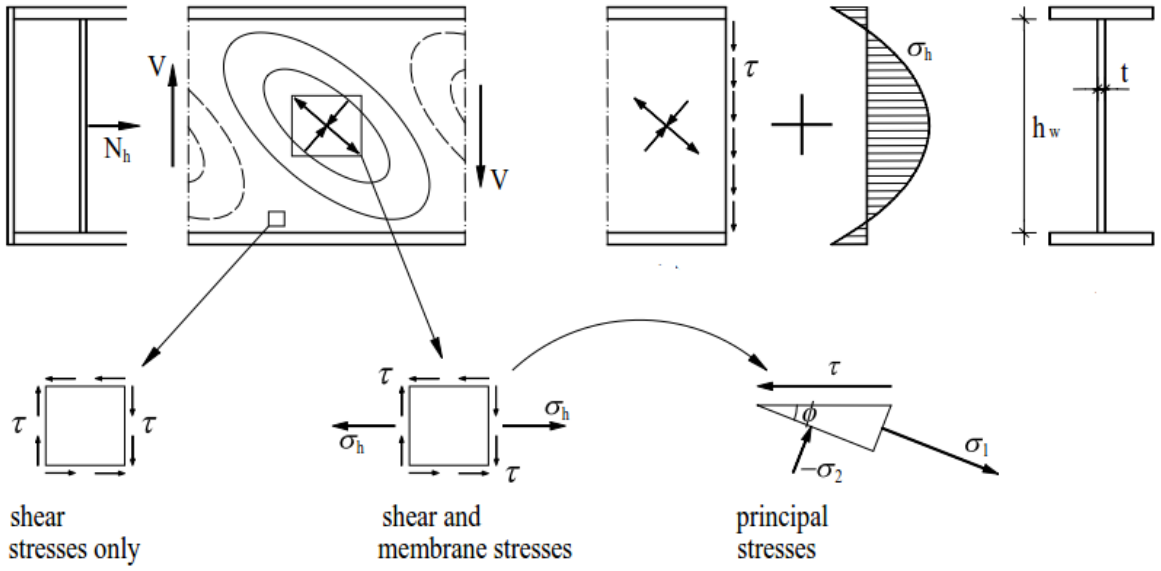


Fig. 4.10 – Mechanical model of the rotated stress field (from *Commentary and Worked Examples to EN1993-1-5*, ECCS, 2007)

The rotated stress field method was adopted in EN1993-1-5 because it provides adequate results regardless of the aspect ratios of the web plate panels. The design shear buckling resistance as given in EN1993-1-5 §5.2 is comprised of contributions from the web and the flanges, but always limited to the plastic resistance of the web alone:

$$V_{b,Rd} = V_{bw,Rd} + V_{bf,Rd} \quad \leq \quad \frac{\eta \cdot f_{yw} \cdot h_w \cdot t_w}{\sqrt{3} \cdot \gamma_{M1}} \tag{4.12}$$

Where

$V_{bw,Rd}$ - is the contribution from the web

$V_{bf,Rd}$ - is the contribution from the flanges

η - is a factor to be taken as 1.0 for all steel grades as per EN1993-1-5 §NA.2.2

h_w - is the depth of the web plate between flanges

t_w - is the thickness of the web plate

f_{yw} - is the design yield strength of the web plate

γ_{M1} - is the partial material factor of steel for resistance of members to instability, taken as 1.10 as per Table 6.1 of EN1993-2.

The contribution of the flanges can only be considered provided that the design working stress of the flanges is lower than the yield strength of the flange plate. An economic design will typically strive to make the most efficient use of materials, hence it is unlikely that there will be an available stress range in the flanges to consider. For this reason the flange contribution is customarily ignored for design purposes.

The web contribution for the design shear buckling resistance is obtained by considering a shear buckling reduction factor χ_w that accounts for components of pure shear as well as anchorage of membrane forces by transverse stiffeners due to tension field action (Beg et al, 2010).

$$V_{bw,Rd} = \frac{\chi_w \cdot f_{yw} \cdot h_w \cdot t_w}{\sqrt{3} \cdot \gamma_{M1}} \tag{4.13}$$

Where

χ_w - is the shear buckling factor

h_w - is the depth of the web plate between flanges

t_w - is the thickness of the web plate

f_{yw} - is the design yield strength of the web plate

γ_{M1} - is the partial material factor of steel for resistance of members to instability, taken as 1.10 as per Table 6.1 of EN1993-2.

As mentioned previously, the flexural stiffness of the transverse stiffners governs the anchorage of the stress field, and hence EN1993-1-5 makes a distinction in Table 5.1 between webs with rigid and non-rigid end posts for the calculation of the shear buckling factor χ_w.

Table 4.2 - Shear buckling factor as per Table 5.1 of EN1993-1-5.

Non-Dimensional Slenderness λ_w	χ_w Rigid End Post	χ_w Non-Rigid End Post
$\bar{\lambda}_w < 0.83/\eta$	η	η
$0.83/\eta \le \bar{\lambda}_w < 1.08$	$0.83/\bar{\lambda}_w$	$0.83/\bar{\lambda}_w$
$\bar{\lambda}_w \ge 1.08$	$1.37/(0.7+\bar{\lambda}_w)$	$0.83/\bar{\lambda}_w$

The shear buckling factor is obtained as function of the modified slenderness , which in turn is dependant on the critical shear buckling stress of the web plate:

$$\bar{\lambda}_w = \sqrt{\frac{f_{yw}/\sqrt{3}}{\tau_{cr}}} \tag{4.14}$$

With

$$\tau_{cr} = k_\tau \cdot \sigma_E \tag{4.15}$$

Where

f_{yw} - is the design yield strength of the web plate

τ_{cr} - is the critical shear buckling stress of the web plate

k_τ - is the shear buckling coefficient of the web plate as per Annex A.3 of EN1993-1-5

σ_E - is the elastic critical plate buckling stress as per Annex A.1 of EN1993-1-5

As can be seen in the above equations the critical shear buckling stress τ_{cr} of the web plate is obtained from the elastic critical plate buckling stress σ_E by means of the shear buckling coefficients k_τ. The elastic critical plate buckling stress σ_E as obtained from first principles is given in EN1993-1-5 §A.1(2).

$$\sigma_E = \frac{\pi^2 \cdot E_a \cdot t_w^2}{12 \cdot (1 - v^2) \cdot h_w^2} = 190\,000 \cdot \left(\frac{t_w}{h_w}\right)^2 \quad [\text{MPa}] \tag{4.16}$$

Where

E_a - is the modulus of elasticity of the steel

h_w - is the depth of the web plate between flanges

t_w - is the thickness of the web plate

When observing the reduction curves for shear buckling it becomes apparent how the post-critical reserve allows for a more efficient use to be made of the web plate's shear resistance (Fig. 4.11). As the non-dimensional slenderness of the web plate increases it can be seen that so does the difference between the shear buckling stress $\chi_w f_y$ and the critical shear buckling τ_{cr} stress. If the design of slender web plates was to be based on elastic critical stresses alone the shear resistance of plate girders would be severely hampered (Rueda, 2009).

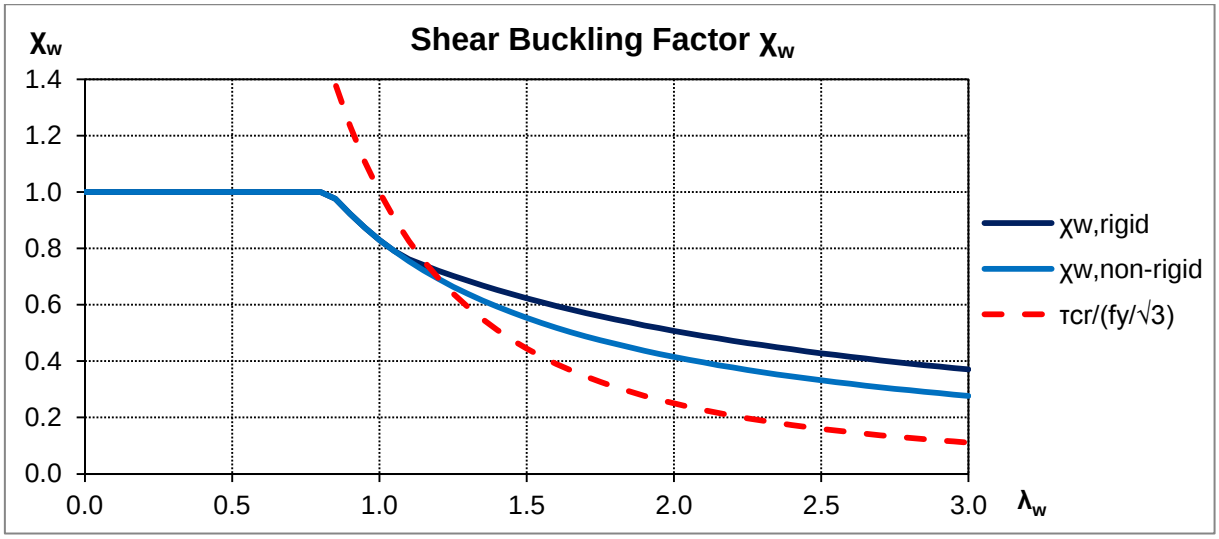


Fig. 4.11 – Reduction curves for shear buckling and critical shear stress

In internal spans of continuous girders with transverse stiffners at the supports the tension field action can be assumed to be anchored since the membrane forces developed in the web to either side of the support section must be in equilibrium. In the case of an end support the flexural stiffness of the support stiffener determines the ability of the end web panels to develop post-critical shear resistance, hence the need for a distinction between rigid and non-rigid end posts. The requirements regarding intermediate transverse stiffeners and end post stiffeners are given in Section 9 of EN1993-1-5.

4.2.2.3. Bending and Vertical Shear Interaction

In instances where the vertical shear force V_{Ed} exceeds half the design shear resistance V_{Rd} allowance needs to be made for the effects of bending and shear interaction in assessment of the cross-section resistance moment in accordance with EN1994-2 §6.2.2.4.

For cross-sections in Class 1 or 2 the recommended approach in §6.2.2.4(2) accounts for the influence of vertical shear in the resistance to bending by considering a reduced design steel strength $(1-\rho)\cdot f_y$ for the web plate (Fig. 4.12). The reduction factor ρ is given by:

$$\rho = \left(2 \cdot \frac{V_{Ed}}{V_{Rd}} - 1\right)^2 \qquad (4.17)$$

Where

V_{Ed} - is the vertical shear force

V_{Rd} - is the design shear resistance $V_{pl,Rd}$ or V_{bRd}, whichever is smaller

Evidently the calculation of the plastic resistance moment accounting for the reduced design steel strength of the web plate will determine a new location of the plastic neutral axis so that all internal forces are in equilibrium. Whereas in sagging moment regions it is unlikely that a change in the position of the plastic neutral axis would affect the cross-section classification as the neutral axis typically lies in the concrete flange, in hogging moment regions a greater depth of web panel under compression could alter its classification.

However, as stated in §6.2.2.4(4) the change in the position of the plastic neutral axis should not be taken into account for cross-section classification purposes and hence there is no need to reclassify the web plate in accordance with EN1993-1-1 §5.5. The reduction of steel strength to cater for the effect of shear in the bending resistance intends to translate observed test results. The added complexity of reclassifying the cross-section would be unjustified given the scatter of data observed for section classification (Hendy and Johnson, 2006).

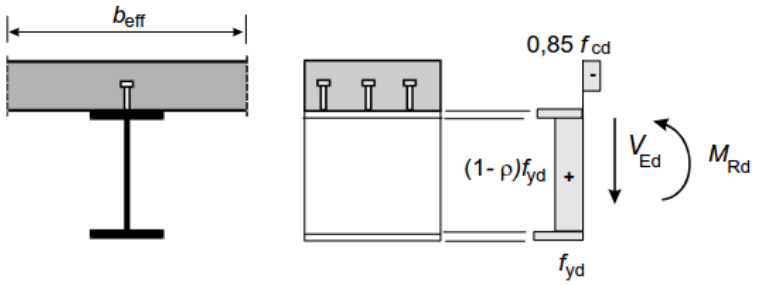


Fig. 4.12 – Plastic stress distribution modified by the effect of vertical shear (from *EN 1994-2:2005*, BSI, 2008)

In the case of Class 3 or 4 cross-sections §6.2.2.4(3) recommends that the prescriptions of EN1993-1-5 §7.1 be adhered to, although subject to modification to consider the load effects and resistances of the composite cross-section. The interaction formula for the resistance check as given in EN1993-1-5 §7.1(1) is:

$$\bar{\eta}_1 + \left(1 - \frac{M_{f,Rd}}{M_{pl,Rd}}\right) \cdot \left(2 \cdot \bar{\eta}_3 - 1\right)^2 \le 1.0 \quad \text{for} \, \bar{\eta}_1 \ge \frac{M_{f,Rd}}{M_{pl,Rd}} \tag{4.18}$$

Where

$M_{pl,Rd}$ - is the design plastic resistance moment of the cross section considering the fully effective web irrespective of its section class

$M_{f,Rd}$ - is the design plastic resistance moment of the section consisting only of the flanges

$$\bar{\eta}_1 = \frac{M_{Ed}}{M_{pl,Rd}}$$

$$\bar{\eta}_3 = \frac{V_{Ed}}{V_{bw,Rd}}$$

$V_{bw,Rd}$ - is the contribution of the web for the design shear resistance

Altough the resistance criteria given in EN1993-1-5 §7.1 relates to plated structural elements EN1994-2 §6.2.2.4(3) allows its extension to composite members by using M_{Ed} as the total bending moment on cross-section and taking both $M_{pl,Rd}$ and $M_{f,Rd}$ of the composite cross-section. The reason for the use of plastic bending properties in the interaction check for Class 3 and 4 cross-sections lies on test results on bare steel beams showing very weak interaction with shear. Since minor interaction typically developed only after 80% of the shear resistance had been reached the use of plastic bending resistances in the interaction formula aims to force the observed test behaviour (Hendy and Johnson, 2006).

In effect, the interaction formula proposed for Class 3 and 4 cross-sections demands that a dual criteria is verified so that the effects of interaction need to be given consideration. The first criteria translates whether or not the shear force can be resisted by the web alone, and the second if the bending moment can be resisted by the flanges only.

$$\begin{cases} \bar{\eta}_3 = \dfrac{V_{Ed}}{V_{bw,Rd}} \geq 0.5 \\ \bar{\eta}_1 \geq \dfrac{M_{f,Rd}}{M_{pl,Rd}} \Leftrightarrow \dfrac{M_{Ed}}{M_{pl,Rd}} \geq \dfrac{M_{f,Rd}}{M_{pl,Rd}} \Leftrightarrow M_{Ed} \geq M_{f,Rd} \end{cases} \tag{4.19}$$

Typically the interaction criterion needs to be checked for the web panels closest to the support sections in multi-span continuous girders, where high hogging moments will be coexistant with considerable shear forces.

It should be noted that both the bending moment and shear force vary along the panel, and that their maximum values at the support are usually overestimated since the beneficial effect of the real width of the bearing is often neglected. Considering that shear buckling is a panel failure mode with a buckle usually inclined less than 45° and that η_1 is a single section criterion it might prove overly conservative to check the support section for interaction. As such, EN1993-1-5 §7.1(2) states that the interaction criterion should be checked for all sections except those at a distance less than $h_w/2$ of a support section with vertical stiffeners (Fig. 4.13) (Beg et al, 2010).

Several theories for the post-critical shear buckling resistance of Class 3 and 4 webs under combined bending and vertical shear have been compared with test results. The method proposed in EN1993-1-5 §7.1 was found to provide accurate predictions for web panels with aspect ratios greater than 1.5 and conservative results for shorter panels (Hendy and Johnson, 2006).

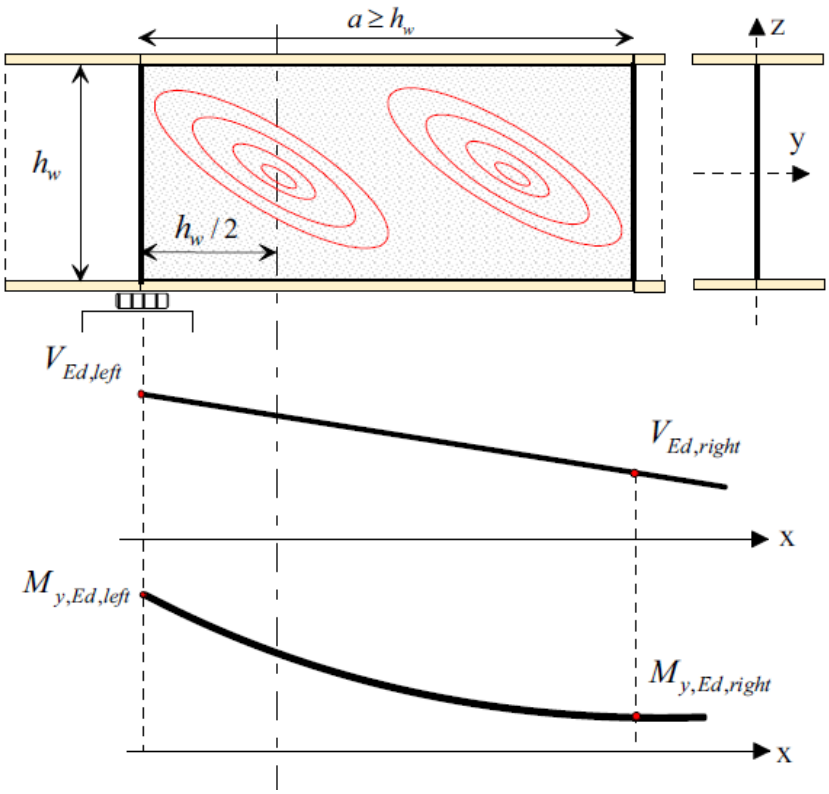


Fig. 4.13 – Region to consider the interaction of bending moment and shear force (from *Design of Plated Structures*, ECCS, 2010)

4.2.3. Cross Section Resistance to Longitudinal Shear

The transfer of longitudinal shear forces between the elements of a steel-concrete composite section needs to be assured to enable composite action to fully develop. For the flanges and web that make up the steel section this transfer is guaranteed by the welds, whereas at the steel-concrete interface a shear connection is needed for the transfer of forces to take place.

The design of the shear connection is the subject of Section 6.6 of EN1994-2, with its governing principles being given in §6.6.1:

- A shear connection together with transverse reinforcement in the concrete slab must be provided to transmit longitudinal shear between concrete and steel. The natural bond effect between the two materials will be ignored in the connection design.
- The shear connectors adopted must possess adequate deformation capacity to justify any inelastic redistribution of shear assumed in the cross-section design, namely when plastic bending resistances are considered. Ductile connectors are those with a deformation capacity consistent with the assumptions regarding ideal plastic behaviour of the shear connection.
- The shear connectors must be capable of preventing separation at the steel-concrete interface.
- Longitudinal shear failure, as well as splitting of the concrete slab due to introduction of concentrated forces by the shear connectors, must be prevented.

Numerous types of shear connectors have been used in composite bridges throughout Europe since the 1950's, such as hooks, spirals, angles and "T" sections, the headed stud connector rapidly gained prominence since its introduction in Germany in the early 1960's. While initially hampered by a

higher cost due to patent licensing issues its combined qualities of a broad range of sizes, high quality automated welding procedure, ease of execution, and simplification of detailing made them a widely adopted solution. Since the 1980's the use of headed stud connectors in design and construction of composite bridges has become almost universal (Larena, 2004) and is the typical UK practice today.

Altough EN1994-2 does not exclude the use of other types of shear connectors it is in line with the state-of-the-art of construction industry practice in that it only provides formulae for the design resistance of headed stud connectors, which are addressed in §6.6.3. The use of other types of shear connectors requires that the behaviour assumed in design be validated by testing, as stated in §6.6.1.1(12).

4.2.3.1. Longitudinal Shear Force for Beams in Bridges

In accordance with §6.6.2.1 the longitudinal shear force per unit length at the steel-concrete interface $v_{L,Ed}$ should be calculated from the rate of change of the longitudinal force in either the steel section or the concrete slab. Where cross-section bending resistance is calculated by linear elastic theory the rate of change of the longitudinal force can be obtained from the vertical shear force envelope.

Unless the effects of tension stiffening are taken into account, the elastic properties of the uncracked composite section should be used in determing the longitudinal shear force $v_{L,Ed}$, even where the effects of cracking of the concrete were considered in the global analysis, as stated in §6.6.2.2.

$$v_{L,Ed} = \frac{V_{Ed} \cdot A \cdot \bar{z}}{I} \tag{4.20}$$

Where

V_{Ed} - is the design vertical shear force

A - is the effective area on the side of the horizontal plane at the steel-concrete interface that does not include the centroid of the section

$\bar{z}$ - is the distance from the centroid of area A to the elastic neutral axis of the composite section

I - is the second moment of area of the effective uncracked composite cross-section

The reason for the use of uncracked section properties even in regions assumed to be cracked in flexure is due to the dependance of the elastic longitudinal shear flow on the consideration of cracking of the concrete slab. If the slab was assumed to be fully cracked and the longitudinal shear flow was calculated based on the shear modulus of the cracked section the longitudinal shear force would be underestimated due to the tension stiffening effect of the concrete between cracks and possible over-strength of the concrete (Hendy and Johnson, 2006). The use of uncracked section properties provides a conservative estimate of the longitudinal shear force.

When plastic bending resistances are considered in the design of Class 1 or Class 2 cross-sections the use of elastic theory for determining the longitudinal shear force is no longer valid. Due to the redistribution of direct stresses in the steel section the rate of change of the longitudinal shear force is no longer proportional to the vertical shear force. The non-linear relation between vertical and longitudinal shear within inelastic lengths of a member should be considered whenever the total design bending moment M_{Ed} exceeds the elastic bending resistance $M_{el,Rd}$, as per §6.6.2.2(1).

For regions where the concrete slab is in compression, that is to say in sagging bending, a simplified procedure for the calculation of the shear connection is proposed in §6.6.2.2(2). The total force $V_{L,Ed}$ to be resisted by the shear connectors within an inelastic length L_{A-B} is given as the difference between the normal forces $N_{c,el}$ and N_{cd} acting in the concrete slab at cross-sections A and B (Fig. 4.14).

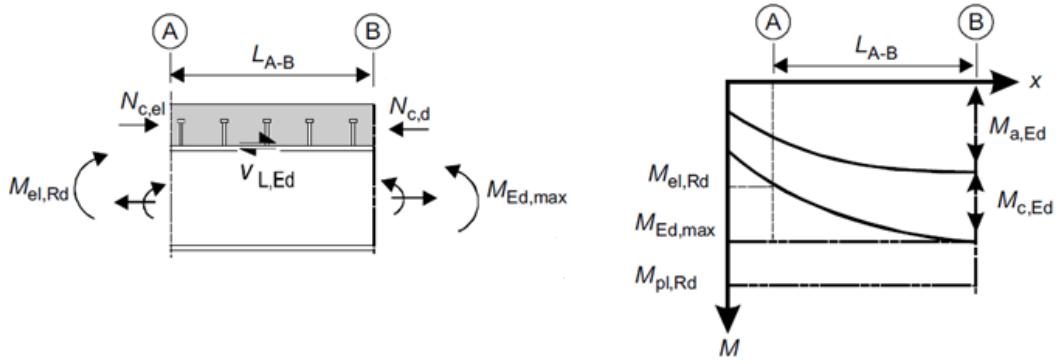


Fig. 4.14 – Definition of an inelastic length for the determination of longitudinal shear force (from *EN 1994-2:2005*, BSI, 2008)

In cases where the design bending moment M_{Ed} is lower than the plastic bending resistance $M_{pl,Rd}$ the normal force N_{cd} in the concrete slab at section B may be related to the acting bending moment M_{Ed} by either of the following simplified diagrams (Fig. 4.15):

- The bi-linear diagram given in Fig. 6.6 of EN1994-2 pertaining to the simplified method for calculation of non-linear bending resistance as per §6.2.1.4(6);
- The simplified linear diagram as given in Fig. 6.11 of EN1994-2 §6.6.2.2(2).

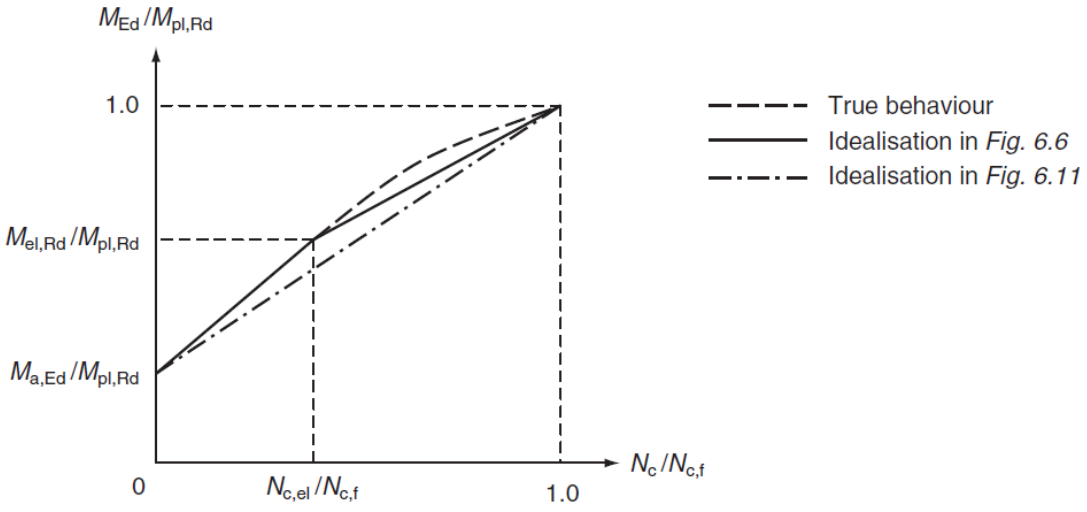


Fig. 4.15 – Variation of normal force in the concrete slab with bending moment (from *Designers Guide to EN1994-2*, Thomas Telford, 2006)

It should be noted that by using the simplified linear diagram the calculated normal force in the concrete slab will always be higher than if determined with the bi-linear diagram. The former typically yields very unfavourable results, which may lead to an unnecessary over-design of the number of shear connectors (Davaine et al, 2007).

For regions where the concrete slab is in tension, i.e. in hogging bending, §6.6.2.2(3) states that where inelastic behaviour is taken into account the longitudinal shear force distribution should also be determined from the difference between the normal force in the concrete slab within the inelastic length. The effects of tension stiffening from concrete between cracks and over-strength of concrete shoul be considered. Alternatively, §6.6.2.2(4) allows the longitudinal shear force to also be determined by elastic theory considering uncracked section properties. The use of elastic theory is a justifiable simplification attending to the fact that the assumption of a fully uncracked concrete section offsets the unconservative neglect of inelastic behaviour (Hendy and Johnson, 2006).

The calculation of the longitudinal shear forces at the steel-concrete interface as per §6.6.2.1 and §6.6.2.2 accounts only for the effects of vertical loads and the secondary effects of temperature and shrinkage. It is also necessary to account for the anchorage of the concentrated longitudinal shear forces at the free ends of the deck arising from the primary effects of temperature and shrinkage.

In accordance with §6.6.2.4(3), where the primary effects of temperature or shrinkage cause a design longitudinal shear force $V_{L,Ed}$ to be transferred at a free end of a member its distribution may be assumed as triangular, with a maximum shear force per unit length $v_{L,Ed,max}$ given by:

$$v_{L,Ed,max} = 2 \cdot V_{L,Ed} / b_{eff} \tag{4.21}$$

Where

$V_{L,Ed}$ - is the design longitudinal shear force (equal to N_{cs} for primary effects of shrinkage)

b_{eff} - is the effective flange width used in the global analysis

It is noted that where headed stud shear connectors are used a rectangular shear flow distribution along length b_{eff} may be considered for ultimate limit states, in which case the design longitudinal shear force per unit length $v_{L,Ed}$ can be simplified to $v_{L,Ed}=V_{L,Ed}/b_{eff}$ (Fig. 4.16).

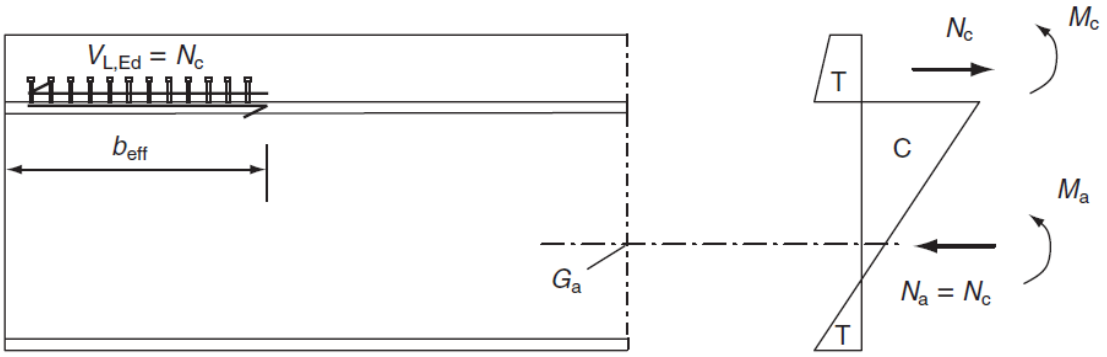


Fig. 4.16 – Determination of the longitudinal shear force from primary shrinkage at the end of a beam (from *Designers Guide to EN1994-2*, Thomas Telford, 2006)

The effects of the vertical loads together with secondary effects of temperature and shrinkage generate a shear flow that is opposite in direction to the shear flow from primary effects of temperature and shrinkage. For this reason the calculation of the longitudinal shear flow should be performed separately for the above and the shear connection designed for the most adverse effect. The shear connection design is usually not governed by the anchorage of longitudinal shear forces from primary effects of temperature and shrinkage (Davaine et al, 2007).

4.2.3.2. Design Resistance of Headed Stud Connectors

As previously stated EN1994-2 provides resistance formulas only for headed stud shear connectors. The design shear resistance P_{Rd} of a headed stud automatically welded in accordance with the requirements of EN (ISO) 14555 *"Arc stud welding of metallic materials"* is given in §6.6.3.1.

$$P_{Rd} = \min \begin{cases} 0.8 \cdot f_u \cdot \left(\pi \cdot d^2/4\right)/\gamma_V \\ 0.29 \cdot \alpha \cdot d^2 \cdot \sqrt{f_{ck} \cdot E_{cm}}/\gamma_V \end{cases} \tag{4.22}$$

With

$$\alpha = \begin{cases} 0.2 \cdot \left(\frac{h_{sc}}{d} + 1\right) \quad \text{for} \quad 3 \le h_{sc}/d \le 4 \\ 1.0 \quad \text{for} \quad h_{sc}/d > 4 \end{cases} \tag{4.23}$$

Where

f_u - is ultimate tensile strength of the stud, but not greater than 500N/mm^2

f_{ck} - is the characteristic cylinder compressive strength of the concrete at the age considered

E_{cm} - is the secant modulus of elasticity of concrete

d - is the stud shank diameter, 16<d<25mm

h_{sc} - is the overall nominal height of the stud

γ_V - is the partial factor for shear connection, taken as 1.25 as per §NA.2.3 of the UK National Annex to EN1994-2

In verifications of ultimate limit states other than fatigue §6.6.1.2 states that the connector size and spacing may be constant over any length where the design longitudinal shear per unit length $v_{L,Ed}$ does not exceed resistance by more than 10%, provided that the total design shear force $V_{L,Ed}$ does not exceed the total resistance within that same length (Davaine et al, 2007). The verification criteria can be expressed as:

$$v_{L,Ed}(x) < 1.1 \cdot \frac{n_i}{L_i} \cdot P_{Rd} \quad [kN/m] \tag{4.24}$$

And

$$V_{L,Ed} = \int_{L_i} v_{L,Ed}(x)\, d_x < n_i \cdot P_{Rd} \quad [kN] \tag{4.25}$$

Where

$v_{L,Ed}(x)$ - is the design longitudinal shear per unit length at abscissa *x*

L_i - is the length of the segment under consideration

n_i - is the total number of shear studs within the segment length L_i

P_{Rd} - is the design resistance of the shear stud as per §6.6.3.1

4.2.3.3. Detailing of the Shear Connection

The conformity of the shear connection with the general principles given in §6.6.1 is dependant to an extent in the abbeyance of the detailing rules provided in §6.6.5, which aim to assure that the behaviour assumed in the conceptual model of the connection is effectively mobilised.

The requirements regarding the dimensions and spacings of headed shear studs are given in §6.6.5 in relation to the stud diameter *d* and slab thickness:

- The overall height of a stud should not be less than 3*d*;
- The stud head should have a diameter and depth not less than 1.5*d* and 0.4*d*, respectively;
- The surface of a connector resisting separation forces such as the underside of the head of a stud should extend not less than 30mm clear above the bottom reinforcement;
- The spacing of studs should not be less than 5*d* in the direction of the shear force and not less than 2.5*d* in the transverse direction;
- The maximum longitudinal spacing of individual studs should not exceed either 800mm or four times the slab thickness, whichever is lesser;
- The distance e_D between the edge of a connector and the edge of the flange to which it is welded should not be less than 25mm;
- The diameter of a welded stud *d* should not be greater than 2.5 times the thickness of the part to which it is welded, with the exception of studs located directly over the web.

As noted in §6.6.1.1(9) headed stud connectors complying with the above requirements may be assumed to provide adequate resistance to uplift and prevent separation of the slab.

In accordance with §6.6.6.1 the premature longitudinal shear failure or longitudinal splitting of the concrete slab must be prevented so that the longitudinal shear flow can be transmitted from the concrete flange to the steel section. The transverse reinforcement in the concrete slab shall be designed to meet this requirement for the ultimate limit state.

The design longitudinal shear stress for any potential failure surface within the slab must be checked against the design longitudinal shear strength of the surface considered, with the design longitudinal

shear stress v_{Ed} determined from the design longitudinal shear per unit length, $v_{L,Ed}$. Typical failure surfaces to consider are shown on Fig. 4.17.

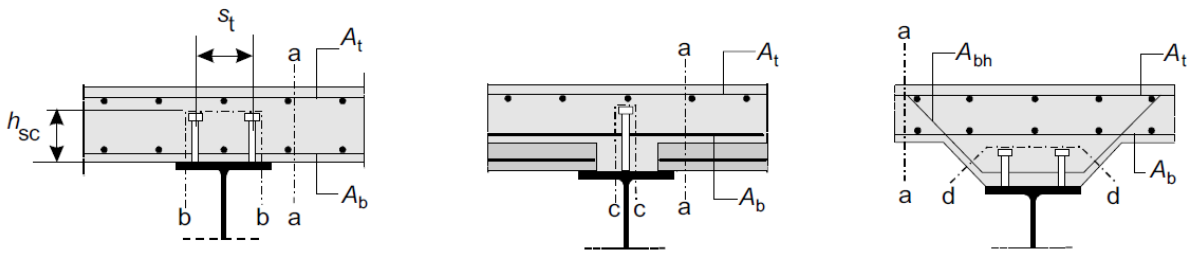


Fig. 4.17 – Typical potential surfaces of shear failure (from *EN 1994-2:2005*, BSI, 2008)

The design shear strength of the concrete flange should be determined as for shear between the webs and flanges of T-sections in accordance with EN1992-1-1 §6.2.4, with the effective areas of transverse reinforcement per unit length A_{sf} / s_f to be determined by calculation being related to the failure surface considered.

4.3. CROSS-SECTION VERIFICATION FOR SERVICEABILITY LIMIT STATES

The serviceability limit state verifications of a structure aim to ensure its adequate functioning under normal use, guarantee user comfort, limit deformations that would affect function or appearance, limit vibrations, and control damage that impacts durability and/or function. Compliance with the serviceability criteria is essential to guarantee the durability of the structure and ensure its intended service life.

The serviceability criteria that should be met regarding steel structures are given in EN1993-2 §7.1, and can be summarised as follows:

- Restriction of the steelwork to elastic behaviour in order to limit excessive yielding and deformation;
- Limitation of deflections and curvatures;
- Limitation of natural frequencies to prevent vibrations due to traffic or wind which are unacceptable to pedestrians or car users;
- Limitation of plate slenderness to avoid excessive plate ripling, web breathing and reduction of stiffness due to plate buckling;
- Adequate detailing to reduce corrosion and wear improving durability;
- Ease of maintenance and repair to ensure acessability of structural parts for maintenance and inspection, as well as the replacement of bearings and expansion joints.

In order to cater for aspects that are particular to composite structures EN1994-2 §7 adds the following criteria:

- Stress limitations in the concrete and reinforcing steel to avoid excessive creep and inelastic strains respectively;
- Control of cracking of concrete in tension in order to limit crack widths;
- Limitation of the longitudinal shear force per shear connector to prevent fatigue damage.

4.3.1. STRESS LIMITATIONS FOR BRIDGES

The cross-section stresses to consider for serviceability limit states should be obtained by means of a linear-elastic global analysis of the structure, taking into account the effects of shear lag, creep and shrinkage of concrete, concrete cracking and tension stiffening of concrete between cracks, as well as the construction sequence. Other effects that may be of relevance in particular situations are also stated in EN1994-2 §7.2.1.

Since the local buckling of elements of the cross-section in compression is addressed by the classification system defined in EN1993-1-1 §5.5.2 and the effects of shear lag may be taken into account by adopting an effective flange width as per EN1994-2 §5.4.1.2, the cross-sections to consider are the same as for ultimate limit states. The effects of creep and shrinkage may be accounted for by the use of modular ratios, and the primary effects of shrinkage may be neglected in cracked sections. Similarly to ultimate limit states, the tensile strength of concrete must be neglected in the section analysis.

The stress limitations for bridges are given in EN1994-2 §7.2.2 by cross-reference with EN1992-1-1/2 for concrete compressive stresses, EN1992-1-1 for tensile stresses in reinforcing steel and prestressing tendons, and EN1993-2 for steelwork stresses.

4.3.1.1. Concrete Compressive Stress Limits

The limitation of the maximum compressive stress of the concrete aims to ensure durability by avoiding longitudinal cracks, micro-cracking and high levels of creep. In accordance with EN1994-2 §7.2.2(2) the compressive stress in the concrete should be limited to the values $k_i \cdot f_{ck}$ given in EN1992-1-1 §7.2:

$$\sigma_c \leq 0.45 \cdot f_{ck} \text{ , for Quasi-Permanent Combinations} \tag{4.26}$$

$$\sigma_c \leq 0.60 \cdot f_{ck} \text{ , for Characteristic Combinations} \tag{4.27}$$

Where

σ_c - is the compressive stress in the concrete

f_{ck} - is the characteristic compressive cylinder strength of the concrete

The verification of the quasi-permanent stress limit means that linear creep may be assumed, and implicitly validates the simplified procedure of accounting for the effects of creep by using modular ratios (Davaine et al, 2007). While the stress limit for characteristic combinations is only indicated in EN1992-1-1 §7.2(2) for exposure classes XD, XF and XS, this criterion has been adopted in EN1994-2 for all exposure classes as a means to overcome any fatigue effects in the concrete slab (Davaine et al, 2007).

4.3.1.2. Reinforcing Steel Tensile Stress Limits

In accordance with EN1994-2 §7.2.2(3) inelastic strains in the reinforcing steel and prestressing tendons shall be avoided, which should achieved by limiting the stresses in the reinforcement and the tendons to the values k_i and k_5 given in EN1992-1-1 §7.2(5):

$$\begin{cases} \sigma_s \leq 0.80 \cdot f_{sk} & \text{for global bending} \\ \sigma_s \leq 1.00 \cdot f_{sk} & \text{for imposed deformations} \end{cases} \tag{4.28}$$

$$\sigma_p \leq 0.75 \cdot f_{pk} \tag{4.29}$$

Where

σ_s - is the stress in the reinforcing steel resulting from characteristic load combinations

f_{sk} - is the characteristic yield strength of the reinforcing steel

σ_p - is the stress in the prestressing tendons resulting from characteristic load combinations

f_{pk} - is the characteristic tensile strength of the prestressing steel

4.3.1.3. Steelwork Stress Limits

The stress limitations in the structural steelwork are of importance in the design of composite sections to assess their behaviour in service conditions, where inadequacy could go unnoticed by ultimate limit state verifications only (Rueda, 2009). Such verifications are all the more relevant when plastic bending resistances are used. The stresses in the structural steelwork should thus be limited in accordance with EN1993-2 §7.3(1):

$$\sigma_{Ed,ser} \leq \frac{f_y}{\gamma_{M,ser}} \tag{4.30}$$

$$\tau_{Ed,ser} \leq \frac{f_y / \sqrt{3}}{\gamma_{M,ser}} \tag{4.31}$$

$$\sqrt{\sigma_{Ed,ser}{}^2 + 3 \cdot \tau_{Ed,ser}{}^2} \leq \frac{f_y}{\gamma_{M,ser}} \tag{4.32}$$

Where

$\sigma_{Ed,ser}$ - is the direct stress resulting from characteristic load combinations

$\tau_{Ed,ser}$ - is the shear stress resulting from characteristic load combinations

f_y - is the design yield strength of the cross-section fibre under consideration

$\gamma_{M,ser}$ - is the partial factor for steelwork stress, taken as 1.00 as per §NA.2.24 of the UK National Annex to EN1993-2

The Von Mises equivalent stress criterion should be checked for concomitant stresses at the most unfavourable fibre of the cross-section. While it may not be known beforehand which fibre will govern the check it is evident that it will either be one of the extreme fibres of the flanges (where direct stresses are highest), or the roots of the web (where high direct stress coexists with shear stress).

An additional check is given in §7.3(2) limiting the nominal stress range $\Delta\sigma_{freq}$ for frequent load combinations considering reversals of sign of stress to $1.5 \cdot f_y / \gamma_{M,ser}$. The purpose of this verification is to ensure that the frequent stress variations remain confined to the strictly linear part of the stress-strain diagram ($\pm 0.75 \cdot f_y$) overcoming any fatigue issues for a low number of cycles (Davaine et al, 2007).

4.3.1.4. Limitation of Longitudinal Shear Force of Connectors

In accordance with EN1994-2 §7.2.2(6) the longitudinal shear force per connector for serviceability limit states should be limited as per §6.8.1(3). Section 6.8 of EN1994-2 deals with fatigue resistance of composite structures subject to repeated stress cycles, which is an ultimate limit state verification. However, as a serviceability criteria to avoid possible fatigue damage, it is recommended in §6.8.1(3) that the longitudinal shear force per connector under characteristic combinations of actions should not exceed the following:

$$P_{Ed,ser} \leq k_s \cdot P_{rd} \tag{4.33}$$

Where

$P_{Ed,ser}$ - is the longitudinal shear force per connector

k_s - is a factor taken as 0.75 as per §NA.2.11 of the UK National Annex to EN1994-2

P_{Rd} - is the design resistance of the headed stud connector

4.3.2. WEB BREATHING

When motorway traffic travels along the deck the web of the steel section at a given location will deform sligthly out of its plane with the passage of each vehicle, then returning to its initial shape. The out-of-plane deflection follows the deformed shape of the first buckling mode of the web panel for in-plane loading. This repeated deformation is commonly referred to as web breathing, and may generate fatigue cracks at the weld joints between the web and flange or between the web and the transverse stiffener (Davaine et al, 2007).

In accordance with EN1994-2 §7.2.3 the slenderness of web plates should be limited as per EN1993-2 §7.4 to avoid excessive web breathing. For road bridges, web panels without longitudinal stiffeners need not be checked for web breathing where the criterion given in §7.4(2) is met:

$$\frac{h_w}{t_w} \leq 30 + 4 \cdot L \quad \leq 300 \tag{4.34}$$

Where

h_w - is the depth of the web plate between flanges

t_w - is the thickness of the web plate

L - is the span length in metres, but not less than 20m

If the slenderness criterion is not satisfied web breathing must be checked explicitly in accordance with §7.4(3):

$$\sqrt{\left(\frac{\sigma_{x,Ed,ser}}{k_\sigma \cdot \sigma_E}\right)^2 + \left(\frac{1.1 \cdot \tau_{Ed,ser}}{k_\tau \cdot \sigma_E}\right)^2} \leq 1.1 \qquad (4.35)$$

With

$$\sigma_E = 190000 \cdot \left(\frac{t_w}{b_p}\right)^2 \quad \left[N/mm^2\right] \qquad (4.36)$$

Where

$\sigma_{x,Ed,ser}$ - is the design longitudinal stress resulting from frequent load combinations

$\tau_{Ed,ser}$ - is the design shear stress resulting from frequent load combinations

k_σ - is the plate buckling coefficient of the web plate as per Table 4.1 of EN1993-1-5

k_τ - is the shear buckling coefficient of the web plate as per Annex A.3 of EN1993-1-5

t_w - is the thickness of the web plate

b_p - is the lesser of the stiffener spacing a and the web panel height h_w

For road bridges the web breathing criterion given in §7.4(2) is typically verified by a wide margin with the explicit verification only being necessary in particular situations (Davaine et al, 2007).

4.3.3. CRACKING OF CONCRETE

The limitation of crack widths in bridges is key to ensure durability of the structure. As stated by EN1994-2 §7.4.1 the general considerations of EN1992-1-1 as modified by EN1992-2 apply to composite structures, with the requirements regarding permissible crack widths in relation to the exposure classes being the same as for concrete structures.

Table 4.3 - Recommended values of w_{max} as per Table 7.101N of EN1992-2.

Exposure Class	Reinforced members and prestressed members with unbounded tendons	Prestressed members with bounded tendons
	Quasi-Permanent Combination	Frequent Combination
X0, XC1	0.3	0.2
XC2, XC3, XC4	0.3	0.2
XD1, XD2, XS1, XS2, XS3		Decompression

A new aspect brought about by EN1994-2 to previous UK practice for control of crack widths was the differentiated approach for cracking due to restraint to imposed deformations and applied loading. The current design rules prescribe two distinct procedures:

- Quantification of a minimum reinforcement to be provided for all cross sections that could be subjected to significant tension by restrained deformations, such as the effects of shrinkage;
- Calculation of a required area of reinforcement to control cracking due to direct loading.

4.3.3.1. Minimum Reinforcement for Restraint of Imposed Deformations

In accordance with EN1994-2 §7.4.2(1) a required minimum reinforcement area should be provided at all sections where the concrete slab is subject to significant tension due to restraint of imposed deformations such as the primary and secondary effects of shrinkage.

$$A_s = k_s \cdot k_c \cdot k \cdot f_{ct,eff} \cdot A_{ct} / \sigma_s \tag{4.37}$$

With

$$k_c = \frac{1}{1 + h_c / (2 \cdot z_0)} + 0.3 \leq 1.0 \tag{4.38}$$

Where

$f_{ct,eff}$ - is the mean value of the tensile strength of concrete at time when cracks are first expected to occur. Values may be taken as f_{ctm} or, when age of concrete at cracking is not less than 28 days, a minimum of $3N/mm^2$ may be used.

k - is a coefficient allowing for the effects of self-equilibrating stresses and may be taken as 0.8

k_s - is a coefficient allowing for the force transfer from the slab to the steelwork due to initial cracking and local slip of the shear connection, which may be taken as 0.9

k_s - is a coefficient accounting for the stress distribution within the section immediately prior to cracking

h_c - is thickness of the concrete slab

z_0 - is the vertical distance between the centroids of the uncracked concrete flange and the uncracked composite section, calculated using the modular ration n_0 for short-term loading

σ_s - is the maximum stress permitted in the reinforcement immediately after cracking

A_{ct} - is the area tensile zone, which may be taken as the area of the concrete section within the effective width

As an initial assumption the reinforcement stress σ_s may be taken as the characteristic yield strength f_{sk}, with the minimum reinforcement area being determined by equalizing the force in the reinforcing steel and in the concrete tensile zone. To check compliance with the permissible crack width w_k the reinforcement stress should be compared with the stress limit for each bar size given in Table 7.1 of EN1994-2, and the minimum reinforcement area re-calculated if need be.

The maximum bar diameter for design crack width in Table 7.1 of EN1994-2 may be increased to account for higher concrete bond strength:

$$\varphi = \varphi^* \cdot f_{ct,eff} / f_{ct,0} \tag{4.39}$$

Where

$f_{ct,0}$ - is a reference tensile strength of concrete of 2.9 N/mm^2

φ^* - is the maximum bar size given in Table 7.1

It is worth noting that in situations where the slab is compressed over the entire structure, as is the case for simply supported bridges, there is no permissible crack width to be checked. In this instance it is recommended to adopt a minimum reinforcement with bars working to their characteristic yield strength f_{sk} over the whole slab (Davaine et al, 2007).

4.3.3.2. Control of Cracking Due to Direct Loading

In accordance with EN1994-2 §7.4.3 the internal forces acting on the structure to consider for the control of cracking due to direct loading should be obtained from an elastic analysis, taking into account the effects of cracking of concrete. The calculation of stresses in the reinforcing steel should account for the effects of tension stiffening of concrete, for which §7.4.3(3) provides the following expression:

$$\sigma_s = \sigma_{s,0} + \Delta\sigma_s \tag{4.40}$$

With

$$\Delta\sigma_s = \frac{0.4 \cdot f_{ctm}}{\alpha_{st} \cdot \rho_s} \tag{4.41}$$

$$\alpha_{st} = \frac{A \cdot I}{A_a \cdot I_a} \tag{4.42}$$

Where

$\sigma_{s,0}$ - is the stress in the reinforcement calculated neglecting concrete in tension

ρ_s - is the reinforcement ratio, given by $\rho_s = A_s / A_{ct}$

A_{ct} - is the effective area of the concrete flange within the tensile zone

A_s - is the total area of longitudinal reinforcement within the effective are A_{ct}

A, I - are the area and the second moment area of the composite section neglecting concrete in tension

A_a, I_a - are the area and the second moment area of the structural steel section

The calculated reinforcement stresses can then checked against the permissible stress limits for maximum bar diameters or maximum bar spacing, given in Table 7.1 and Table 7.2 respectively, that will ensure compliance with the permissible crack width w_k.

5
CASE STUDY – THE RIVER SEIONT VIADUCT

5.1. INTRODUCTION AND BACKGROUND

5.1.1. THE A487 CAERNARFON TO BONTNEWYDD BYPASS

The A487 Fishguard to Bangor Trunk Road is a single carriageway road running along the western Welsh shoreline from Haverfordwest in the south to Bangor in the north. It is classified and maintained as a strategic route by the North and Mid Wales Trunk Road Agency on behalf of the Welsh Government.

The Caernarfon to Bontnewydd section in North Wales has experienced congestion problems from increased traffic volumes, which are adversely affecting the area. The high volumes of traffic have resulted in community severance and reduced quality of life of residents adjacent to the A487 and the lack of connectivity on the A487 southwards from Bangor is deemed to hinder the economic development of the region (Spence, 2015).

Since the early 1990's studies have been undertaken commisioned by the Welsh Office to identify traffic problems around Caernarfon and investigate possible bypass routes to increase network capacity. As the result of an investigation of route options and following two public consultations the Purple Route (Fig.5.1) was announced by the Minister for Local Government and Communities as the Preferred Route in July 2012. Due to budgetary pressures the Minister for Economy, Science and Transport decided to review the options and in May 2013 the Yellow Route (Fig.5.1) was adopted instead (Spence, 2015).

Following the choice of the Preferred Route a TR111 route protection was issued to prevent future development to encroach on the route line. This statutory instrument will allow for future improvement of the scheme to benefit connections of the A487 to local trunk roads around Caernarfon and Bontnewydd.

In 2014 the Welsh Government appointed Employer's Agent E.C. Harris and consultant Ramboll to prepare the A487 Caernarfon to Bontnewyd Bypass scheme for an Early Contractor Involvement tender process. In December 2014 it was announced that a Balfour Beatty/Jones Brothers Joint Venture with WSP | Parsons Brinckerhoff and TACP Architects as designers won the commission (Spence, 2015).

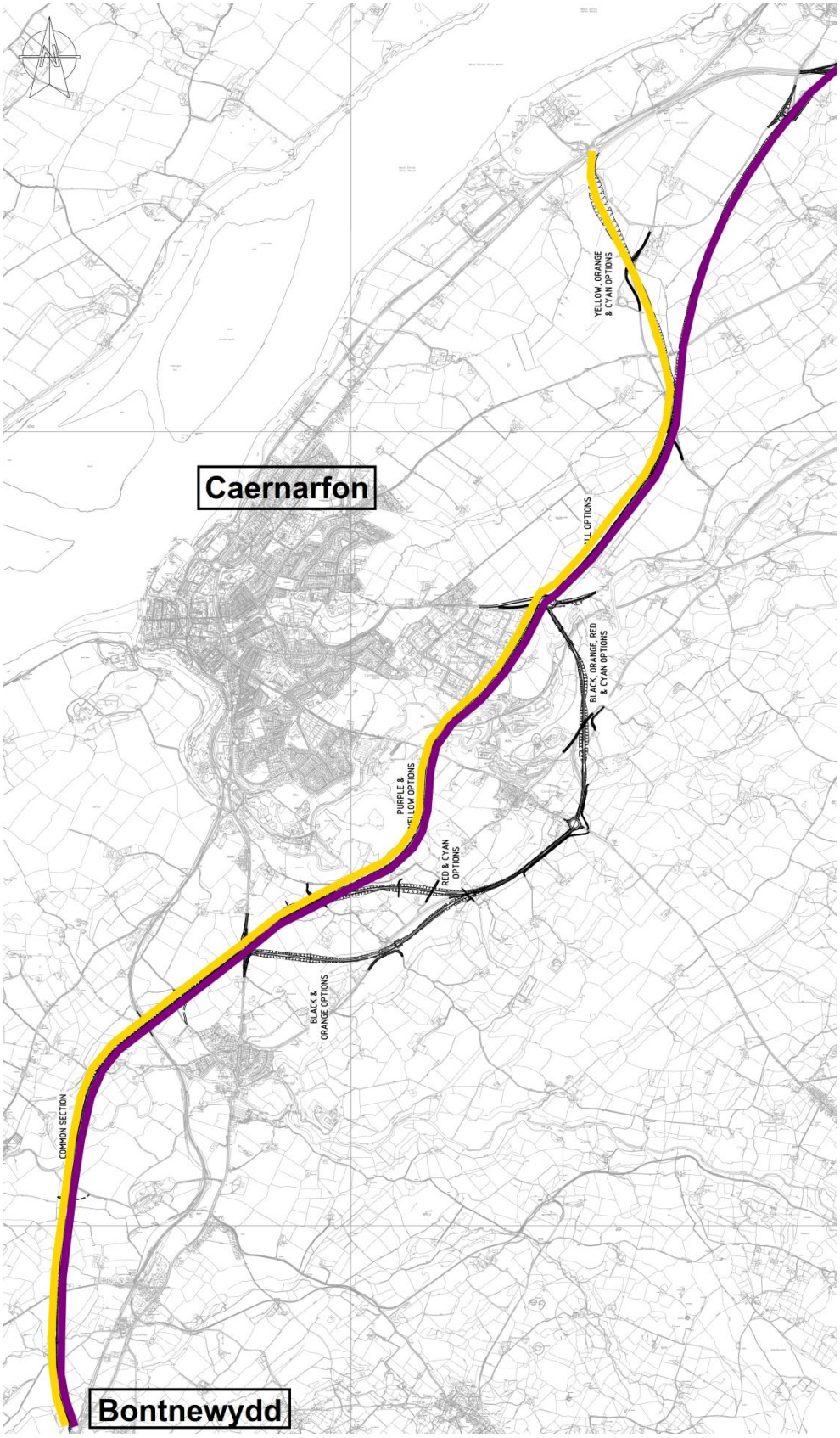


Fig. 5.1 – A487 Caernarfon to Bontnewydd Bypass Preferred Routes

A *"Design Options Report Highways"* that describes the work undertaken to arrive at an optimal highway solution with associated crossing points in relation to physical constraints was produced in which the structures needed to support the highway solution were defined. This report was subsequently supplemented by a *"Structures Design Options Report"* that explored the range of options that could provide an adequate solution for each of the structure's required by the scheme (Spence, 2015).

5.1.2. Options Development for The River Seiont Viaduct

Located midway through the A487 Caernarfon to Bontnewydd Bypass the River Seiont Viaduct will be one of the major structures of the scheme. Its purpose is to carry the A487 main line over the River Seiont and its valley.

The horizontal alignment of the A487 main line at this location is a 510m radius curve to the right (i.e. looking north) (Fig.5.2). The curve radius gives rise to the need of a 7% super elevation of the carriageway and the horizontal curve implies a 3.6m wide inside verge due to forward visibility requirements. As for the vertical alignment, it is a straight 1.2% gradient rising from south to north that enters the valley about 5m above existing ground level and exits it way up the steep north slope in slight cutting.

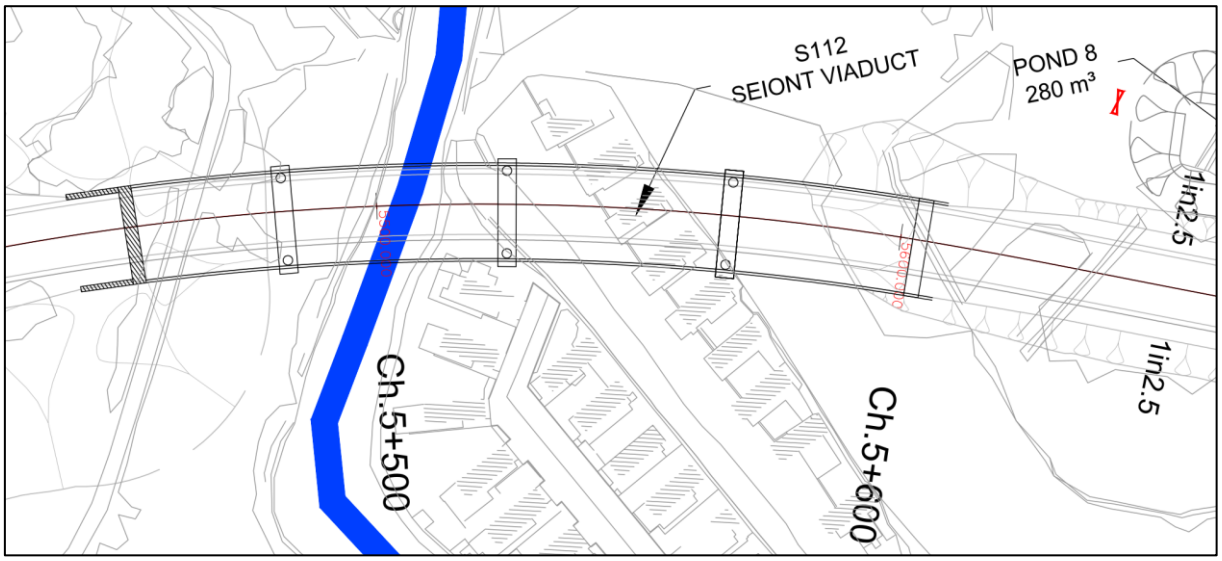


Fig. 5.2 – Horizontal alignment of the A487 over River Seiont

The production of the *"Structures Design Options Report"* would run paralell with numerous iterations of the highway alignment design with the respective iterations for earthworks cut-fill balance, with the ground investigation and topographical survey works, flood modelling, as well as Public Information Exhibitions and other stakeholder liasion. The report would start by developing solutions that responded to the various constraints for comparative purposes which would be refined as the detailed information became available.

The key constraints that governed the design options for the River Seiont Viaduct were:

- The mandatory budget assumptions regarding the viaduct length, the carriageway cross section and the levels;
- The plan location and the extents of the River Seiont's flood plain;
- The provision of a minimum freeboard above maximum flood level of 600mm;
- The requirement from the Welsh Government of a 3.0m soffit clearance to ground level to prevent unauthorised access to soffit;
- The provision of an passage around the substructure to facilitate river maintenance acess along the river banks;
- The restricted access into the river valley for construction;
- The horizontal curve of the highway alignment and the significant super-elevation it implied.

The *"Structures Design Options Report"* considered and reviewed five different options for the structural form of the viaduct to arrive at the solution with the least whole life cycle cost. The options were all continuous multispan superstructures with the mandated total length of 260m:

- Option 1- Steel-concrete composite multi girder deck
    - A superstructure with main spans 35-40m comprising 6 paralell steel girders with integral steel crossheads at intermediate supports with the deck slab spanning transversely;
    - The substructure would comprise 3 reinforced concrete columns at each pier.
- Option 2 - Steel-concrete composite ladder deck
    - A superstructure with main spans 40-50m formed by two main longitudinal girders and transverse beams at 3-4m centres with the deck slab spanning longitudinally;
    - The substructure would comprise 2 reinforced concrete columns at each pier.
- Option 3 - Steel-concrete composite box girder deck
    - A superstructure with main spans of about 50m composed 4 trapezoidal open top steel box girders with the deck slab spanning transversely;
    - The substructure would comprise 4 reinforced concrete columns at each pier.
- Option 4- Precast prestressed concrete deck
    - A superstructure with main spans of 32m comprised of 6 precast prestressed W14 beams with integral concrete crossheads over the piers with the deck slab spanning transversely;
    - The substructure would comprise either 1 or 2 concrete leaf piers per line of supports;
- Option 5 - Post-tensioned concrete deck
    - A superstructure with main spans of 72m with 2 paralell post-tensioned prestressed concrete box girders;
    - The substructure would comprise 2 concrete leaf piers per line of supports.

All options would provide for reinforced concrete abutments with inspection galleries at both ends of the viaduct. The articulation arrangements would also be similar for all, with fixed longitudinal bearings at the southern abutment and mechanical guided bearings along one of the alignments set out radially from the fixed point. The remainder of the bearings would be mechanical with all translation free (Groves, 2015).

The composite multigirder considered for Option 1 required particular consideration of stability of the girders during erections. The works at height required by the integral crossheads whose connections involve lare groups of bolts also presented concerns. The steel consumption of the deck would be greater than that of the other composite superstrucutres.

The construction arrangement for the Option 2 ladder deck consisted in the assembly of complete spans at ground level and lifting them onto the piers by large capacity cranes, thus overcoming stability problems during construction. To cater for the transverse cross fall of the deck the longitudinal girders would be stepped vertically relative to each other and the closely spaced cross girders arranged paralell to the cross fall, allowing for a constant concrete slab thickness.

For the Option 3 composite box girder deck it was deemed that while they provided improved aesthetics, offered reduced maintenance due to a lesser exposed surface to be painted, and reduced flange sizes in comparison with plate girders, the added fabrication costs would offset any potential savings.

It should be noted that given the proximity to the Welsh shoreline weathering steel could not be used in the composite superstructures, which would need the application of protective coatings. A complete grit blast and reapplication of the protective system to the structural steelwork would be required at 25 year intervals. The resulting future maintenance costs of the steel-concrete superstructures would higher than that of the prestressed concrete solutions.

The Option 4 prestressed precast beam deck would require transport to site of 32m long beams with a weight of 80t that would then be erected one by one with large capacity cranes onto temporary bearings. After the integral crossheads were cast over the piers and the superstructure made continuous the temporary supports would be removed and the deck rest on its permanent bearings. The construction process would therefore be more complex and take longer than for steel options. Despite the reduced maintenance requirements of the concrete superstructure the savings were not enough to offset the inital capital cost.

The post-tensioned concrete box girder of Option 5 would consider span-by-span casting on conventional falsework, as the use of movable scaffolding systems or incremental launching of the deck were not economical given the lenght of the viaduct. This solutions was found to have the highest capital cost.

From the exercise undertaken the twin girder ladder deck of Option 2 was found to yield the lowest whole life cycle cost, and was selected as the option to develop in preliminary design (Groves, 2015).

5.2. PROPOSED STRUCTURE

The inclusion of mandatory budget assumptions regarding the viaduct length and the carriageway cross section in the tender brief had had the objective to make the proposals from the bidders comparable like-for-like. Once the preferred bidder had been selected it would then be possible for him to present to Welsh Government a value engineering exercise justifying an alternative design.

It had been identified that an improved cut-fill balance of the entire scheme could be achieved by lengthening the embankment at the south end of River Seiont valley. This would reduced the total length of the viaduct from the mandated 260m to about 145m. Given that the relative costs of the options developed are primarily a function of the superstructure type the conclusions of the *"Structures Design Options Report"* remained valid. This proposal for a shortened ladder deck viaduct was accepted by Welsh Government.

5.2.1. DESCRIPTION OF STRUCTURE AND DESIGN WORKING LIFE

The proposed structure will be a continuous four span curved steel-concrete composite ladder deck with main spans of 42.5m supported over three support alignments with cantilever abutmens at each end. The proposed span arrangement for the structure is 28.0 + 42.5 + 42.5 + 35.0, with the total lenght of the viaduct being 148.0m between abutment bearing centrelines (Fig. 5.3 and Fig. 5.4).

The superstructure is comprised of two curved longitudinal steel plate girders of constant depth with cross girders at 3.5m spacings. A reinforced concrete deck slab of constant thickness spans longitudinally between the cross girders and cantilevers transversely from the main girders. The deck has no skew, with support lines arranged radially to the plan 510m radius curvature of the carriageway centreline.

The substructure will consist of two circular reinforced concrete columns per each line of supports and reinforced concrete abutments with integral cantilever wingwalls at both ends of the viaduct. The foundations of the southern abutment and the first two pier alignments (P1 and P2) will be shallow spread foundations, whereas the last pier (P3) and the northern abutment will require piled foundations.

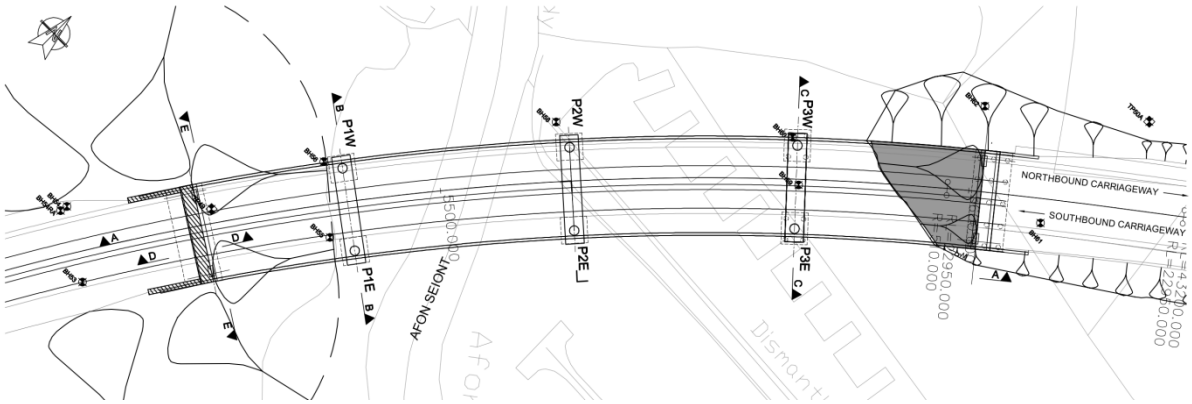


Fig. 5.3 – Plan of River Seiont Viaduct.

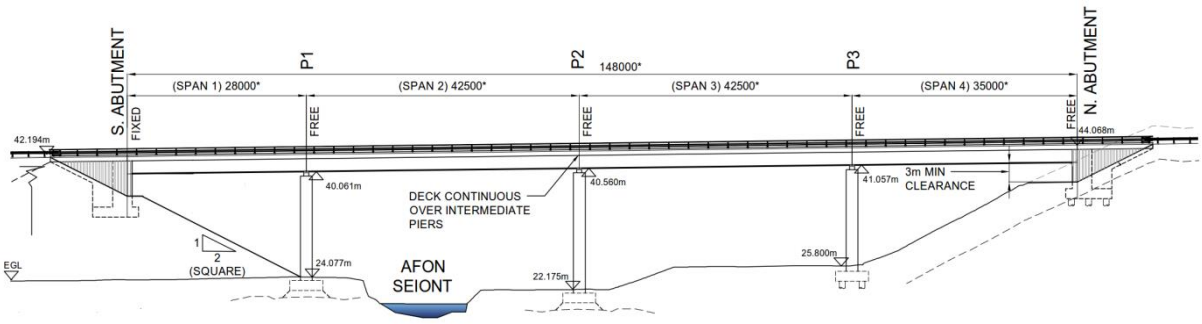


Fig. 5.4 – Elevation of River Seiont Viaduct.

The superstructure will be supported on proprietary pot bearings, one per girder per line of supports. The longitudinal translation will be fixed at the southern abutment with expansion and contraction movement being accomodated at the expansion joint of the northern abutment. Transverse movement

will be restrained at all bearings supporting the eastern girder whereas the bearings below the western girder will be free translation. The bearings on the eastern girder will be arranged radially from the fixed bearing on the southern abutment.

The cross-section of the main line of the A487 over the viaduct is comprised of a 0.60m wide verge to the western edge, a 13.50m wide single carriageway and a 3.60m wide verge to the eastern edge (Fig. 5.5). The two-way single carriageway will carry two lanes of traffic in each direction.

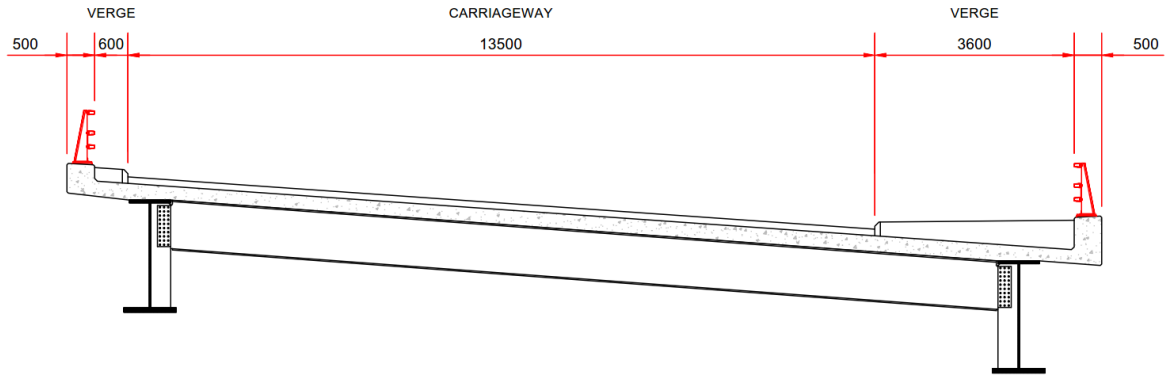


Fig. 5.5 – A487 Carriageway over River Seiont Viaduct

The design working life of the structure and its components were specified in abidance with the recommendations of Highways Agency document *Interim Advice Note 124/14(W)*. This document provides the requirements and gives guidance for the use of Eurocodes in the design of highway structures for the Welsh Trunk Road network. The requirements depend on the design working life category of the item under consideration, and are given in Table A.1 of IAN124/14(W):

- For the structure, a design working life greater than 120 years (design working life category 5);
- For the bearings, a design working life of at least 50 years (design working life category 4);
- For replaceable structural parts including expansion joints, waterproofing systems, safety barriers and parapets a design working life of up to 50 years (design working life category 2).

5.2.2. Deck Cross-Section of the Viaduct

The cross-section of the A487 at the location of the viaduct will have a total width of 17.70m and will be carried over the River Seiont valley by a single bridge deck. With the provision of edge beams for fixing of safety barriers the total deck width comes to 18.70m.

The construction of the 250mm thick reinforced concrete deck slab between the longitudinal girders will use *Omnia* precast concrete planks spanning longitudinally between cross girders as permanent formwork. As for the edge cantilevers, these will be constructed using the *Paraslim* formwork system supported from the main girders. With the adoption of a 1.50m edge cantilever to allow for a constant thickness of the slab the resulting spacing between the longitudinal girders is 15.70m.

The large spacing between the longitudinal girders is towards the high-end of the range for twin-girder ladder decks. Each girder will be heavily loaded and will require considerably thick flange plates. For

this reason a moderate span-to-depth ratio for a continuous structure of 1/20 was selected. Taking the 42.5m main spans the corresponding total girder depth (including the reinforced concrete slab) of 2275mm was adopted throughout (Fig. 5.6).

The cross girders will span simply supported between the longitudinal girders and will be spaced 3.5m longitudinally. In service the cross girders will distribute the traffic loads to the longitudinal girders acting as a composite member. Attending to the large longitudinal girder spacing a span-to-depth ratio of 1/15 was selected. A total depth of 1150mm was adopted for the cross girders, from which results a 900mm deep steel section after deducting the concrete slab depth (Fig. 5.6).

At pier support lines the cross girders will have to transmit the horizontal forces from wind actions to the substructure and therefore more robust members are required (Fig. 5.6). Since over the supports the transverse members also provide for the stability of the compressed flange these should be as deep as practicable. Additional fabrication costs from complicated connection details will be avoided by having the steel section of the support cross girders stop 550mm short of the longitudinal girder's bottom flanges.

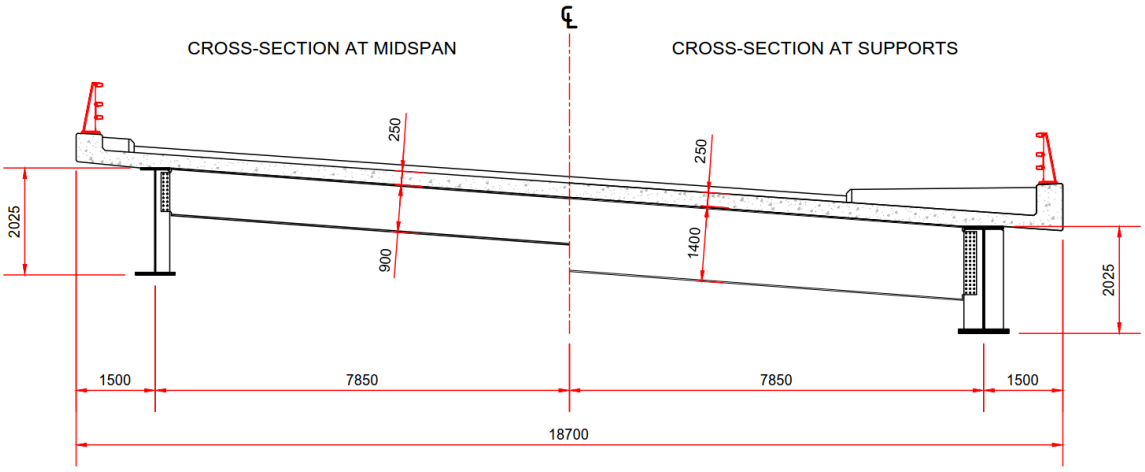


Fig. 5.6 – Typical cross section of River Seiont Viaduct

The preliminary section sizes adopted for the main longitudinal girders at midspan and over the supports, as well as the sections adopted for the cross girders are summarised in Table 5.1.

Table 5.1 – Structural steelwork grades used in the River Seiont Viaduct.

Steel Section	Longitudinal Girders		Transverse Girders	
Element	Midspan	Supports	Intermediate	Supports
Top Flange	550x35	750x50	500x22	400x20
Web Plate	16x1940	25x1895	10x858	14x1360
Bottom Flange	750x50	950x80	550x20	500x20

5.2.3. MATERIALS

The materials used in the construction of the River Seiont Viaduct are to assure adequate performance, durability and minimise future maintenance. The structural steelwork grades are all to be in accordance with the prescriptions of EN10025-1. Given the proximity of the marine environment the use of weathering steels with improved atmospheric corrosion resistance is not suitable and protective systems will need to be applied to the structural steelwork.

Table 5.2 – Structural steelwork grades used in the River Seiont Viaduct.

Element	Plate Thickness	Steel Grade
Web and Flanges	t ≤ 55mm	S355J2+N
Flanges	t > 55mm	S355K2+N

The concrete grades were selected in accordance with the requirements of BS EN206 and adhering to the recommendations of BS8500. The prevalent use of de-icing salts for winter road maintenance in the UK and the proximity to the shoreline required severe exposure classes to be considered.

Table 5.3 – Concrete grades used in the River Seiont Viaduct.

Element	Strength Class	Exposure Class
In-situ deck slab	C40/50	XC3/4, XD1
Parapet edge beams	C40/50	XC3/4, XD3, XF4
Pier Columns	C40/50	XC3/4, XD3, XF1
Abutments walls	C40/50	XC3/4, XD3, XF2
Abutment foundations	C40/50	XC3/4, XD3
Piles	C32/40	XC3/4, XD3

5.3. DESIGN ACTIONS AND COMBINATIONS

5.3.1. PERMANENT ACTIONS

The permanent actions considered in the analysis of the structure were the dead loads from the self-weight of structural elements of the deck, namely the steelwork and reinforced concrete deck slab, and the superimposed dead loads from permanent non-structural elements. In both instances the corresponding loads were calculated from the dimensions of the elements of the cross-section (Fig 5.7) and the material densities given in Table A.1 of EN1991-1-1.

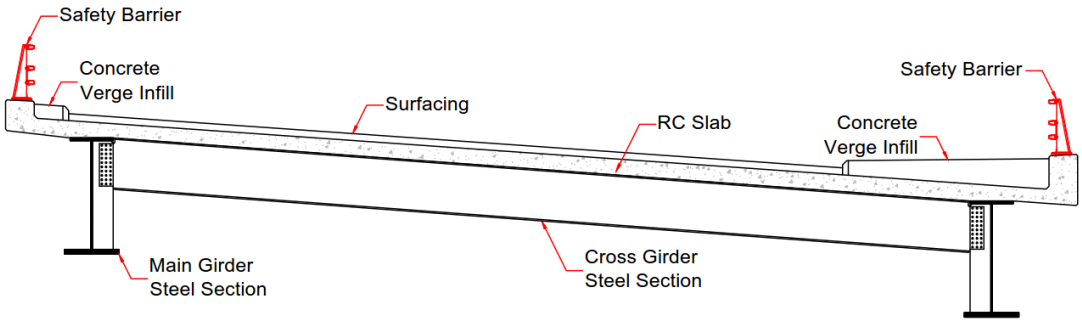


Fig. 5.7 – Elements of the deck cross-section of River Seiont Viaduct

The permanent actions applied to both longitudinal girders and their respective partial load factors for persistent design situations defined in Table NA.A2.4(B) of the UK National Annex to EN1990 are summarised in Table 5.3.

Table 5.4 – Permanent actions on River Seiont Viaduct.

Permanent Actions	$\gamma_{G,sup}$	$g_{k,LEFT}$ (kN/m)	$g_{k,RIGHT}$ (kN/m)
Dead Loads			
• Self-weigth of steelwork	1.20	14.8	14.8
• Self-weight of concrete deck	1.35	58.4	58.4
Superimposed Dead Loads			
• Safety barrier	1.20	1.0	1.0
• Safety barrier concrete upstand	1.20	3.8	7.5
• Concrete fill to verges	1.20	3.7	36.0
• Carriageway surfacing	1.20	35.9	24.4

5.3.2. SHRINKAGE

The quantification of the shrinkage strains should contemplate a scenario at traffic opening immediately after the end of construction (age t_0) and another at the end of the service life where all shrinkage strains would have occurred (age t_∞). For the purpose of a preliminary design only the final shrinkage strains were considered. The long-term shrinkage strain ε_{cs} was calculated from the final autogenous and drying strains in accordance with EN1992-1-1 §3.1 and Annex B.2.

The autogenous shrinkage strain ε_{ca} is a linear function of the concrete strength. For the C40/50 concrete strength class of the deck slab it resulted in a value of:

$$\varepsilon_{ca}(\infty) = 2.5 \cdot (f_{ck} - 10) \cdot 10^{-6} \Rightarrow \varepsilon_{ca}(\infty) = 7.5 \times 10^{-5} \quad (5.1)$$

As for the drying shrinkage strain ε_{cd} its final value will depend on the notional thickness of the concrete slab, relative humidity and cement type. In the calculation of the notional thickness of the slab only the soffit was considering in the drying perimeter since a waterproofing membrane will be applied to the top. The relative humidity was taken as 80% and a normal type cement was assumed.

The basic drying shrinkage strain $\varepsilon_{cd,0}$ was calculated from the basic equations given in Annex B.2 of EN1992-1-1.

$$\varepsilon_{cd,0} = 0.85 \cdot \left[(220 + 110 \cdot \alpha_{ds1}) \cdot \exp\left(- \alpha_{ds2} \cdot \frac{f_{cm}}{f_{cm0}} \right) \right] \cdot 10^{-6} \cdot \beta_{RH} \Rightarrow \varepsilon_{cd,0} = 23.8 \times 10^{-5} \quad (5.2)$$

The final value of the drying shrinkage ε_{cd} strain was obtained by applying the correction factor for notional thickness of the deck slab.

$$\varepsilon_{cd}(\infty) = k_h \cdot \varepsilon_{cd,0} = 0.7 \times 23.8 \times 10^{-5} = 16.7 \times 10^{-5} \quad (5.3)$$

The long-term shrinkage strain ε_{cs} to consider in the calculation of the primary and secondary effects of shrinkage amounted to:

$$\varepsilon_{cs}(\infty) = \varepsilon_{ca}(\infty) + \varepsilon_{cd}(\infty) = 7.5 \times 10^{-5} + 16.7 \times 10^{-5} = 24.2 \times 10^{-5} \quad (5.4)$$

5.3.3. Thermal Actions

The bearing arrangement proposed for the structure allows it to expand and contract freely under uniform temperature ranges, with only vertical temperature differences giving rise to internal forces on the deck.

From the two approaches given in EN1991-1-5 §6.1.4 the simplified procedure for Approach 2 was adopted. The effects of temperature difference components are assimilated to those of a temperature difference due to heating or cooling of the concrete slab in relation to the steel girders of $\Delta T_1 = \pm 10^{\circ}C$.

5.3.4. Road Traffic Actions

In order to account for the effects of normal traffic LM1 and LM2 were considered in the design of the structure in accordance with EN1991-2 and subject to the modifications mandated by the UK National Annex.

The special vehicles of LM3 to consider for the effects of General Order Traffic under STGO regulations relate to the type of road being carried by the bridge deck. In accordance with Table A.3 of IAN124/14(W) the type of road is a “Motorway and Trunk Road”. Hence, the bridge is to be designed

for the effects of the SV80, SV100 and SV196 vehicles defined in the UK National Annex to EN1991-2.

The bridge deck will carry a single carriageway with a total width between kerbs of 13.50m. For the application of road traffic actions the carriageway width *w* was divided in a set of notional lanes and a remaining width in accordance with EN1991-2 §4.2.3.

$$w = 13.50\text{m} > 6.00\text{m} \;\Rightarrow\; n_L = \text{Int}\left(\frac{w}{3}\right) = \text{Int}\left(\frac{13.50}{3}\right) = 4\,\text{lanes} \tag{5.5}$$

$$w - 3 \times n_L = 13.50 - 3 \times 4 = 1.50\text{m} \;\; \text{remaining width} \tag{5.6}$$

Where

w - is the carriageway width

n_L - is the number of notional lanes

To obtain the most adverse effects due to traffic loads on either of the longitudinal girders two arrangements of notional lanes were considered. For the most adverse effects on the left girder, the closest lane was numbered as Lane 1, the next as Lane 2, and so forth (Fig. 5.8). The notional lane arrangement for the most adverse effects on the right girder was determined in the same manner starting from opposite side of the carriageway (Fig. 5.9).

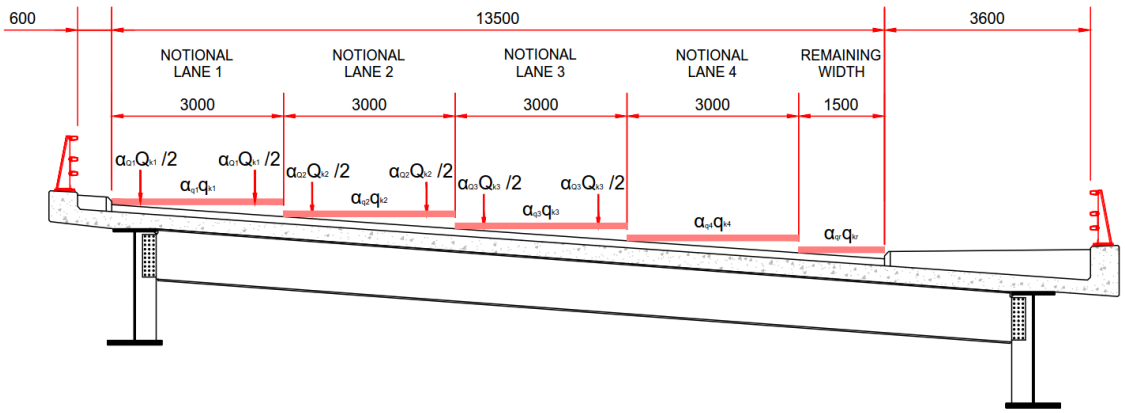


Fig. 5.8 – Notional lanes for most adverse effects on left girder

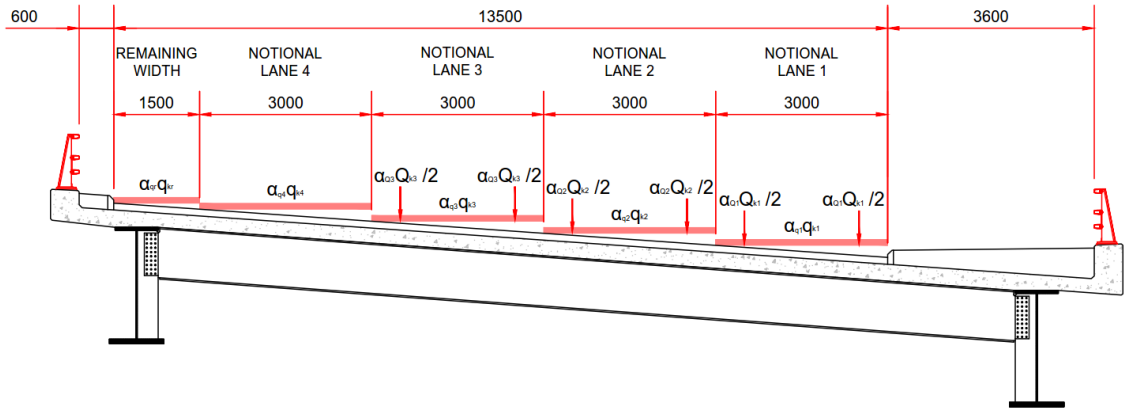


Fig. 5.9 – Notional lanes for most adverse effects on right girder

5.3.5. Combinations of Actions

The purpose of the preliminary design was to validate the section sizes for the main load bearing elements of the structure such as the two main longitudinal girders and the transverse girders. The number of combinations of actions investigated was limited to those expected to yield the most adverse effects. The leading variable actions were chosen based on previous experience with similar works.

It was anticipated that combinations of actions taking load group gr5 as the leading variable action (comprised by the special vehicles from LM3 taken with their characteristic values together with the traffic loads from LM1 at frequent values) accompanied by the temperature difference component were likely to yield the most adverse effect. Combinations of actions taking load group gr1a or the temperature difference component as the leading variable action were also considered.

Table 5.5 – Combinations of actions considered for preliminary design.

	G	S	Q	T
No.	Permanent	Shrinkage	Traffic Loads	Temperature
ULS - Persistent and Transient Design Situation (STR/GEO)				
1	1.35	1.00	1.35×gr5	1.55×0.60
2	1.35	1.00	1.35×0.75×gr1a	1.55
SLS - Characteristic Combination (stress limitation checks)				
1	1.00	1.00	1.00×gr5	0.60
2	1.00	1.00	0.75×gr1a	1.00
SLS - Quasi-Permanent Combination (concrete crack width checks)				
1	1.00	1.00	0	0.50

5.4. GLOBAL ANALYSIS OF THE VIADUCT

5.4.1. EFFECTIVE WIDTH OF FLANGES FOR SHEAR LAG

The effective width b_{eff} of the concrete flanges to account for the effects of shear lag was assessed in accordance with EN1994-2 §5.4.1.2. The distance L_e between points of contraflexure was calculated for each span along with the effective widths on each side of the web b_{ei}. The distance b_o between the centres of the outstand connectors was taken as 0.40m. The effective width was obtained from the expressions given in §5.4.1.2(5) and §5.4.1.2(6).

Table 5.6 – Effective widths of the concrete flange.

Span/Pier No.	Type	L (m)	L_e (m)	b_{e1} (m)	b_{e2} (m)	b_{eff} (m)
S1	End Support	28.0	23.8	1.30	2.98	3.93
S1	Mid-Span	28.0	23.8	1.30	2.98	4.68
P1	Int. Support	-	17.6	1.30	2.20	3.90
S2	Mid-Span	42.5	29.8	1.30	3.72	5.42
P2	Int. Support	-	21.2	1.30	2.65	4.35
S3	Mid-Span	42.5	29.8	1.30	3.72	5.42
P3	Int. Support	-	19.4	1.30	2.43	4.13
S4	Mid-Span	35.0	29.8	1.30	3.72	5.42
S4	End Support	35.0	29.8	1.30	3.72	4.49

In regards to the consideration of shear lag effects in the global analysis of the structure the effective width b_{eff} of the concrete flanges at mid-span was assumed constant over the whole of the spans as per §5.4.1.2(4).

5.4.2. MODULAR RATIOS FOR CONCRETE

The assessment of the modular ratios that account for the effects of concrete creep as per EN1994-2 §5.4.2.2 is based on the short term modular ratio n_0, the creep coefficient φ_t and the creep multiplier ψ_L.

The modular ratio for short-term loading was calculated as the ratio between the modulus of elasticity of structural steel, E_a, and the modulus of elasticity of concrete, E_{cm}.

$$n_0 = E_a / E_{cm} = 210/35 = 6.00 \quad (5.7)$$

The creep coefficient φ_t was obtained from the basic equations in Annex B of EN1992-1-1. Long-term, the creep coefficient φ_t will tend to the value of the notional creep coefficient φ_0, and hence the equation for its calculation can assume a simplified form.

$$\varphi(t,t_0) = \varphi_0 \cdot \beta_c(t,t_0) \quad \Rightarrow \quad \varphi_t = \varphi(\infty,t_0) = \varphi_0 \tag{5.8}$$

A relative humidity of 80% and a normal type cement were assumed in the calculations. For permanent loads, the age of the concrete at loading t_0 was taken as the mean age at the end of the construction of the deck. This was conservatively set at 21 days.

$$\varphi_0 = \varphi_{RH} \cdot \beta(f_{cm}) \cdot \beta(t_0) = 1.128 \times 2.423 \times 0.516 \quad \Rightarrow \quad \varphi_0 = 1.412 \tag{5.9}$$

For shrinkage, the age of the concrete at loading was assumed to be 1 day as per EN1994-2 §5.4.2.2(4), and the notional creep coefficient recalculated accordingly.

$$\varphi_0 = \varphi_{RH} \cdot \beta(f_{cm}) \cdot \beta(t_0) = 1.128 \times 2.423 \times 0.909 \quad \Rightarrow \quad \varphi_0 = 2.488 \tag{5.10}$$

The modular ratios n_L for permanent loads and shrinkage were obtained from the short-term modular ratio n_0 with the notional creep coefficients φ_t and the creep multipliers ψ_L to account for the type of loading. Taking the creep multiplier of 1.10 for permanent loads the respective modular ratio was then calculated.

$$n_L = n_0 \cdot (1 + \psi_L \cdot \varphi_t) = 6.0 \times (1 + 1.10 \times 1.412) \quad \Rightarrow \quad n_L = 15.32 \tag{5.11}$$

A creep multiplier of 0.55 was used for the modular ratio for primary and secondary effects of shrinkage.

$$n_L = n_0 \cdot (1 + \psi_L \cdot \varphi_t) = 6.0 \times (1 + 0.55 \times 2.488) \quad \Rightarrow \quad n_L = 14.21 \tag{5.12}$$

Given the similar values obtained for the modular ratios for the effects of permanent loads and shrinkage it was deemed adequate for a preliminary design to adopt a single long-term modular ratio n_L of 15 for both.

5.4.3. Effects of Cracking of Concrete

EN1994-2 allows the consideration of the effects of concrete cracking on the distribution of internal forces and moments by either the general method described in §5.4.2.3(2) or the simplified method in §5.4.2.3(3). Given that the cross-section type and adjacent span ratios of the superstructure are within its range of validity the simplified method was chosen.

The effect of concrete cracking was accounted for by using the flexural stiffness of the cracked section E_aI_2 over 15% of the span to each side of internal support sections and the uncracked flexural stiffness E_aI_1 elsewhere. In the calculation of the flexural stiffness of the cracked section E_aI_2 the reinforcing steel of the deck slab was taken as B25 bars at 150mm centres for both the top and bottom layers.

The mid-span and support cross-sections for each span were draw to scale using computer drafting software. The concrete flange width was reduced by the appropriate modular ratio n_L to obtain the section properties in steel units for use with the short-term and long-term structural models (Fig. 5.10). For the definition of the cracked cross-section the reinforced concrete deck slab was replaced by two small rectangles with an equivalent section area to the reinforcement within the effective width of the slab.

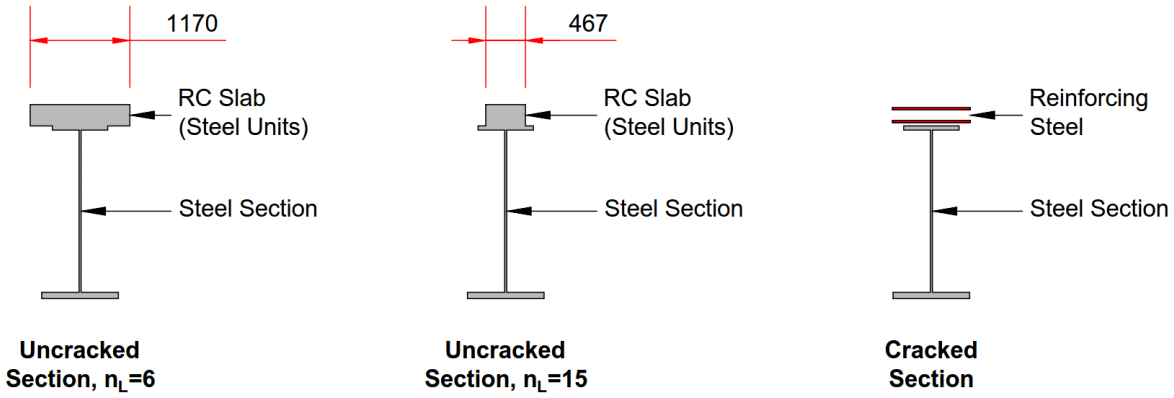


Fig. 5.10 – Notional cross-sections of spans 2 and 3.

5.4.4. Structural Analysis Model

For a preliminary design stage it was desirable that the model of choice could be set up quickly and enabled the swift extraction of analysis results for use in the cross-section checks. Attending to the type of cross-section of the viaduct, which is comprised of twin longitudinal girders with transverse girders girders at close spacing, it was deemed that a three-dimensional beam model would be adequate to replicate the actual behaviour of the structure.

The structure was modelled as a grillage with longitudinal and transverse girders represented by Timoshenko three-dimensional beam elements (Fig. 5.11). The piers were also included and the connection to the deck elements modelled with joint elements assigned a local coordinate system to replicate the radial orientation of the bearings from the fixed point at the south abutment.

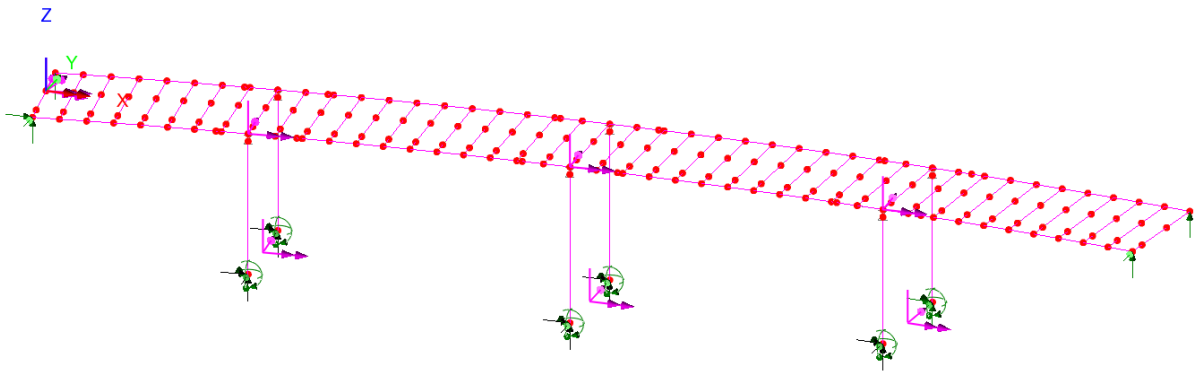


Fig. 5.11 – Three-dimensional line beam model of River Seiont Viaduct.

The geometry of the model accounted for the plan curvature of the deck, whilst the vertical position of the centroid of each section was taken as constant. The effects of the shift in the position of the neutral axis at the transition between different cross-sections were considered in the calculation of the moments due to shrinkage applied to the model.

The design values of material coefficients of concrete and steel assigned to the analysis model were taken from EN1992-1-1 §3.1 and EN1993-1-1 §3.2.6:

- Structural Steel
  - Modulus of elasticity, $E_a = 210\,000\,N/mm^2$;
  - Shear modulus, $G = \frac{E}{2\cdot(1+\upsilon)} = 81\,000\,N/mm^2$;
  - Poisson ratio, $\upsilon = 0.3$;
- Concrete
  - Modulus of elasticity, $E_c = 35\,000\,N/mm^2$;
  - Poisson ratio, $\upsilon = 0.2$;
- Coefficient of thermal expansion, $\alpha = 10\times10^{-6}\ per\ ^\circ C$.

To account for the changes in the cross-sections at each stage and the long-term effects of creep four separate models were analysed:

- A model with the cross sections assigned steel-only properties was used to obtain the effects of the self-weigth of the steelwork and the casting of the concrete slab in the span regions;
- A model with composite cross-sections in the span and steel-only over the supports was used to assess the effects of the casting of the concrete slab over the piers;
- A model considering composite cross-sections using the long-term modular ratio n_L=15 for the effects of permanent actions;
- A model considering composite cross-sections using the short-term modular ratio n_L=6 for the effects of variable actions.

5.4.5. LINEAR ELASTIC ANALYSIS

The internal forces on the members of the superstructure were obtained by linear-elastic analysis of the four models of the superstructure described in the previous section. The total bending moments due to the permanent actions resulted from the superposition of the action effects due to self-weight of the steelwork, self-weight of concrete and superimposed dead loads obtained from the different models considered (Fig. 5.12).

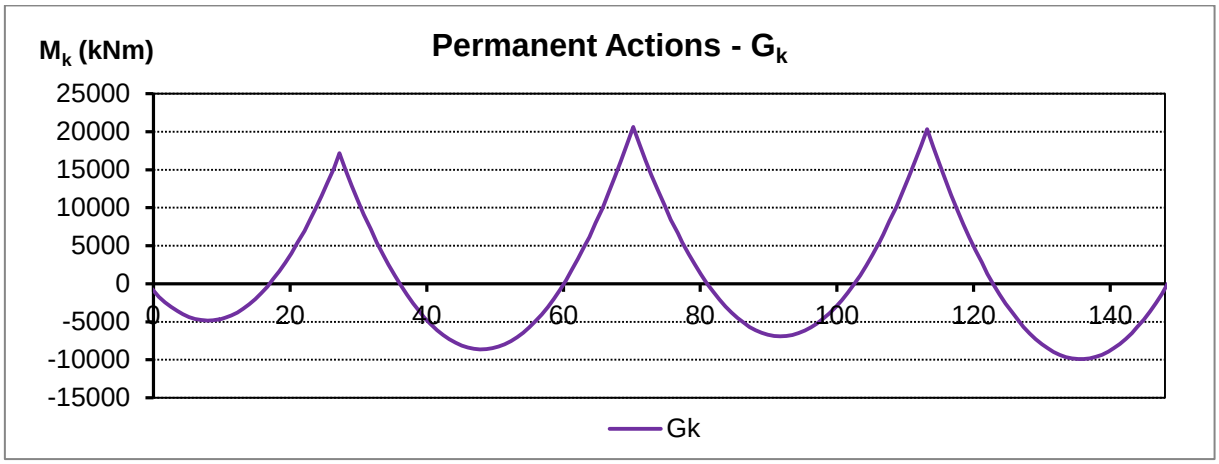


Fig. 5.12 – Bending moment diagram due to effects of permanent actions.

The total effects of shrinkage were extracted from the long-term model to which the axial forces and moments calculated with the long-term shrinkage strain had been applied. The primary effects were neglected over the cracked regions. The secondary effects were obtained by deducting the primary effects from the total effects (Fig. 5.13).

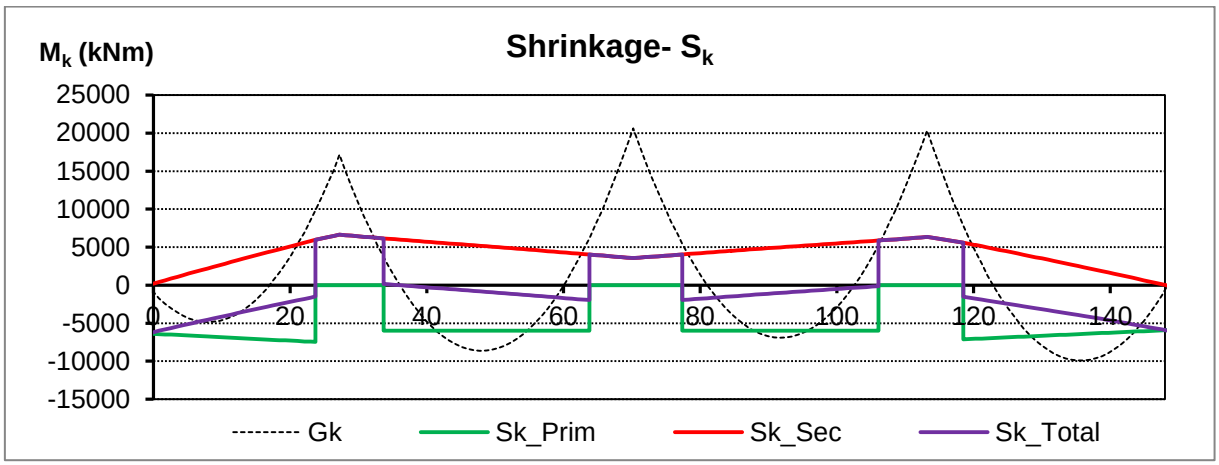


Fig. 5.13 – Bending moment diagrams due to effects of shrinkage.

The envelopes of the effects of road traffic actions were determined by using moving loads representing the tandem systems of load model LM1 and the special vehicles of LM3 travelling along the deck. As for the effects of the uniformly distributed load its envelope was obtained by considering all the possible arrangements within the four spans of the deck. The individual envelopes were then combined by superposition to determine the total effects of load models LM1 and LM3 (Fig. 5.14). The most adverse effects for load model LM3 were due to the SV196 vehicle. All effects of road traffic actions were calculated using the short-term model.

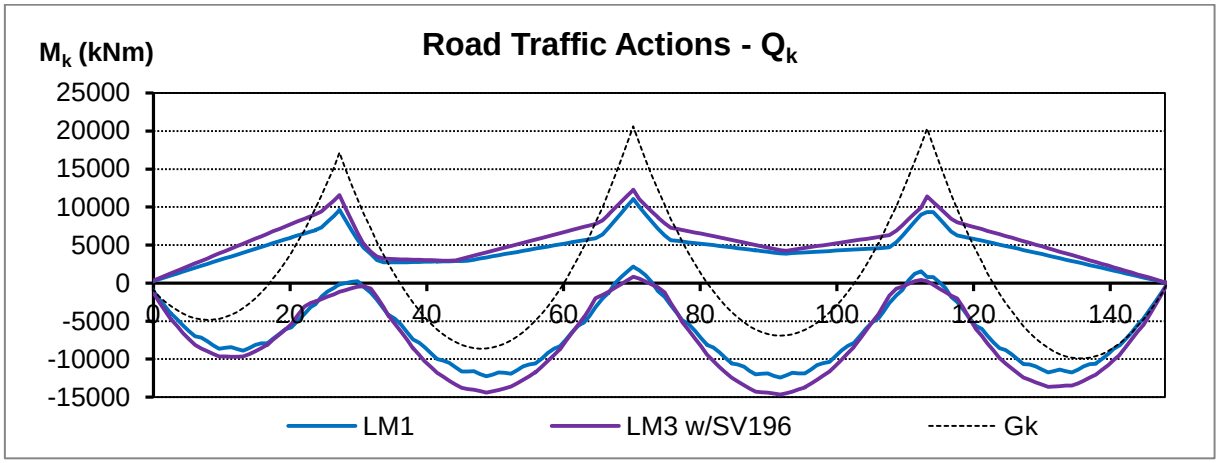


Fig. 5.14 – Bending moment envelopes due to effects of road traffic actions.

The effects of the temperature difference component were obtained from the short-term model in the same manner as the shrinkage effects considering the axial forces and moments due to the temperature difference T_k=±10°C between the concrete slab and the steel section (Fig. 5.15).

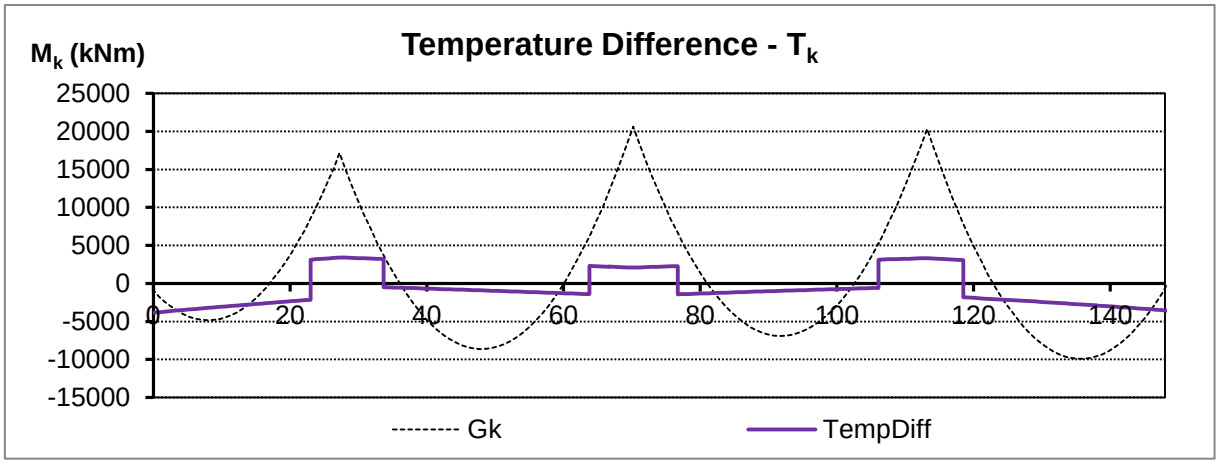


Fig. 5.15 – Bending moment diagram due to effects of temperature difference.

The bending moment and shear force envelopes for the ultimate limit state combinations considered were determined by superposition of the effects from permanent loads and shrinkage with the envelopes of the effects of variable actions, each factored by the appropriate partial factor. As anticipated, the combination with road traffic actions from LM3 as the leading variable action yielded the most onerous effects (Fig. 5.16 and Fig. 5.17).

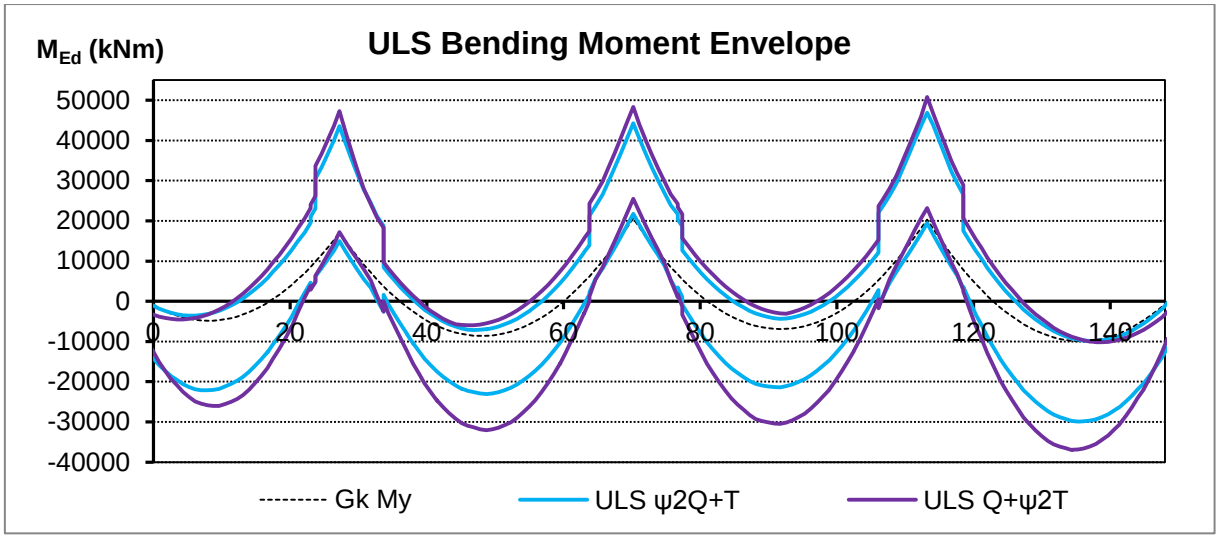


Fig. 5.16 – ULS bending moment envelope.

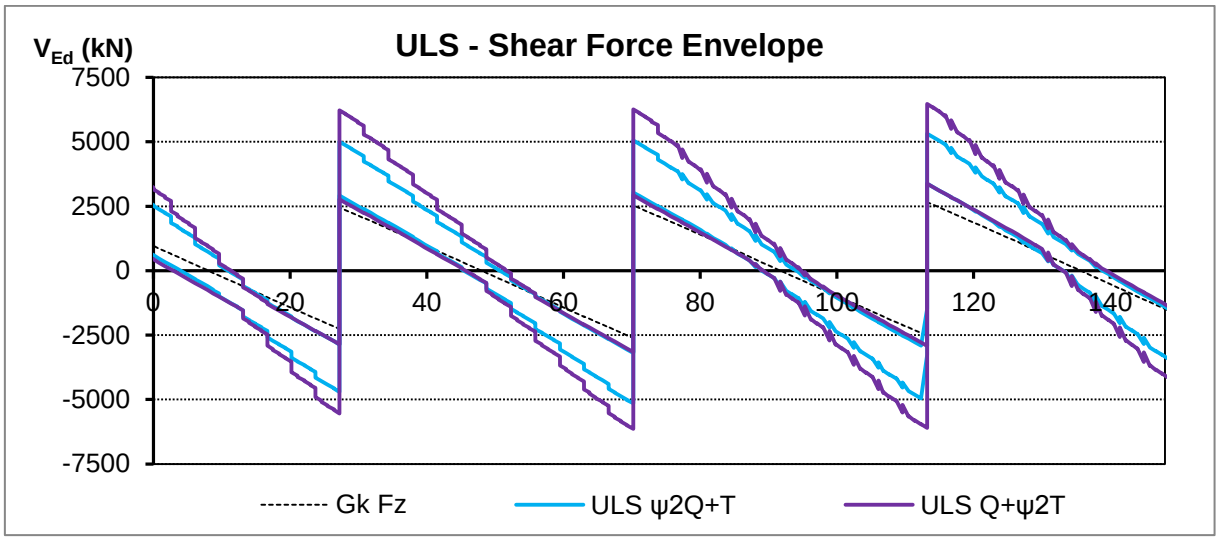


Fig. 5.17 – ULS shear force envelope.

5.5. CROSS-SECTION VERIFICATION AT ULS

The material resistances used in the calculation of the cross-section resistances to bending and vertical shear were:

- Characteristic yield strength of structural steelwork as per EN10025-1,
  - For $t \le 16mm$, $f_y = 355\,N/mm^2$;
  - For $16 < t \le 40mm$, $f_y = 345\,N/mm^2$;
  - For $40 < t \le 80mm$, $f_y = 335\,N/mm^2$.
- Characteristic concrete cylinder strength as per Table 3.1 of EN1992-1-1,
  - For a C40/50 strength grade, $f_{ck} = 40\,N/mm^2$;
- Characteristic yield strength of reinforcing steel as per EN1992-1-1 §3.2,
  - For B500B grade, $f_{sk} = 500\,N/mm^2$.

5.5.1. BENDING RESISTANCE OF THE SPAN CROSS-SECTION

By inspection of the bending moment envelope it can be seen that the highest sagging moment occurs in span 4 of the viaduct. Attending to the fact that the effective width b_{eff} of the last span is 5.40 m, as opposed to the 7.00m of spans 2 and 3, it is evident that this will be the section governing the design.

For classification purposes a plastic stress distribution in the cross-section was assumed and once position of the plastic neutral axis had been determined the hypothesis checked. In order to determine whether or not the plastic neutral axis lays within the depth of the concrete slab the total force on the steel section and on the slab must be calculated.

Table 5.7 – Axial forces on the steel section elements.

Steel Section Element	Dimensions (mm)	Yield Strength fy (N/mm^2)	Section Area (mm^2)	Axial Force (kN)
Top Flange	550x35	345	19250	6641.2
Web Plate	16x1940	355	31040	11019.2
Bottom Flange	750x50	345	37500	12937.5
$N_{pl,a}=\Sigma F_i$	-	-	77790	30597.5

The maximum compressive force that can be mobilised by the concrete slab is:

$$N_c = 0.85 \cdot f_{cd} \cdot b_{eff} \cdot h = 0.85 \times \frac{40 \times 10^3}{1.5} \times 5.4 \times 0.25 = 30600kN \quad (5.13)$$

Since the maximum tensile force $N_{pl,a}$ of the steel section is less than the maximum compressive force N_c of the concrete slab the plastic neutral axis lies within the thickness of the slab. The depth of the plastic neutral axis is given by:

$$x = \frac{N_{pl,a}}{0.85 \cdot f_{cd} \cdot b_{eff}} = \frac{30597.5}{0.85 \times 40^3 / 1.5 \times 5.4} = 0.250\text{m} \tag{5.14}$$

There is no need to check the width-to-thickness ratio of the parts of the steel section as it is fully in tension. The composite cross-section is Class 1 in sagging bending.

Since the section is compact its plastic resistance moment can be mobilised. To calculate the plastic resistance moment the internal forces and lever arms of all elements of the composite cross-section were determined.

Table 5.8 – Axial forces and lever arms of the composite cross-section elements.

Cross-Section Element	Axial Force F_i (kN)	Centroid z_i (mm)	Moment $F_i \cdot z_i$ (kNm)
Concrete slab, N_c	30600	125.0	3825.0
Top Flange, N_{tf}	-6641.2	-17.5	116.2
Web Plate, N_w	-11019.2	-1005.0	11074.3
Bottom Flange, N_{bf}	-12937.5	-2000.0	25875.0
$M_{pl,Rd} = \Sigma F_i \cdot z_i$	-	-	40890.5

The cross-section is adequate at ultimate limit state, as the plastic resistance moment $M_{pl,Rd}$ is greater than the acting bending moment M_{Ed}.

$$\eta = \frac{M_{Ed}}{M_{pl,Rd}} = \frac{36975.9}{40890.5} = 0.90 < 1.00 \tag{5.15}$$

The utilisation ratio obtained η=0.90 appears somewhat high for a preliminary design but it should be borne in mind that this refers to the most adverse scenario. The bending moments in spans 1, 2 and 3 are all considerably lower and so will be their utilisation factors. Observing the bending moment envelope it is apparent that the sagging moment on span 4 is about 20% higher than elsewhere, hence it can be concluded that it would be advantageous to adjust slightly this end span.

5.5.2. BENDING RESISTANCE OF THE PIER CROSS-SECTION

At sections over the supports the effective width b_{eff} of the concrete flange for cross-section analysis is no longer equal to the width used in the global analysis of the structure. Different effective widths were obtained for all three pier sections, as shown in Table 5.6.

The effective width width b_{eff} at pier P3 is marginally larger than of pier P1 but has to cater for a bending moment about 10% higher. For this reason it was deemed that the section at pier P3 will govern the design, and its effective width of 4.10m was adopted in the cross-section analysis for hogging bending.

For classification of the cross-section in hogging bending a plastic stress distribution was assumed and this hypothesis subsequently checked once position of the plastic neutral axis had been determined. Since the concrete slab is in tension only the areas of the top and bottom layers of reinforcement (B25mm bars at 150mm centres) within the effective width were considered.

Table 5.9 – Axial forces on cross-section elements for plastic stress distribution.

Cross-Section Element	Yield Strength fy (N/mm^2)	Section Area (mm^2)	Axial Force (kN)
Top Reinforcement, $N_{s,top}$	435	13420.7	5838.0
Bottom Reinforcement, $N_{s,bot}$	435	13420.7	5838.0
Top Flange, N_{tf}	335	37500	12562.5
Bottom Flange, N_{bf}	335	76000	25460.0

The net force on the web of the steel section N_w was determined from equilibrium considerations:

$$N_{s,top} + N_{s,bot} + N_{tf} + N_w - N_{bf} = 0 \Leftrightarrow$$

$$5838.0 + 5838.0 + 12562.5 + N_w - 25460 = 0 \quad \Leftrightarrow \quad N_w = 1221.5\text{kN} \tag{5.16}$$

The positive value obtained means that the net axial force on the web is tensile. The distance Δz_{PNA} of the plastic neutral axis to mid-height of the web was then determined with the following expression:

$$\Delta z_{PNA} = \frac{N_w/2}{t_w \cdot f_{yw}} = \frac{1221.5/2}{25\times10^{-3}\times345\times10^{3}} = 0.07081\text{m} = 70.8\text{mm} \tag{5.17}$$

With the depth of the plastic neutral axis defined at 70.8mm below the web's mid-height the tension and compression forces on the web could now be calculated.

Table 5.10 – Axial forces on the cross-section web for plastic stress distribution.

Cross-Section Element	depth (mm)	Yield Strength fy (N/mm^2)	Section Area (mm^2)	Axial Force (kN)
Web (tens), $N_{w,t}$	1018.3	345	25457.5	8782.8
Web (comp), $N_{w,c}$	876.7	345	21917.5	7561.5
Web, $N_w = N_{w,t} + N_{w,c}$	1895	345	47375.0	1221.3

Having determined the depth of the web in compression all the parts of the cross-section could now be classified and the initial assumption of a compact cross-section verified. The class of each of the compression parts of the cross-section was obtained from their width-to-thickness ratios in accordance with Table 5.2 of EN1993-1-1.

- Class of the top flange:
  - Top flange in tension, Class 1.
- Class of the compressed part of the web:
  - Check for Class 1 limit:

$$\alpha = \frac{h_{w,c}}{h_w} = \frac{876.7}{1895} = 0.463 < 0.5 \quad \Rightarrow \quad \frac{c}{t} < \frac{36 \cdot \varepsilon}{\alpha}$$

$$\frac{c}{t} = \frac{1895}{25} = 75.8 > \frac{36 \cdot \varepsilon}{\alpha} = \frac{36 \times 0.81}{0.463} = 63.0 \rightarrow \text{Not Class 1} \qquad (5.18)$$

  - Check for Class 2 limit:

$$\alpha = \frac{h_{w,c}}{h_w} = \frac{876.7}{1895} = 0.463 < 0.5 \quad \Rightarrow \quad \frac{c}{t} < \frac{41.5 \cdot \varepsilon}{\alpha}$$

$$\frac{c}{t} = \frac{1895}{25} = 75.8 > \frac{41.5 \cdot \varepsilon}{\alpha} = \frac{41.5 \times 0.81}{0.463} = 72.6 \rightarrow \text{Not Class 2} \qquad (5.19)$$

  - Check for Class 3 limit:

    The Class 3 limit is based on an elastic stress distribution and hence requires that the position of the elastic neutral axis z_{ENA} be known. The position of the elastic neutral axis was defined as the distance from the outer compression fibre to the centroid of the cross-section, z_{ENA}=982.5mm.

$$\psi = -\frac{h_{w,t}}{h_{w,c}} = -\frac{1895-982.5}{982.5} = -0.929 > -1 \quad \Rightarrow \quad \frac{c}{t} < \frac{42\cdot\varepsilon}{0.67+0.33\cdot\psi}$$

$$\frac{c}{t} = \frac{1895}{25} = 75.8 < \frac{42\cdot\varepsilon}{0.67+0.33\cdot\psi} = \frac{42\times 0.81}{0.67+0.33\times(-0.929)} = 93.6 \rightarrow \text{Class 3} \tag{5.20}$$

- Class of the bottom flange:
  - Check for Class 1 limit:

$$\frac{c}{t} = \frac{(950-25)/2}{80} = 5.78 < 9\cdot\varepsilon = 9\times 0.81 = 7.29 \rightarrow \text{Class 1} \tag{5.21}$$

The cross-section has a Class 3 web with Class 1 flanges. In accordance with EN1994-2 §5.5.2(3) it may be treated as an effective Class 2 cross-section, provided that an effective web is considered as per EN1993-1-1 §6.2.2.4.

The effective web is defined by replacing the compressed part of the web by two compression blocks of depth $20\cdot\varepsilon\cdot t_w$, one adjacent to the compression flange and the other just below the plastic neutral axis (Fig. 5.18). The plastic resistance moment of the effective Class 2 cross-section was used in the assessment of the bending resistance.

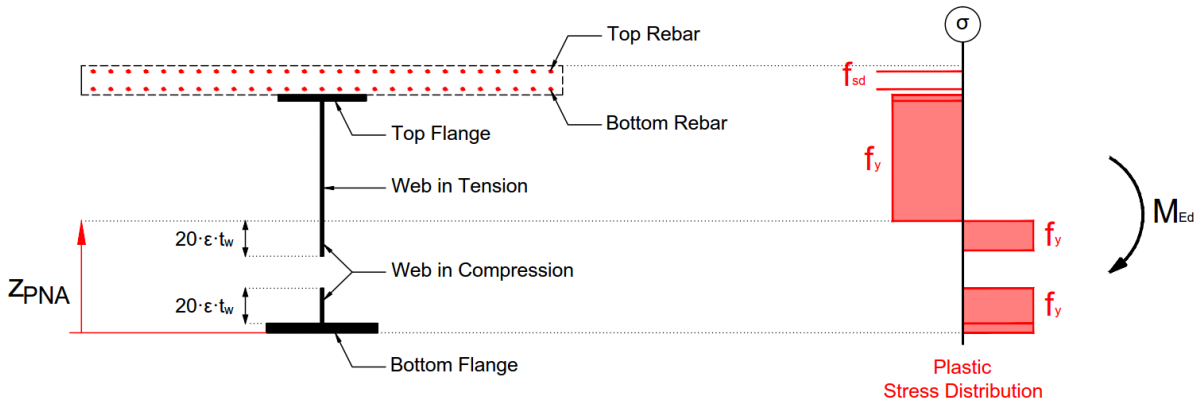


Fig. 5.18 – Plastic stress distribution on effective Class 2 cross-section.

As before, the position of the plastic neutral axis can be determined from the equilibrium of forces in the cross-section. The forces in the reinforcement and in both flanges are known and the compression force on the web can be readily obtained from the area of the two compression blocks.

$$N_{w,c} = 2 \times (t_w \times 20 \cdot \varepsilon \cdot t_w) \cdot f_{yw} \Leftrightarrow$$

$$N_{w,c} = 2 \times (25 \times 20 \times 0.81 \times 25) \times 10^{-6} \times 345 \times 10^3 = 6986.3\text{kN} \quad (5.22)$$

With the axial forces on all other elements quantified the tensile force on the web could now be determined:

$$N_{w,t} = N_{bf} + N_{w,c} - N_{s,top} - N_{s,bot} - N_{tf} \Leftrightarrow$$

$$N_{w,t} = 25460.0 + 6986.3 - 2 \times 5838.0 - 12562.5 = 8207.8\text{kN} \quad (5.23)$$

After finding the corresponding depth of the web in tension, the position z_{PNA} of the plastic neutral axis was calculated:

$$h_{w,t} = \frac{N_{w,t}}{t_w \cdot f_{yw}} = \frac{8207.8}{25 \times 10^{-3} \times 345 \times 10^3} = 0.9516\text{m} = 951.6\text{mm} \quad (5.24)$$

$$z_{PNA} = h - t_{tf} - h_{w,t} = 2025 - 50 - 951.6 = 1023.4\text{mm} \quad (5.25)$$

With the plastic neutral axis located the lever arms of the internal forces in the cross-section are defined, and the plastic moment resistance can be readily obtained.

Table 5.11 – Axial forces and lever arms of the effective cross-section elements.

Cross-Section Element	Axial Force N_i (kN)	Centroid z_i (mm)	$M_i = F_i \cdot z_i$ (kNm)
Top Reinforcement, $N_{s,top}$	-5838.0	-1201.6	7014.9
Bottom Reinforcement, $N_{s,bot}$	-5838.0	-1051.6	6139.2
Top Flange, N_{tf}	-12562.5	-1026.6	12896.7
Web (tens), $N_{w,t}$	-8207.8	-525.8	4315.7
Web (comp), $N_{w,c1}$	3493.1	202.5	707.3
Web (comp), $N_{w,c2}$	3493.1	740.9	2588.0
Bottom Flange, N_{bf}	25460.0	983.4	25037.4
$M_{pl,Rd} = \Sigma F_i \cdot z_i$	-	-	58699.2

The web cut-out was found to be only 133.4mm deep, which is in line with the findings during cross-section classification that the web marginally exceeded the Class 2 limit.

$$h_{cut} = h_w - h_{w,t} - 2 \times (20 \cdot \varepsilon \cdot t_w) = 1895 - 951.6 - 2 \times (20 \times 0.81 \times 25) = 133.4mm \quad (5.26)$$

The cross-section was deemed adequate at ultimate limit state, as the plastic resistance moment $M_{pl,Rd}$ is greater than the acting bending moment M_{Ed}.

$$\eta = \frac{M_{Ed}}{M_{pl,Rd}} = \frac{50805.0}{58699.2} = 0.86 < 1.00 \quad (5.27)$$

5.5.3. Shear Resistance of Pier Cross-Section

The ladder deck cross-section obliges the use of closely spaced transverse girders which require transverse stiffeners at every connection to the longitudinal girders. In the River Seiont viaduct a cross girder spacing a of 3.50m was adopted, which together with the girder depth h_w defines the dimensions of the web panels (Fig. 5.19).

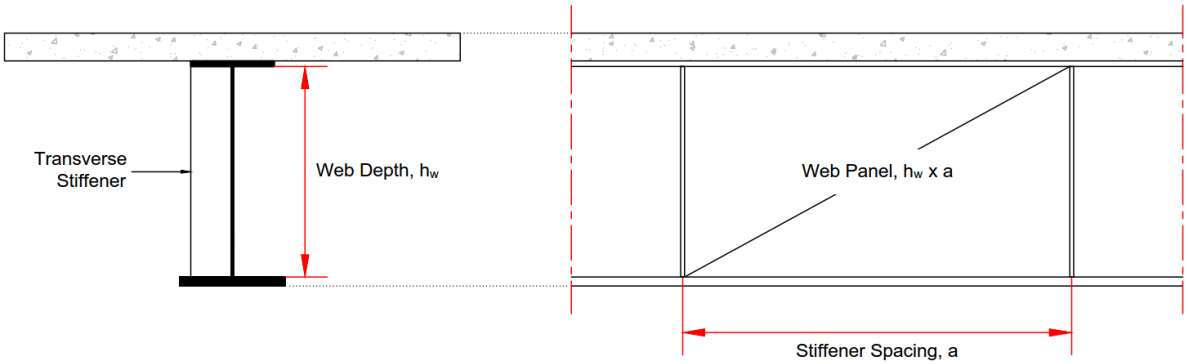


Fig. 5.19 – Web panels on longitudinal girders of River Seiont Viaduct.

The plastic shear resistance $V_{pl,a,Rd}$ of the web of the longitudinal plate girders was calculated in accordance with EN1993-1-1 §6.2.6.

$$V_{pl,a,Rd} = \frac{A_v \cdot \left(f_y / \sqrt{3}\right)}{\gamma_{M0}} = \frac{h_w \cdot t_w \cdot f_{yw}}{\sqrt{3} \cdot \gamma_{M0}} \Leftrightarrow$$

$$V_{pl,a,Rd} = \frac{(1895 \times 25) \times 10^{-6} \times 345 \times 10^3}{\sqrt{3} \times 1.0} = 9436.4\text{kN} \quad (5.28)$$

The web plate slenderness was checked in regards to susceptibility to shear buckling as per EN1993-1-5 §5.1(2) considering the limits for stiffened webs. The shear buckling coefficient k_τ was calculated in accordance with the expressions given in Annex A.3 of EN1993-1-5.

$$\begin{cases} k_\tau = 5.34 + 4.00 \cdot (h_w/a)^2 & \text{, when } a/h_w \geq 1 \\ k_\tau = 4.00 + 5.34 \cdot (h_w/a)^2 & \text{, when } a/h_w < 1 \end{cases} \Leftrightarrow$$

$$k_\tau = 5.34 + 4.00 \cdot (1895/3500)^2 = 6.513 \quad (5.29)$$

With the shear buckling coefficient k_τ determined the web panel slenderness was then checked:

$$\begin{cases} \frac{h_w}{t_w} > \frac{72}{\eta} \cdot \varepsilon & \text{, for unstiffened webs} \\ \frac{h_w}{t_w} > \frac{31}{\eta} \cdot \varepsilon \cdot \sqrt{k_\tau} & \text{, for stiffened webs} \end{cases} \Leftrightarrow$$

$$\frac{h_w}{t_w} = \frac{1895}{25} = 75.8 > \frac{31}{\eta} \cdot \varepsilon \cdot \sqrt{k_\tau} = \frac{31}{1.0} \times 0.81 \times \sqrt{6.513} = 64.1 \rightarrow \text{SlenderWeb} \quad (5.30)$$

The web panel was found to exceed the slenderness limit, hence its shear buckling resistance $V_{b,Rd}$ would need to be determined in accordance with EN1993-1-5 §5.2. In the assessment of the shear buckling resistance only the contribution from the web $V_{bw,Rd}$ would be considered.

To quantify the shear buckling resistance the critical shear buckling stress τ_{cr} of the web panel was first calculated:

$$\tau_{cr} = k_\tau \cdot \sigma_E = k_\tau \cdot 190000 \cdot \left(\frac{t_w}{h_w}\right)^2 = 6.513 \times 190000 \times \left(\frac{25}{1895}\right)^2 = 215.4\text{MPa} \quad (5.31)$$

Followed by the modified slenderness λ_w of the web plate:

$$\bar{\lambda}_w = \sqrt{\frac{f_{yw}/\sqrt{3}}{\tau_{cr}}} = \sqrt{\frac{345/\sqrt{3}}{215.4}} = 0.962 \tag{5.32}$$

The web panel of the cross-section at pier P3 relates to an internal support. Accordingly, the reduction factor for shear buckling χ_w was obtained from the expressions in Table 5.1 of EN1993-1-5 considering a rigid end post condition.

$$\frac{0.83}{\eta} \le \bar{\lambda}_w \le 1.08 \Rightarrow \chi_w = \frac{0.83}{\bar{\lambda}_w} \quad \Leftrightarrow \quad 0.83 \le \bar{\lambda}_w = 0.962 \le 1.08 \Rightarrow \chi_w = \frac{0.83}{0.962} = 0.863 \tag{5.33}$$

The contribution from the web to the shear buckling resistance of the web panel was then calculated from the expression given in EN1993-1-5 §5.2(1).

$$V_{bw,Rd} = \frac{\chi_w \cdot f_{yw} \cdot h_w \cdot t_w}{\sqrt{3} \cdot \gamma_{M1}} = \frac{0.863 \times 345 \times 10^3 \times (1895 \times 25) \times 10^{-6}}{\sqrt{3} \times 1.10} = 7403.3\text{kN} \tag{5.34}$$

The resistance to vertical shear V_{Rd} of the web panel is the lesser of the plastic shear resistance $V_{pl,a,Rd}$ and the shear buckling resistance V_{bRd}, and in this case is governed by the former. The web panel resistance was found to be adequate at ultimate limit state.

$$\eta = \frac{V_{Ed}}{V_{Rd}} = \frac{6466.1}{7403.3} = 0.87 < 1.00 \tag{5.35}$$

5.5.4. Bending and Vertical Shear Interaction of Pier Cross-Section

The utilisation ratio of the cross-section in shear is greater than 50%, which implies that the effect of the shear force in the bending resistance must be considered in accordance with EN1994-2 §6.2.2.4. For cross-sections in Class 1 or 2 this effect is taken into account by using a reduced steel strength given by $(1-\rho)\cdot f_y$ in the web of the steel section.

$$\rho = \left(2 \cdot \frac{V_{Ed}}{V_{Rd}} - 1\right)^2 = \left(2 \times \frac{6466.1}{7403.3} - 1\right)^2 = 0.558 \tag{5.36}$$

$$(1-\rho)\cdot f_{yw} = (1-0.558)\times 345 = 152.5\text{MPa} \tag{5.37}$$

Once the reduced steel strength of the web was determined the location of the plastic neutral axis needed to be recalculated from the equilibrium of the internal forces in the cross-section. The forces in the reinforcement and flanges are known, as well as the compression force on the web which was obtained from the area of the two compression blocks taking the reduced steel strength.

$$\begin{aligned} N_{w,c} &= 2\times(t_w \times 20\cdot\varepsilon\cdot t_w)\cdot(1-\rho)\cdot f_{yw} \Leftrightarrow \\ N_{w,c} &= 2\times(25\times 20\times 0.81\times 25)\times 10^{-6}\times 152.5\times 10^{3} = 3088.1\text{kN} \end{aligned} \tag{5.38}$$

The tensile force on the web was determined from the equilibrium of internal forces:

$$\begin{aligned} N_{w,t} &= N_{bf} + N_{w,c} - N_{s,top} - N_{s,bot} - N_{tf} \Leftrightarrow \\ N_{w,t} &= 25460.0 + 3088.1 - 2\times 5838.0 - 12562.5 = 4309.6\text{kN} \end{aligned} \tag{5.39}$$

By calculating the web depth in tension the position z_{PNA} of the plastic neutral axis was obtained:

$$h_{w,t} = \frac{N_{w,t}}{t_w\cdot(1-\rho)\cdot f_{yw}} = \frac{4309.6}{25\times 10^{-3}\times 152.5\times 10^{3}} = 1.1304\text{m} = 1130.4\text{mm} \tag{5.40}$$

$$z_{PNA} = h - t_{tf} - h_{w,t} = 2025 - 50 - 1130.4 = 844.6\text{mm} \tag{5.41}$$

The plastic resistance moment of the cross-section was calculated from the revised forces on the web and taking the centroids of the forces in the cross-section elements relative to the new location of the plastic neutral axis.

Table 5.12 – Axial forces and lever arms considering reduced steel strength of web.

Cross-Section Element	Axial Force N_i (kN)	Centroid z_i (mm)	$M_i=F_i \cdot z_i$ (kNm)
Top Reinforcement, $N_{s,top}$	-5838.0	-1380.4	8058.8
Bottom Reinforcement, $N_{s,bot}$	-5838.0	-1230.4	7183.1
Top Flange, N_{tf}	-12562.5	-1155.4	14514.7
Web (tens), $N_{w,t}$	-4309.6	-565.2	2435.8
Web (comp), $N_{w,c1}$	1544.0	202.5	312.7
Web (comp), $N_{w,c2}$	1544.0	562.1	867.9
Bottom Flange, N_{bf}	25460.0	804.6	20485.1
$M_{pl,Rd}=\Sigma F_i \cdot z_i$	-	-	53867.1

The cross-section was found to be adequate at ultimate limit state, as the plastic resistance moment $M_{pl,Rd}$ was greater than the acting bending moment M_{Ed}.

$$\eta = \frac{M_{Ed}}{M_{pl,Rd}} = \frac{50805.0}{53867.1} = 0.94 < 1.00 \tag{5.42}$$

The utilisation ratio obtained is fairly high for a preliminary design stage. It should be noted that conservatively the most onerous shear force and bending moment were taken, as opposed to concomitant values. Furthermore, in accordance with EN1993-1-5 §7.1(2) the combined bending and resistance check should be met at all sections other than those located at a distance $h_w/2$ from the support. If instead the bending moment in a section 900mm to the left of the support of pier P3 was considered a similar utilisation ratio to that of the bending resistance would be obtained.

$$\eta = \frac{M_{Ed}}{M_{pl,Rd}} = \frac{45921.5}{53867.1} = 0.85 < 1.00 \tag{5.43}$$

5.6. MATERIAL QUANTITIES AND STEEL CONSUMPTION

The preliminary design undertaken validated the cross-sections of the longitudinal girders of the viaduct. The resistances of the intermediate and support cross girders and of the reinforced concrete slab were also checked for ultimate limit states. With the section sizes and required reinforcement defined for all the elements of the superstructure the material quantities to be used in the construction of the viaduct were estimated.

Table 5.13 – Structural steelwork quantities based on preliminary design.

Superstructure Element	Area A (m^2)	Length L_i (m)	Volume V_i (m^3)	Tonnage M_i (t)
Main Girders				
• Span	0.088	185.0	16.24	127.5
• Pier	0.161	112.0	18.02	141.4
Cross Girders				
• Intermediate	0.031	575.2	17.83	139.9
• Support	0.037	77.3	2.86	22.5
Stiffening (10% ΣM_i)	-	-	-	43.1
Total Steel Tonnage	-	-	-	474.4

The structural steelwork consumed in the superstructure amounts to 474 tonnes. The corresponding average steel consumption per metre square of deck is 171.4kg, which is in line with the values provided by the simplified expression from Eq. 3.1.

6 CONCLUSIONS

6.1. CLOSING REMARKS

This dissertation intended to characterise the state-of-the-art of steel-concrete composite bridge structures as the result of an incremental evolution of steel bridges from the first examples born in Britain in the late 1700's.

It was described how the technological evolution of steel bridges developed as part of a larger on-going process that changed the fabric of Western European societies: the Industrial Revolution. The impressive rate of innovation of this period was fuelled by the combination of the advances in scientific knowledge, the use of a new energy source, and the development of new manufacture processes.

The rapid development of steel bridge design and construction in the century after the first cast iron bridge at Coalbrookedale in 1779 was highlighted. As engineers grew more experienced with steel new bridge types were developed to make a more efficient use of its properties. The appearance of the riveted steel plate girder in the 19th century provided the ancester for today's welded steel plate girders.

The reconstruction Europe after World War II and the postwar expansion of motorways were shown to have provided the setting for steel-concrete composite bridges to appear. Following these early prototypes some of the first standards for the design of composite structures were published. Lessons learned from accidents and extensive investigation programs on plate buckling led to the development of modern design codes. The designs of today's steel-concrete composite bridges reflects the confidence engineers have in their assessment of the behaviour of these structures.

A quantitative analysis of road bridges in service in Wales appraised the share that composite bridges currently have within existing bridges. The span ranges for which they have been the preferred option was commented upon. This was followed by an overview of the most common types of steel-concrete composite decks in use in the UK and their favored field of application. A breakdown of the typical fabrication costs of steel plate girders showed how key factors other than minimum weight affect overall economy.

Following the historical appraisal of the state-of-the-art the global analysis of composite bridge decks was presented. The permanent and variable actions to consider for design were laid out, with emphasis on aspects that are particular to the UK in regards to temperature gradients and especially road traffic

actions. The rules that define combinations of actions for serviceability and ultimate limit states were explained and the combination factors and partial load factors noted.

Consideration of the time-dependant properties of concrete that are creep and shrinkage is essential to the design of composite bridges. The methods given by the Eurocodes for their quantification were explained and the typical ranges of values for shrinkage strains and creep coefficients provided.

The options at the disposal of the designer regarding the modelling for structural analysis of composite decks were listed and their strong points and limitations pointed out. The implications of the choice of model on the allowance for shear lag effects was discussed, as was the use of modular ratios to account for the effects of concrete creep. The influence of cracking of concrete on the distribution of the sectional forces was argued and the methods proposed by the Eurocodes to account for its effects explained.

An overview of the design of composite cross-sections started by presenting the section classification process adopted by the Eurocodes. The link between the cross-section classification and the resistances which may be used of was exposed.

The verifications of resistance of composite cross-sections customary of bridge decks for ultimate limite states were discoursed upon. The assessment of the resistance to bending flexure, to vertical shear and to their combined effects was explained. The verification of the shear connection for the effects of longitudinal shear, which is a key aspect of composite structures, was presented in detail.

The stress limitations imposed by serviceability limit state verifications for structural steelwork, reinforcing steel and concrete were listed and their relevance in ensuring adequate design of the cross-section for service conditions emphasized. The quantification of the required reinforcement to limit crack widths in regions where the concrete slab is in tension and its importance to guarantee the durability of the structure was addressed.

In order to illustrate how the selection of deck type, global analysis methods and cross-section verifications all come together in the design of a bridge structure a case study of the preliminary design of a viaduct with a steel-concrete composite deck was presented. The structure under consideration was the River Seiont Viaduct on the A487 Caernarfon to Bontnewydd Bypass, in Wales.

The option for a ladder composite structure was justified by a comparative exercise in which 5 different options were evaluated to select the one which best responded to the mandatory assumptions of the tender brief and the constraints on site. The development of the structural form regarding span arrangement, span-to-depth ratio of the longitudinal girders, the depth and spacing of the cross girders and arrangement of the deck slab was then explained.

The type of model chosen for the structural analysis of the viaduct was described and the methodology of analysis adhered to explained, and the section properties used in the models presented. The permanent and variable actions considered as well as the combinations of actions deemed to be relevant for the superstructure design were listed. Their effects were illustrated in the form of bending moment and shear force diagrams. The envelopes of the effects of actions considered for ultimate limit state checks were provided.

The cross-section classification for the span and pier cross-sections was presented and the differences between the two commented. The assessment of bending resistance for the midspan cross-section and

for the cross-section over the piers was presented in detail. The calculation of the resistance to vertical shear was exposed and commented upon. The verification of the combined effects of bending and vertical shear at the cross-section over the piers was justified and the calculation process explained.

With the preliminary cross-section design finalised an overview of the material quantities that the construction of the viaduct will require provided a point of reference for the economy of design. The steel consumption per metre square of deck highlights the competitiveness of this type of twin girder composite deck. This factor, together with its technical merits and ease of construction, demonstrates how well adapted ladder decks are for medium spans with wide carriageways which are often required for highway structures.

6.2. FUTURE WORKS

The UK government investment plan for infrastructure outlined in the 2013 report *"Investing in Britain's Future"* commits to publicly fund a pipeline of transportation projects with over £70 billion pounds. Included in these projects are the biggest road investment programme since the 1970's (£16 billion), the construction of High Speed 2 that will link northern England to the capital in just two hours (over £15 billion) and the upgrading of the existing rail network (£22.5 billion) (HM Treasury, 2013).

The volume of works that this investment plan requires will be substantial and undoubtedly require the construction of a large number of road and rail bridges. Engineering consultants can expect to receive a rising number of task orders in the period up to 2021. As with all publicly funded projects the best possible use and allocation of resources is essential. Steel-concrete composite structures can make a significant contribution by offering value-for-money in terms of whole life-cycle cost.

The benefits from emerging technologies and new practices in the field of composite construction tested elsewhere in Europe will likely be put to use in the UK. Bridges with double composite action where bottom composite flanges are used over the support sections, a type of solution that has been tested in Spain with great success since the late 1970's (Millanes Mato, 2004), could expand the economical span ranges of composite structures. Solutions with a proven track record that have been used in viaducts in the Spanish high-speed railway network could be transferrable to works for High Speed 2. Strict-box composite decks provide increased torsional stiffness and enhanced dynamic behaviour while keeping the simple construction of plate girders, whereas steel-concrete composite truss decks provide an alternative for long span viaducts (Millanes Mato, 2009).

The near future will provide bridge engineers in the UK with the opportunity and the challenge to design the next generation of infrastructure. Owing to the know-how of the engineering consultants and the capabilities of the construction companies it is likely that over the next decade some remarkable structures will add to the works of historical significance of the past two centuries.

REFERENCES

BOOKS AND PUBLISHED PAPERS

Akesson, B. (2008) *Understanding Bridge Collapses*, Taylor and Francis, London, ISBN 978-0-415-43623-6

Andrews, A. and Pascoe, M. (2008). *Clifton Suspension Bridge. Bristol*, Broadcast Books, ISBN 978-1-874092-49-0

Beg, D., Kuhlman, U., Davaine, L. and Braun, B. (2010) *Design of Plated Structures*, Berlin, ECCS, ISBN 978-92-9147-100-3

Binding, J. (1997), *Brunel's Royal Albert Bridge*. Truro, Twelveheads Press, ISBN 0-906294-39-8

Bridle, R. (2009). *125 Years of Steel Bridges in Britain (Part 1)*, Proceedings of the Institution of Civil Engineers, Engineering History and Heritage 162, Institution of Civil Engineers, London

Brunel, I. (1870). *The life of Isambard Kingdom Brunel, Civil Engineer*, London, Longmans Green and Co.

BSI (2002) *BS EN 1990:2002 Eurocode: Basis of structural design*, BSI, London

BSI (2002) *BS EN 1991-1-1:2002 Eurocode 1: Actions on structures - Part 1-1: General actions — Densities, self-weight, imposed loads for buildings*, BSI, London

BSI (2003) *BS EN 1991-1-5:2003 Eurocode 1: Actions on structures - Part 1-5: General actions — Thermal actions*, BSI, London

BSI (2003) *BS EN 1991-2:2003 Eurocode 1: Actions on structures - Part 2: Traffic loads on bridges*, BSI, London

BSI (2005) *BS EN 1993-1-1:2005 Eurocode 3: Design of steel structures - Part 1-1: General rules and rules for buildings*, BSI, London

BSI (2006) *BS EN 1993-1-5:2006 Eurocode 3 - Design of steel structures - Part 1-5: Plated structural elements*, BSI, London

BSI (2006) BS EN 1993-2:2006 Eurocode 3 — Design of steel structures - Part 2: Steel bridges, BSI, London

BSI (2004) *BS EN1994-1-1:2004 Eurocode 4: Design of composite steel and concrete structures - Part 1-1: General rules and rules for buildings*, BSI, London

BSI (2005) *BS EN1994-2:2005 Eurocode 4 — Design of composite steel and concrete structures - Part 2: General rules and rules for bridges*, BSI, London

Calgaro, J., Tschumi, M., Shetty, N. and Gulvanessian, H. (2010) *Designer's Guide to Eurocode 1: Actions on Bridges. EN 1991-2, EN 1991-1-1, -1-3 to -1-7 and EN 1990 Annex A2*, London, Thomas Telford, ISBN 978-0-7277-3158-6

Clarck, E. (1849) *General Description of Britannia and Conway Tubular Bridges*, London, Chapman and Hall

Cossons, N. and Trinder, B. (2002). *The Iron Bridge: symbol of the Industrial Revolution*, Phillimore. ISBN 978-1-86077-230-6

Davaine, L., Imberty, F. and Raoul, J. (2007) *Eurocodes 3 and 4. Application to steel-concrete composite road bridges*, Bagneux, SETRA, ISRN EQ-SETRA-07-ED31-FR+ENG

Dintenfass, M. and Dourmois, J. (1999) *The British Industrial Decline*, London, Routledge, ISBN 978-0415172318

Groves, A. (2015) *A487 Caernarfon to Bontnewydd Bypass. Structures Design Options Report*, Manchester, WSP | Parsons Brinckerhoff, Doc. No. 3513874-PB-XX-XX-RP-S-00001

Hayward, A. (2002a). *Steel Bridges. A Practical Approach to Design for Efficient Fabrication and Construction*, BCSA, London, ISBN 0-85073-040-6

Hayward, A. (2002b) *Composite Steel Highway Bridges*, Scunthorpe, Corus Construction Centre, CL&I:SML:3000:UK:02/2002

Hayward, A. (2015). *125 Years of Steel Bridges in Britain (Part 1)*, The Structural Engineer Vol.93 Issue 3, Institution of Structural Engineers, London

Hendy, C. and Johnson, R. (2006) *Designer's Guide to EN1994-2. Eurocode 4: Design of composite steel and concrete structures. Part 2: General rules and rules for bridges*, London, Thomas Telford, ISBN 978-0-7277-3161-0

Hendy, C. and Iles, D. (2010) *Steel Bridge Group: Guidance Notes on best practice in steel bridge construction (5th Issue) (P185)*, SCI, Ascot, ISBN 978-1-85942-196-3

Highways Agency (2014) *Interim Advice Note 124/14(W) Interim requirements for the use of Eurocodes in the design of highway structures*, Highways Agency, Guilford

HM Treasury (2013) *Cm8669 Investing in Britain's Future*, London, The Stationery Office, ISBN 978-0-1018-6692-7

Holt, G. (1986) *The North West, A Regional History of the Railways of Great Britain 10*, David St John Thomas, ISBN 0-946537-34-8

Iles, D. (1994) *Design Guide for Composite Box Girder Bridges. (P140)*, SCI, Ascot, ISBN 1-85942-006-0

Iles, D. (2010) *Composite Highway Bridge Design. (P356)*, SCI, Ascot, ISBN 978-1-85942-188-8

Johansson, B., Maquoi, R., Sedlacek, G., Muller, C. and Beg, D. (2007) *Commentary and Worked Examples to EN1993-1-5 "Plated Structural Elements"*, JRC-ECCS, ISSN 1018-5593

Labrum, E. (1994) *Civil Engineering Heritage*, London, Thomas Telford, ISBN 978-0-727-71970-6

Landes, D. (1969). *The Unbound Prometheus: Technological Change and Industrial Development in Western Europe from 1750 to the Present*, Cambridge, New York: Press Syndicate of the University of Cambridge. pp. 90–93. ISBN 0-521-09418-6

Larena, J. (2004) *Evolucion Tipologica y Estetica de los Puentes Mixtos en Europa*, Universidad Politecnica de Madrid, Madrid

Lucas, R. (2002). *Lectures on Economic Growth*, Cambridge, Harvard University Press, ISBN 978-0-674-01601-9

Millanes Mato, F. (2004) *1ª Jornada 2004 APTA. Construir en Acero los Puentes de Luces Medias*, Madrid, APTA

Millanes Mato, F., Rubio, L., Cornejo, M., Agromayor, D. and Bujalance, E. (2009) *VII Congresso de Construçao Metálica e Mista. Development of steel and composite solutions for outstanding viaducts on the Spanish H.S.R. lines*, Coimbra, CMM

Pannell, J. (1964). *An Illustrated History of Civil Engineering*, London, Thames & Hudson, ISBN 978-0500260012

Rosenberg, N. (1982). *Inside the Black Box: Technology and Economics*, New York, Cambridge University Press. ISBN 0-521-27367-6

Rolt, L. (1984). *George and Robert Stephenson: The Railway Revolution*, London, Penguin. ISBN 0-14-007646-8

Rueda, L., Salcedo, J. (2009) *Proyecto e Construcción de Puentes Metálicos e Mixtos*, Madrid, APTA, ISBN 978-84-692-3057-2

Skempton, A., Rennison, R., Cox, R., Ruddock, T., Cross-Rudkin, P. and Chrimes, M. (2002) *The Biographical Dictionary of Civil Engineers in Great Britain and Ireland, Volume 1*, London, Thomas Telford Publishing for the ICE, ISBN 0-7277-2939-X

Smiles, S. (1862) *Lives of the Engineers, Volume 2*, John Murray, London

Smith, D. (2008) *Civil Engineering Heritage: London & The Thames Valley*, Thomas Telford, London, ISBN 07277 2876 8

Smith, S. (1979) *A View from the Iron Bridge*, Ironbridge Gorge Museum Trust, ISBN 0-903971-09-7

Spence, S. (2015) *A487 Caernarfon to Bontnewydd Bypass. S112 Afon Seiont Newydd (WG No. A487 621) Approval in Principle*, Cardiff, WSP | Parsons Brinckerhoff, Doc. No. 3513874-PB-SBR-112-RP-S-00001

Timoshenko, S. (1953) *History of Strength of Materials*, Dover Publications, New York, 978-04-866-1187-7

Tomlinson, W. (1915). *The North Eastern Railway: Its Rise and Development*, Andrew Reid and Company, OCLC 504251788

Vayas, I. and Iliopoulos, A. (2014) *Design of Steel-Concrete Composite Bridges to Eurocodes*, London, Taylor and Francis, ISBN 978-1-4665-5745-1

Warren, L. (2009). *A Critical Analysis of the Hulme Arch Bridge, Manchester. Proceedings of Bridge Engineering 2 Conference*, Bath University, Bath

WEBSITES

English Heritage (2011) *History and Research: Iron Bridge*. Available from:

https://www.english-heritage.org.uk/daysout/properties/iron-bridge/history-and-research/

[Accessed 4th April 2014]

Engineering Timelines (2015) *Buildwas Bridge*. Available from:

http://www.engineering-timelines.com/

[Accessed 25th January 2015]

Royal Commission on the Ancient and Historical Monuments of Wales (2010) *The Aqueducts*. Available from:

http://www.rcahmw.gov.uk/HI/ENG/Heritage+of+Wales/World+Heritage+Wales/The+Aqueducts/

[Accessed 25th January 2015]

Wikipedia (2015) Bessemer Process. Available from:

http://en.wikipedia.org/wiki/Bessemer_process

[Accessed 8th February 2015]

Severn River Crossing PLC. Available from:

http://www.severnbridge.co.uk/index.html

[Accessed 1st March 2015]

River Usk Crossing, Newport Southern Distributor Road. Available from:

http://www.steelconstruction.org/resources/design-awards/2005/award/river-usk-crossing-newport-southern-distributor-road.html

[Accessed 14th March 2015]

M4. Wales. Available from:

http://www.ukmotorwayarchive.org/en/motorways/motorway-listing/m4/index.cfm

[Accessed 2nd April 2015]

Welsh Government (2013) *A487 Caernarfon to Bontnewydd Bypass*. Available from:

http://gov.wales/topics/transport/roads/schemes/a487/a487caernarfon/?lang=en

[Accessed 15th January 2016]